UiT
THE ARCTIC
UNIVERSITY
OF NORWAY

Department of Physics and Technology

Quantifying influence of local air pollution on measurements in Ny-Ålesund and at the Zeppelin station

—

Alena Dekhtyareva

FYS-3900 Master's Thesis in Physics

May 2014

UNIVERSITY OF TROMSØ

Abstract

In order to keep the scientific significance of the Ny-Ålesund station on Svalbard as the key place for the monitoring of background air it is needed to assess the influence from local human activities on the air quality. Whether research and tourist activity continues to grow or restrictions to be implied the change of impact may affect air chemistry data quality. Therefore the identification of the present sources of local, regional and long-range transport of pollution and estimation of the magnitude of their impact on the data collected at the mountain Zeppelin station and in the Ny-Ålesund village would be very useful for any proposal for the local activity change.

The classical tools of the air pollution dispersion theory cannot be applied alone for such analysis and should be compiled with the knowledge of the local micrometeorological features and unique Arctic air chemistry and physics. Taking it into account the atmospheric stability analysis and local wind field assessment has been applied and the days with possible local pollution from the cruise ship traffic and from the power plant have been defined. Further the long-range sources of pollution have been determined using FLEXTRA air mass trajectories analysis.

In general, the Zeppelin station is proved to be influenced by the local pollution quite rare if was at all and remains a valuable scientific station for the long-range transport research. However, the results of the analysis show that the high rate of uncertainty is still present in the separation of the long-range transport and local pollution due to the absence of the high frequency chemical measurements of the same tracer both in the village and at the Zeppelin station. It would be possible to investigate the influence of the regional pollution from the ships when the ship location statistics is available. On the other hand, the comprehensive local meteorological data analysis done for the area allows to set up a high resolution air dispersion model in the further work.

Content

Introduction

The Zeppelin Observatory is Norwegian atmospheric monitoring facility located approximately 2 km away from the centre of the Ny-Ålesund (a small village in North Western Svalbard). Zeppelin mountain station is pre-eminent for the Global Atmosphere Watch and AMAP programmes as well as for many other research projects because it provides opportunities for such activities as monitoring of ozone and UV-radiation, global distribution of toxic pollutants like heavy metal, CFC, VOC, POPs, VOCs, NO_x, SO_2, CO_2, CO and nutrients deposition in Arctic, meteorological measurements and global modelling.

The coordinates of the Zeppelin mountain (Zeppelinfjellet) station are following 78°54′26"N 11°53′12"E. The station is placed on a mountain ridge (474m above sea level) with steep slopes to the north and south.

As one can see in Figure 1 the glacier Austre Brøggerbreen located south and south-east and higher mountain peaks to the west from the Zeppelinfjellet set the stage for developing of so called valley wind system. Therefore the most expectable wind direction at the Zeppelin observatory would be south and south-east.

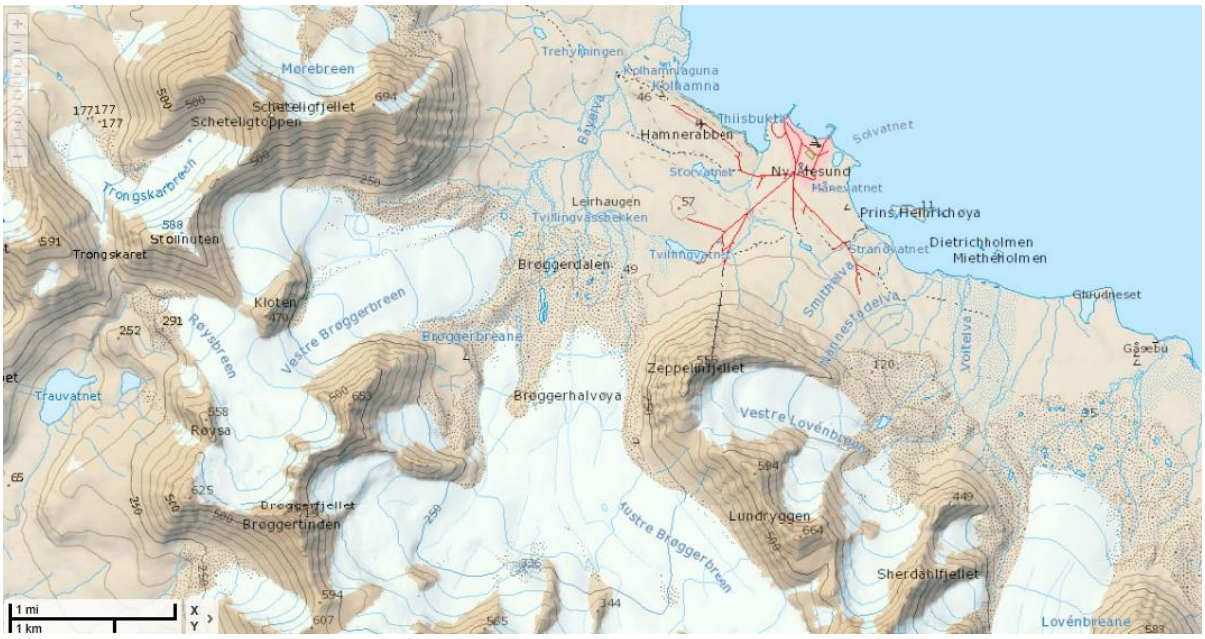

Figure 1 Map of Ny-Ålesund and surroundings (taken from the web-site http://eivind.npolar.no/Geocortex/Essentials/Web/viewer.aspx?Site=svbk_v01_no)

This specific location for the station has been chosen in order to reduce the impact of local pollution on the measurements of high accuracy needed to detect long range transport of substances to the Arctic (Eneroth et al. 2007).

However, measurements of NO_x and aerosol particles at the Ny-Ålesund Zeppelin

mountain station have shown that the measurements are at times influenced by regional and local pollution sources (Beine H. J. et al. 1996).

The largest source of NO_x in Ny-Ålesund is the power station. It is situated north of the monitoring station inside Ny-Ålesund and runs on low sulphur diesel. Another local source of SO_2 and NO_x in Ny-Ålesund is summertime traffic of the tourist ships utilizing heavy oil with high sulphur content (Shears et al. 1998).

Air arrived from SE might be influenced by regional pollution from the settlements Longyearbyen or Barentsburg which are located south-east from Ny-Ålesund. These mining settlements served by small, coal-fired electric power plants are sources of acidification agents in Arctic (AMAP, 1998).

Cruise, research and fishing vessel's traffic around Svalbard might be another regional source of pollutants and should be taken into consideration as well.

Therefore the main aim of the following Master thesis is to develop means of quantifying the influence of local and regional air pollution on Ny-Ålesund and Zeppelin measurements. Particular attention will be paid to utilizing the data collected in the village during the project Local Air Quality Monitoring 2008-2010 in Ny-Ålesund.

For achieving the goal of the thesis the following methods have been implemented:

-literature research of previous scientific investigation results dedicated to identification of sources of local, regional and long-range transported pollution;

-analysis of ground based observations results such as air quality and meteorological measurements from the place of interest and comparison of them with ship traffic statistics;

-examination of the main chemical properties and life-time of the measured substances in order to relate these characteristics with the transport pathways to understand their fate in the atmosphere;

- scrutinize the differences in the filter sample results from the Zeppelin and Ny-Ålesund to quatify the amount of data possibly influenced by local pollution;

-investigation of local boundary layer meteorological characteristics and comparison of different methods of atmospheric stability analysis to estimate how often the polluted air could reach the Zeppelin observatory and what atmospheric conditions were favourable for such event;

-comparison of the local wind field and the stability characteristics of the atmosphere from the meteorological data and the results of the simulation executed on the high resolution Weather Research and Forecasting model;

-study of trajectory modelling (e.g. from FLEXTRA-model) results for distinguishing between local and long-range transport of pollutants with special attention to the unique influences of atmospheric lifetime of constituents in the Arctic.

All the methods (ground-based observations, remote sensing and modelling) used in the thesis have uncertainties which are to be qualitatively described and quantified when possible.

Ny-Ålesund is a place dedicated to research of climate and long-range transport of pollutants and the unique qualities of the location are of paramount importance to maintain and protect therefore in the conclusion of the thesis statements concerning future air quality monitoring have been made.

The scientific and technical work is done in cooperation with the Norwegian Polar Institute, Stockholm University, Alfred Wegener Institute for Polar and Marine Research and the Norwegian Institute for Air Research.

1 Identification of possible sources of local, regional and long-range transport of pollution

The source defining process is closely related to the concept of lifetime, chemical properties and environmental fate of the particular pollutants.

The local pollution is usually characterized by higher pollutant concentrations while long-range transported pollution is more dispersed. However, the Arctic is a unique place due to special atmospheric dynamics and chemistry. In the Arctic layers of polluted air can be brought almost undispersed and avoiding the reactions typical for plume aging and thus this can be misinterpreted for local pollution due to the steep gradients or short timescale variations because of the non-uniform "layer-cake" aerosol concentration of the air masses. In a contrary, local pollution trapped in the fjord surrounded mountains in the presence of local wind flows with low wind speed can lead to diffuse peaks that may be misinterpreted as long range transport.

On the other hand, the shipping fleet around Svalbard can create patterns of pollution that can be difficult to separate from European or other long-range pollution.

Thus both the "classical" regional and local pollution reactions intrinsic to urban areas should be compared with the specialties of the remote Arctic chemistry and atmospheric dynamics.

According to classification presented in (Arya 1999) the local and urban air pollution is characterized by temporal scale from 10^{-1} to 10 and from 10 to 10^2 hours, respectively, while the regional air pollution has a temporal scale from 10 to 10^3 hours.

The regional pollution problems in urban areas are caused by tropospheric ozone (O_3), photochemical oxidants, and sulphur and nitrogen compounds (Arya 1999).

The data available from the project Local Air Quality Monitoring 2008-2010 in Ny-Ålesund represent NO_x and SO_2 monitor measurements, therefore chemical properties and sources of these substances are discussed further where a careful analysis of possible sources of events can give a better insight into how frequently registered events may come from local sources.

There nitrogen oxides play important role in the formation of the tropospheric ozone and photochemical smog (Arya 1999). NO_x is usually defined in the literature as sum of the nitrogen oxide NO and nitrogen dioxide NO_2. The fossil fuel combustion reactions in the mobile sources such as automobiles, snowmobiles, ships and zodiacs and the stationary sources such as power plants start the following chain of reactions.

First NO is formed during high-temperature combustion process with atmospheric oxygen from nitrogen present in the fuel and in the air (Seinfeld and Pandis 2006). Then due to increased temperature some part of NO (0,5-10%) in the exhaust gases is oxidized more deeply and NO_2 is produced (Arya 1999).

The rest of NO is participating in the so called null-cycle where daylight plays an important role:

$$NO + O_3 \rightarrow NO_2 + O_2 \quad (1)$$

$$NO_2 + O_2 + M + h\nu \rightarrow NO + M + O_3 \quad (2)$$

where M is an inert "third body" absorbing excess molecular energies (Wallace and Hobbs 2006).

However, excess O_3 can be produced though the following reaction chain when the nitrogen oxide (NO) concentration is higher than 10pptv (Wallace and Hobbs 2006).

First the hydroxyl radical formed by photodissociation of the ozone molecule in the presence of water vapour

$$O_3 + H_2O + h\nu\ (\lambda \leq 0.32\ \mu m) \rightarrow O_2 + 2OH \quad (3)$$

Then hydroperoxyl radical is formed through the reaction with carbon monoxide (CO)

$$OH + CO + O_2 \rightarrow HO_2 + CO_2 \quad (4)$$

HO_2 is then involved in the NO_x cycle with resulting ozone production

$$HO_2 + NO \rightarrow OH + NO_2 \quad (5)$$

$$NO_2 + h\nu \rightarrow NO + O \quad (6)$$

$$O_2 + O + M \rightarrow O_3 + M \quad (7)$$

The volatile organic compounds (VOCs) in the presence of high NO_x concentration can also be source of ozone production

$$OH + RH + O_2 \rightarrow H_2O + RO_2, \quad (8)$$

where R is the alkyl radical and RO_2 is the peroxy radical. Then the latter reacts with NO in the same manner as HO_2 yielding net O_3 production in the reaction (5). Thus the ozone production in the mid-latitude urban area is limited by the VOC/NO_x and CO/NO_x ratios (Seinfeld and Pandis 2006).

Conversely, in the vicinity to large source of NO loss of ozone can be observed due to reaction (1). The dip in concentration of O_3 is especially pronounced during the night (Chameides et al. 1992).

The evidence the ozone loss process has been observed in Ny-Ålesund and explained by the pollution from the ships (Eckhardt et al. 2013)

During the day NO_2 is removed through reaction with OH-radical (Wallace and Hobbs 2006):

$$NO_2 + OH + M \rightarrow HNO_3 + M \quad (9)$$

Nevertheless, at the night in the absence of sunlight the nitric acid is produced as well but in a different way. The process consists of nitrate radical production during the oxidation of nitrogen oxide by ozone, dinitrogen pentoxide N_2O_5 formation and the hydrolysis of the latter to nitric acid (Seinfeld and Pandis 2006; Wallace and Hobbs 2006).

$$NO_2 + O_3 \rightarrow NO_3 + O_2 \quad (10)$$

$$NO_2 + NO_3 \rightarrow +N_2O_5 \quad (11)$$

$$N_2O_5 + H_2O \rightarrow HNO_3 \quad (12)$$

Then HNO_3 is rapidly removed from the air through dry and wet deposition processes. HNO_3 and ammonia (NH_3) can form ammonium nitrate aerosol NH_4NO_3 as well (Seinfeld and Pandis 2006).

Other sources of NO_x in the troposphere are biomass burning, and emissions from soils, NH_3 oxidation and subsidence from the stratosphere (Wallace and Hobbs 2006).

As a result of the reactions mentioned above NO_x has approximate residence time around one day in the lower troposphere and from 5 to 10 days in the upper troposphere in mid-latitudes. (Arya 1999; Jaeglé et al. 1998).

Sulphur dioxide (SO_2) is mainly released during the combustion of fossil fuel (Wallace and Hobbs 2006). However, such sources as smelting processes, natural gas and petroleum production emissions containing significant amounts of sulphur compounds, emissions from pulp and paper operations, biomass combustion and waste burning may also contribute significantly to the total budget of sulphur substances (Smith et al. 2011).

The natural sources of the sulphur agents such as biological activity of plankton in the oceans and sea-salt spray should also be taken into consideration.

The dimethyl sulphide (CH_3SCH_3; DMS) originated from the metabolite of some marine algae is the most common biogenic sulphur compound sent out to the atmosphere. DMS is a short-lived compound with half day lifetime (Seinfeld and Pandis 2006). The oxidation of DMS by the hydroxyl radical is the major source of H_2SO_4 in the unpolluted marine boundary layer.

The process is highly complex and gives a variety of the transient and final products of the reaction depending on NO_x-free and NO_x-containing conditions (Arsene et al. 2002; Berresheim et al. 2002; Ramírez-Anguita, González-Lafont, and Lluch 2008; Yin, Grosjean,

and H. 1990). Some characteristic reactions showing formation of major products are described below.

There are two ways of the primary oxidation reaction of DMS. One way yields CH_3SCH_2-radical formation and the second one leads to DMS-OH production with adduct reaction with O_2 (Ramírez-Anguita, González-Lafont, and Lluch 2008)

$$CH_3SCH_3 + OH \rightarrow CH_3SCH_2 + H_2O \quad (13)$$

$$CH_3SCH_3 + OH \rightleftarrows CH_3S(OH)CH_3 \xrightarrow[O_2]{} \text{products} \quad (14)$$

Dimethyl sulphoxide ($CH_3S(O)CH_3$: DMSO), dimethyl sulfone ($CH_3S(O)_2CH_3$: $DMSO_2$), methane sulphonic acid ($CH_3S(O)_2OH$: MSA) can act as products in the last reaction (Ramírez-Anguita, González-Lafont, and Lluch 2008).

Methane sulphinic acid ($CH_3S(O)OH$: MSIA) can be further produced from reaction of DMSO with hydroxyl radical (Arsene et al., 2002).

Methylsulphonyl radical (CH_3SO_2) formed from DMS though a set of reactions with hydroxyl radical, nitrogen oxides, O_2 and ozone is further decomposed to SO_2 (Yin, Grosjean, and H. 1990).

The evidences of significance of these natural processes were documented on Svalbard as well. For example, the data from the analysis of composition of the aerosol particles collected at the Zeppelin station showed that the sea spray from oceans plays important role in the wintertime on Svalbard due to annual maximum of the wind speed. Whereas 26% of the non-sea salt sulphur in summer were methanesulphonate, MSA^-, and sulphate, (SO_4^{2-}) from the regional marine biological source. The MSA^- has a summer maximum in concentrations because it is related to seasonal biological activity of phytoplankton and zooplankton (Heintzenberg and Leck 1994).

Both natural and anthropogenic sulphur dioxide yields sulphur acid formation in gaseous phase (Wallace and Hobbs 2006) in following way

$$SO_2 + OH + M \rightarrow HOSO_2 + M \quad (15)$$

$$HOSO_2 + O_2 \rightarrow HO_2 + SO_3 \quad (16)$$

$$SO_3 + H_2O \rightarrow H_2SO_4 \quad (17)$$

Sulphur dioxide also can dissolve in cloud water and then in aqueous phase the oxidation process takes place:

$$SO_2(g) + H_2O(l) \rightleftarrows SO_2 \cdot H_2O(aq) \quad (18)$$

$$SO_2 \cdot H_2O(aq) + H_2O(l) \rightleftarrows HSO_3^-(aq) + H_3O^+(aq) \quad (19)$$

$$HSO_3^-(aq) + H_2O(l) \rightleftarrows SO_3^{2-}(aq) + H_3O^+(aq) \quad (20)$$

Then products of the latter reactions are oxidized to the sulphate ion (SO_4^{2-}) (Wallace and Hobbs 2006).

The classical lifetime of sulphur dioxide and non-sea salt sulphate are 2 days and 5 days, respectively (Seinfeld and Pandis 2006).

However, some specific chemical reactions, physical processes and timescales are intrinsic only to the Arctic.

First of all, the physical environment is very different from the mid-latitudes. According to (Kupfer, Herber, and König-Langlo 2006), the last sunset is 24th of October and first sunrise is 18th of February in Ny-Ålesund. Therefore the photolysis reactions described above are limited, and the air may be retained in the darkness about 10 days in December in the lowest 100 m (Stohl 2006).

Furthermore, the Arctic lower troposphere is separated from the rest of the atmosphere by the Arctic front barrier, formed by the surfaces of constant potential temperature increasing with height. During winter the Arctic front extends further south (up to 50°N) while during summer it is located northerly. This prevents the transport of pollutants from Eurasia during this season, and extends the time air remains continuously in north of 80°N (the Arctic age of the air) in the lower troposphere from 7 days in winter to 14 days summer (Stohl 2006; Weinbruch et al. 2012). Thus local aerosol sources on Svalbard are considered to be more important in this time of year. (Zhan and Gao 2014)

On the other hand, in the winter and spring the Arctic haze, an anthropogenic phenomenon characterized by the transport of highly polluted air masses from Europe and the former Soviet Union, can be observed (Quinn et al. 2007; Stohl 2006). These two main sources of long-range transport of pollution were also noticed in the environmental impact assessment report (Shears et al., 1998).

High concentrations of pollutants in the air results from limited turbulent mixing and surface inversions produced during the radiative cooling of the snow and ice-covered surfaces. Moreover, the air humidity is very low due to temperature-humidity dependence. Therefore both dry and wet deposition of pollutants is confined (Stohl 2006).

When the sun rises above the horizon late in February, the long-range favourable conditions still remain due to cold air temperatures. Such combination leads to the very peculiar photochemical reactions specific for the Arctic.

For example, in the high latitudes the long-range transport of photochemically

produced O_3 from anthropogenic emissions at lower altitudes is accompanied by the local destruction resulting to the ozone depletion events. It has been shown that the ozone concentration rapid variation in the Ny-Ålesund and Alert depends on the advection and mixing of depleted and undepleted air masses therefore not only unique springtime chemistry but also the atmospheric dynamics is very important. (Barrie and Platt 1997)

In general, the maximum of average ozone tropospheric concentration in late winter in Ny-Ålesund, the springtime rapid decrease and a minimum level during summer are observed (Eneroth et al. 2007; Solberg et al. 1996)

The ozone depletion events coincide with non-methane hydrocarbons minimum in spring in the Arctic Basin. This is the result of heterogeneous reactions over the pack ice with bromine and chloride. (Eneroth et al. 2007)

Moreover, the reactions of NO and N_2O_5 with components of sea salt particles such as sodium chloride (NaCl) and bromide (NaBr) may also occur in the gas-aerosol mixture close to the ocean surface (Finlayson-Pitts and Pitts 2000; Li et al. 1990)

$$2NO_2(g) + NaCl(s) \rightarrow ClNO(g) + NaNO_3(s) \quad (21)$$

$$2NO_2(g) + NaBr(s) \rightarrow BrNO(g) + NaNO_3(s) \quad (22)$$

$$N_2O_5(g) + NaCl(s) \rightarrow ClNO_2(g) + NaNO_3(s) \quad (23)$$

$$N_2O_5(g) + NaBr(s) \rightarrow BrNO_2(g) + NaNO_3(s) \quad (24)$$

The atomic chlorine and bromine are the products of photolysis of the gaseous nitrosyl chloride and nitrosyl bromide

$$ClNO(g) \rightarrow Cl + NO(g) \quad (25)$$

$$BrNO(g) \rightarrow Br + NO(g) \quad (26)$$

The chlorine and bromine monoxides are the products of photolysis of the gaseous nitril chloride and bromide

$$ClNO_2(g) \rightarrow ClO + NO(g) \quad (27)$$

$$BrNO_2(g) \rightarrow BrO + NO(g) \quad (28)$$

Halogen products in the last two reactions are closely connected to the tropospheric ozone depletion events known to take place in the Arctic during springtime in connection with air transport across the Arctic ocean (Eneroth et al. 2007; Solberg et al. 1996).

One can see in the Figure 2 that the production of Br_x from HOBr crucial for sufficient ozone loss is documented for acid conditions present in Arctic haze aerosols, and that the cycle may involve nitrous oxides as well (Fan and Jacob 1992) .

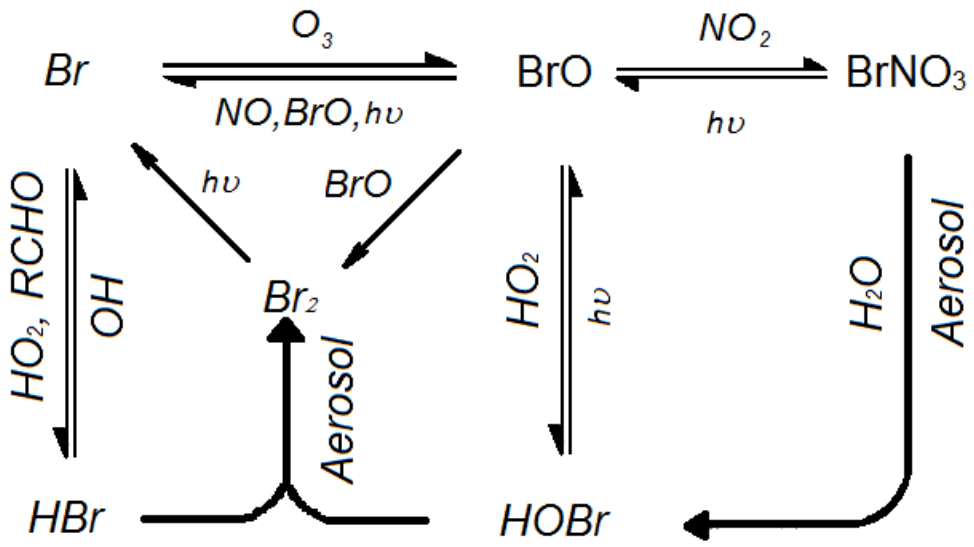

Figure 2 The Br_x production cycle (Fan and Jacob 1992)

The thermal decomposition of peroxyacetyl nitrate (PAN) may also be an important source of NO_x in the high latitudes. The reaction resulting to peroxyacetyl radical and nitrogen dioxide formation is following (Seinfeld and Pandis 2006):

$$CH_3C(O)O_2NO_2 + M \rightarrow CH_3C(O)O_2 + NO_2 + M \quad (29)$$

The PAN lifetime decreases exponentially with increasing temperature (at the temperature -10°C it is around 200hours while at the temperature 15°C it is just about 3hours (Harald J Beine et al. 1997; Seinfeld and Pandis 2006)). It is reflected in the springtime increased NO_x/PAN ratio which has been observed near Ny-Ålesund, Svalbard in 1994 and Poker Flat, Alaska in 1995 (Harald J Beine et al. 1997).

The springtime reactions with nitrous oxides and PAN described above and long aerosol lifetime in winter make the lifetime estimation of these compounds very complicated.

In addition to this, the boreal fires plumes over Siberia could be possible source of ammonia and nitrogen oxides in the Arctic in the summertime if there were favourable conditions for the transportation from this source (Alvarado et al. 2010).

Another common local pollutant in the classical theory is the anthropogenic black carbon (BC). Indeed, the new investigation made in Svea and in Longyearbyen showed 200 higher concentration of elemental carbon (EC) around these settlements than the background level on Svalbard. However, 90% of the total EC pollution on Svalbard has long-range origin. The maximum concentration is measured in winter and spring during Arctic haze periods while in summer cleaner air can be at times influenced by the plumes of boreal fires in Northern Eurasia (Aamaas et al. 2011; Stohl 2006).

The enhanced biomass burning in summer might increase these periods and make even more complicated the process of separation of local and long-range transported emission, therefore both changes in local impact (e.g. new cleaning equipment for the power plant or difference in cruise ship traffic from year to year) must be carefully documented as well as alteration of long-range sources of pollution (Zhan and Gao 2014).

According to the mentioned lifetime for the classical air pollution chemistry the sources of NO_x and SO_2 might be regional or local. However, the conclusion about local nature of these compounds is imprecise for Arctic winter because of very low rates of reaction due to the low temperatures and the absence of sunlight in the polar night time (Harald J Beine et al. 1997). Without dispersion and chemical transformation the lifetimes of NO_x and SO_2 increase during wintertime to 10 days (Beine H. J. et al. 1996) and 4 days (Lee et al. 2011), respectively. The time might also be much higher if one takes into consideration the Arctic age of air and chemical transformation occurring during the transport (e.g. PAN to NO_x conversion).

One can see that the Arctic atmospheric chemistry is highly variable and depends on the time of year, local meteorological conditions and large scale atmospheric dynamics, and therefore it cannot be evaluated using only classical pollution dispersion chemistry theories developed for urban mid-latitude areas. Local and regional sources and sinks can imitate long-range transport and cause misinterpretations of the data set. It is therefore important to be able to eliminate data with local contamination from the dataset and quantify the quality of Ny-Ålesund as a pristine site for environmental monitoring. Hence better measures and understanding of how often the data are disturbed by the activities in Ny-Ålesund are needed. The increases and decreases in the local activity may lead to misinterpretations too. For example, installation of new cleaning equipment at the power plant or improvement of energy saving in the village reduce emissions and this can lead to erroneous conclusion that the background air monitored at the Zeppelin station becomes less polluted therefore it is important to look at possible sources of emissions on Svalbard and, particularly, in Ny-Ålesund.

However, it is also important to remember that the simple time scale analysis cannot be applied and the atmospheric stability analysis can be an important part of a more careful approach of the further source defining process.

1.1 Regional pollution in Svalbard

There is a map of Svalbard in Figure 3 where one can see location of Ny-Ålesund vs other settlements which could be possible sources of the pollution.

Figure 3 Map of Svalbard (taken from the web-site http://eivind.npolar.no/Geocortex/Essentials/Web/viewer.aspx?Site=svbk_v01_no)

Approximate distance from Ny-Ålesund to Barenstburg and to Longyearbyen is 110km and 113km, respectively.

The largest source of SO_2 (92%) is a coal energy production. Big coal-fuelled power plants for the production of electricity and heat are operated in Longyearbyen and Barentsburg. The most of diesel for electricity supply is consumed in Svea (Sveagruva in the map), Ny-Ålesund and Hornsund.

Carbon dioxide (CO_2), methane (CH_4) and black carbon (BC) are released during the coal mining process and from diesel and coal power stations in Longyearbyen (Gruve 7), Svea and Barentsburg. The coal transportation is a local source of air pollution close to the mines located at Svea and Longyearbyen due to high consumption of diesel fuel by heavy duty vehicles which contributes 4% of BC released at Svalbard (Vestreng et al. 2009).

Local elemental carbon (EC) emissions in Norwegian settlements on Svalbard are responsible for 10% reduction of the snowpack albedo on Svalbard (Aamaas et al. 2011) The land based private transport such as cars and snow scooters contribute to significant air pollution by the aromatic hydrocarbons (HC) on local level along scooter tracks and roads (Reimann et al. 2009). Despite these sources are not significant on regional level due to low

diesel and gasoline consumption for private cars (Vestreng et al. 2009), they can play important role in local pollution processes in Ny-Ålesund directly. The snowmobiles are in use in the village in spring time, and the emissions can be trapped between the mountains in Kongsfjorden due to insufficient mixing. The local wind system such as mountain and valley winds and sea breezes are not effective in the dispersion processes due to low speed (<7m/s) and closed trajectory and possible diurnal reversibility of the wind flow. (Oke 2002).

1.1.1 Ship traffic around Svalbard

The shipping industry is responsible for 4-6% of world total sulphur emissions and approximately 14% of world's total nitrogen discharge to air (Norges Rederiforbund 2003).

The combustion engines installed on most of marine vessels including zodiacs produce operational discharges to air containing carbon monoxide (CO), NO_x, HC, CO_2, SO_2, particulate matter, halogens and metals. Emissions of the first three compounds depend on the engine design while released amounts of the rest vary from one type of oil to another (Kalli, Karvonen, and Makkonen 2009; Ziegler and Hansson 2003).

The main regulation is the MARPOL 73/78 Protocol of 1997 (Annex VI) - Regulations for the Prevention of Air Pollution from Ships. It has been ratified by Norway therefore ships operated on Svalbard have to follow these rules.

The Annex VI sets limits on sulphur oxide and nitrogen oxide emissions from ship exhausts and prohibits deliberate emissions of ozone depleting substances. The document includes a limit of 3.5% m/m on the sulphur content of fuel oil from the 1st of January 2012 and declares progressive reductions in nitrogen oxide (NO_x) emissions from marine engines such as shown in Figure 4. There Tier I are diesel engines installed on a ship constructed on or after 1 January 2000 and prior to 1 January 2011 or ships constructed on or after 1 January 1990 but prior to 1 January 2000 with a power output of more than 5000 kW and a per cylinder displacement at or above 90 litres; Tier II are diesel engines installed on a ship constructed on or after 1 January 2011 (Det Norske Veritas AS 2009). Therefore comparing vessels of the same size one can say that higher emission levels of NO_x are intrinsic to older ships.

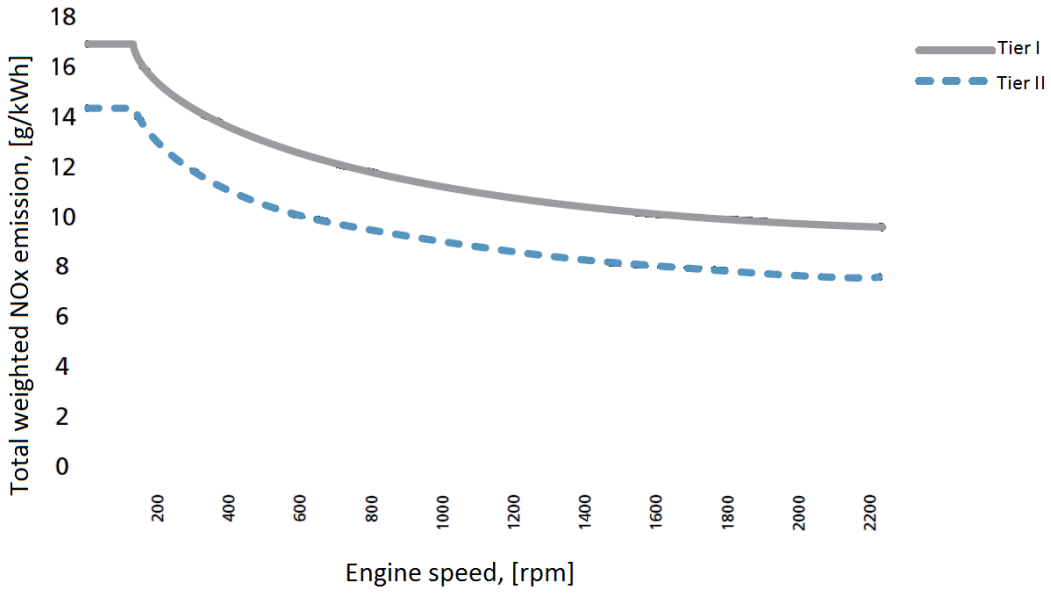

Figure 4 Allowable NO_x emissions from diesel engines (Det Norske Veritas AS 2009)

The type of the fuel used is of high importance in terms of sulphur dioxide emissions. There are following types of oil the most commonly used by shipping industry: Marine Gas Oil (MGO) represented by Distillate DMX, DMA, DMB, DMC Gas Oil; Marine Diesel Fuel such as Intermediate Fuel Oil (IFO 180 and IFO 380) and Residual Fuel Oil (RMA-RML Fuel Oil). The marine distillate fuel is the most sold around the world type of MGO. It contains 0.1-1% of sulphur with average value of 0.35% while the conventional marine residual oil (RO) has 0.5-4% of sulphur with average values of 2.6% and 2.4% for IFO 380 and IFO 180 types of RO, respectively (Corbett and Winebrake 2008).

Most of cruise ships operated by Association of Arctic Expedition Cruise Operators (AECO) use marine gas oil (MGO) (Evenset and Christensen 2011).

The amount of energy needed for the voyages and, consequently, the fuel consumed depends on the operation regimes. Lower temperatures of operation and frequent stops and start-ups of cruise ships due to landing for the excursions within the Svalbard zone may increase the emissions quantities (Vestreng et al. 2009).

For excursions on sea and landings AECO widely use zodiacs (the distance travelled by inflatable boats can be 1000 km per cruise). Emissions from them depend on the outboard engine type used: two-stroke or four-stroke. The two-stroke engines are more fuel-consuming and emit higher values of polycyclic aromatic hydrocarbons (PAHs) and CO (Evenset and Christensen 2011).

According to the information given by AECO in the presentation “Polar cruise tourism

development" the total number of cruise passengers visiting Svalbard was slightly decreasing from 2008 to 2010, however, it rose again in 2012. The dynamics of passenger number is shown in Figure 5.

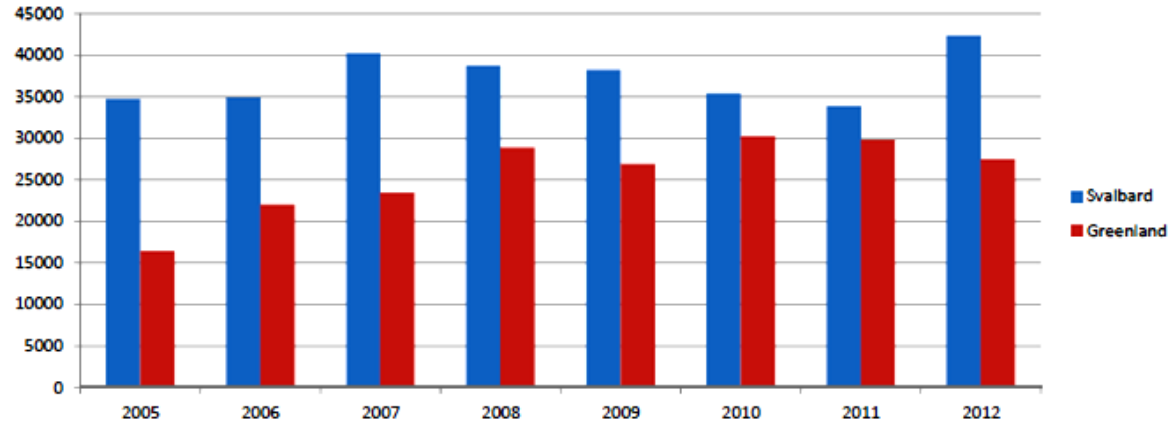

Figure 5 Total number of cruise passengers Svalbard&Greenland (numbers include all commercial cruise traffic (conventional cruise vessels and expedition ones)

The air pollution from cruise ship traffic has been accessed in the report "Climate influencing emissions, scenarios and mitigation options at Svalbard" made by Norwegian Pollution Control Authority. According to this document marine international cruises and marine coal transport from Svea produce 3% of SO_2 emissions on Svalbard. Marine transportation in general contributes approximately 90% to emissions of particulate matter (black carbon (BC, soot) and organic carbon (OC)) and NO_x in 2007 from which 40% originates from cruise ships (Vestreng et al. 2009). The ratio of NO_x emissions from marine activity is shown in Figure 6 and 7 respectively.

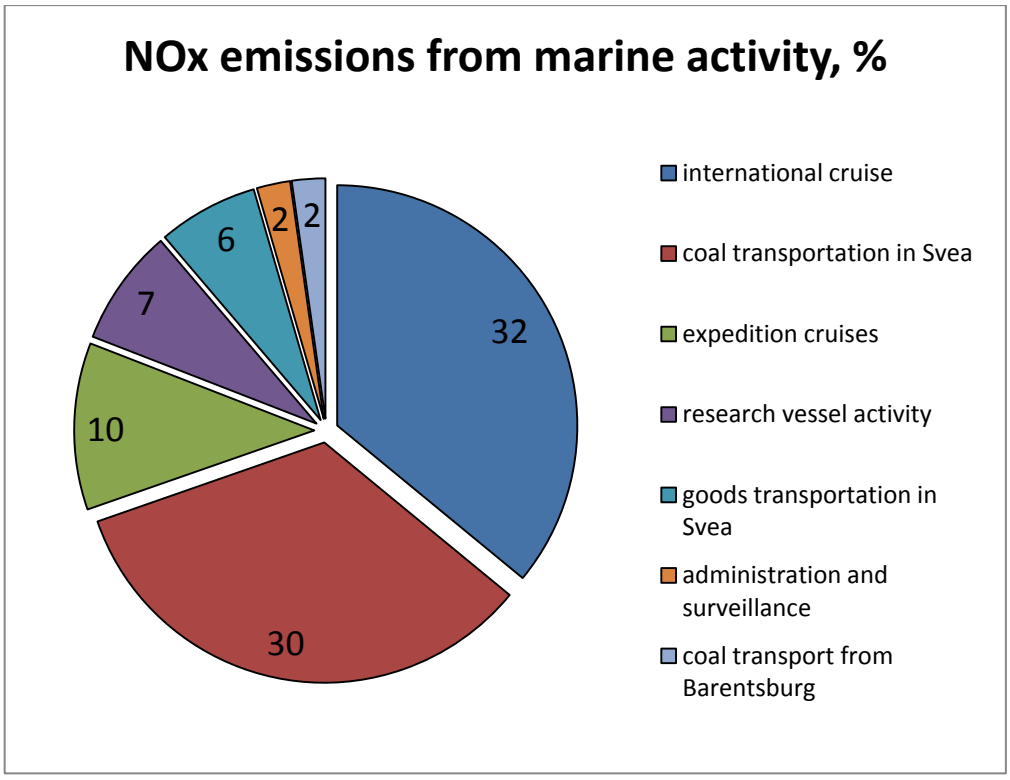

Figure 6 NO_x emissions from marine activity (not including the fishing boats) (Vestreng et al. 2009).

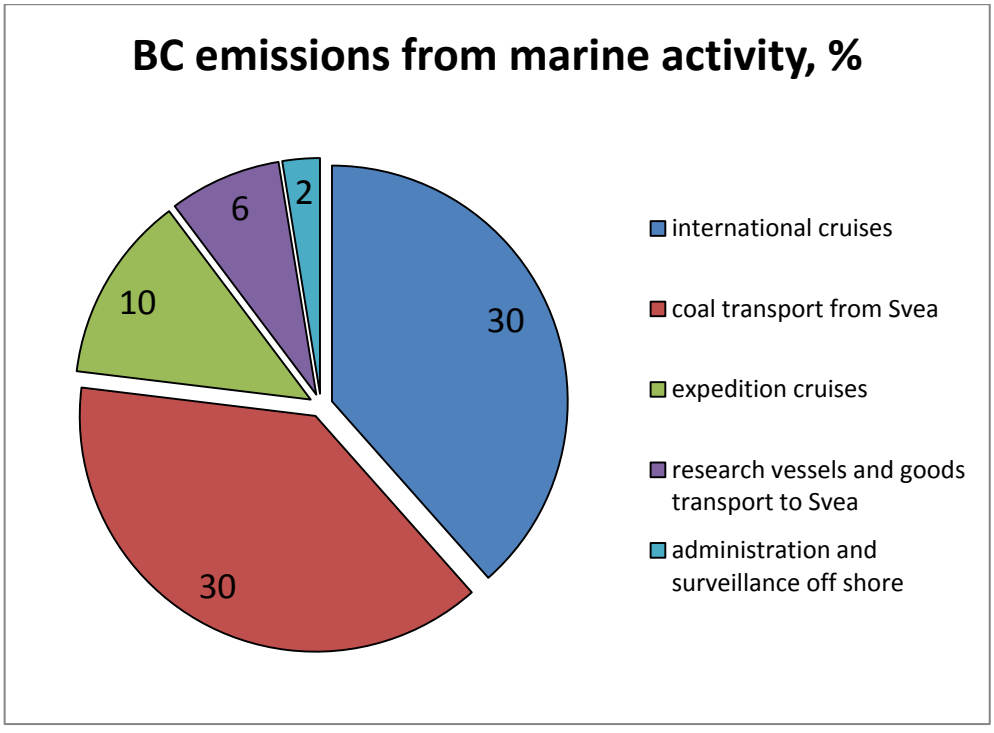

Figure 7 BC emissions from marine activity (not including the fishing boats) (Vestreng et al. 2009).

However, despite the emission source ratio offered by (Vestreng et al. 2009) the

example of the ship traffic around Svalbard during period from 15.07.2010 00:01 to 30.09.2010 23:59 given by AECO in the presentation “Polar cruise tourism development” shows that the most of ships were fishing vessels (10 times as many as the passenger ships) (Figure 8) therefore it is needed to look at fishing industry as another source of air pollution at Svalbard.

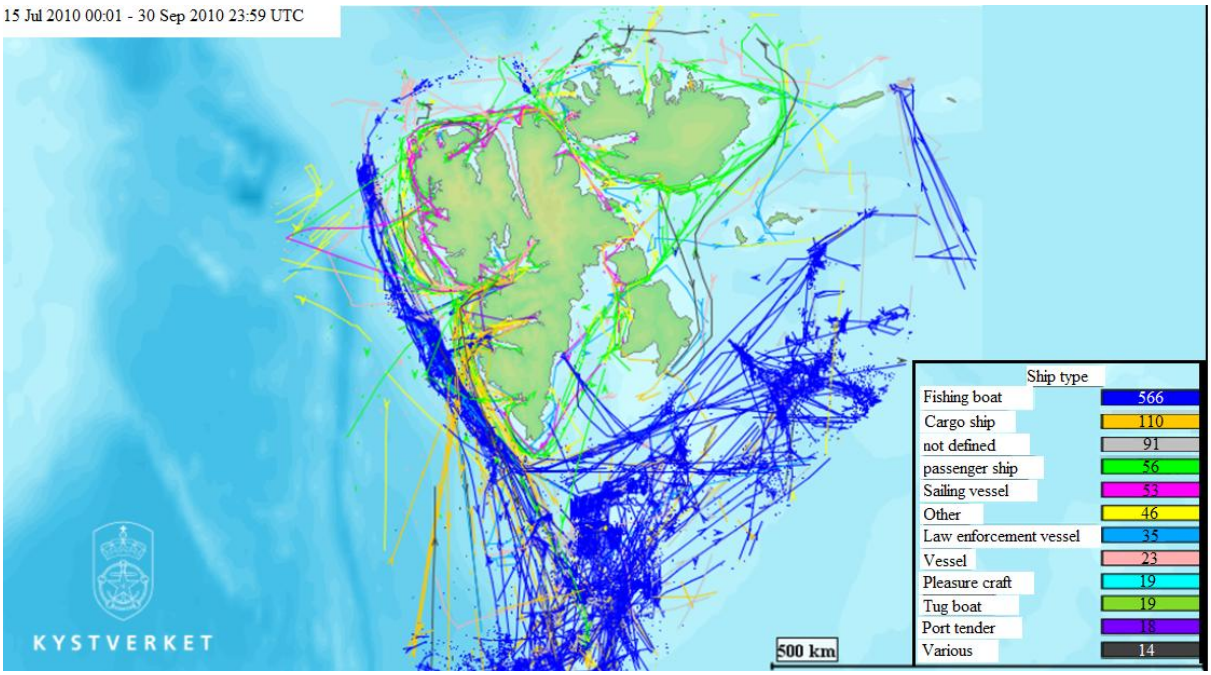

Figure 8 The example of the ship traffic around Svalbard during the period from 15.07.2010 00:01 to 30.09.2010 23:59

The typical fuel used for fishing vessels is marine gas oil (diesel) which has lower sulphur content than the conventional residual oil (Schau et al. 2009). However, the resulting energy performance of fishing vessels depends on the relative abundance and catchability of various targeted species and type of fishing gear employed (Tyedmers 2004).

For the main target fish species in the maritime zones of Svalbard Norwegian spring-spawning (Atlanto-scandian (AS)) herring (*Clupea harengus*), Arctic cod (*Gadus morhua*), haddock (*Melanogrammus aeglefinus*), and shrimp (*Pandalus borealis*) the fuel use coefficients are 0.09 kg/kg fish, 0.35kg/kg fish, 0.40 kg/kg fish, and 1.04 kg/kg fish, respectively (Molenaar 2012; Schau et al. 2009). The most important fishery in the region is the shrimp one, however, the distribution above reflects that the shrimp trawl is the fishing gear with the highest fuel consumption per kilogram of catch while pelagic trawl used for herring is the most fuel efficient gear (Schau et al. 2009).

Therefore it is possible to distinguish the amount of energy ship consumes and pollutants it releases using the data about fishing gear, target species and the information from

the energy audit of fishing vessels (Basurko, Gabiña, and Uriondo 2012; Schau et al. 2009). Data about the location of the particular ship and the type of vessel would allow making an assessment of influence of regional ship traffic emissions on measurements at the Zeppelin station.

1.2 Local pollution in Ny-Ålesund

According to the Environmental impact assessment of the Ny-Ålesund international scientific research and monitoring station made in 1998, the very high significance of conflict between the local air pollution from station operations and vessels and atmospheric monitoring activity was identified (Shears et al. 1998).

Besides the monitoring activities mentioned in the introduction local pollution may have influence on the results of aerosol and BC measurements.

SO_2 and NO_x emitted from local sources may lead to the alteration of fresh sea salt through partial depletion of chloride and replacement by sulphates and nitrates and thus affect the results of aerosol measurements made by several institutions in Ny-Ålesund (Virkkula et al. 2006; Weinbruch et al. 2012).

During the short-term measurement campaign in July 2011 concentrations of equivalent black carbon (EBC) two times higher than the common background summertime level were observed in Ny-Ålesund. According to the results from the ensemble empirical mode decomposition method and analysis of the dispersion and deposition patterns at Ny-Ålesund, about 60-70% of EBC was related to local emissions and they mainly affect the area within 10 km around the settlement (Zhan and Gao 2014).

On the other hand, the long-term monitoring projects such as BC measurements from 1998 to 2007 made by Eleftheriadis, Vratolis, and Nyeki, 2009 show that only 0.2% of all episodes were attributed to local pollution cases which is correlated with the seasonal Arctic circulation pattern described in the beginning of the first chapter. However, the number of such cases might rise if the local anthropogenic influence would increase or decrease resulting to the misinterpretations of the records. However, Weinbruch et al. 2012 suggested that the summer cruise ship traffic in the Ny-Ålesund result to short-term BC peaks only, which can be separated from the general seasonal pattern.

The local power plant, cruise ships, vehicles such as snowmobiles and cars and aircraft are sources of atmospheric pollutants in Ny-Ålesund. Additionally, occasional emissions from the construction work cause considerable local atmospheric pollution of NO_x, dust particles and HC (Shears et al. 1998).

However, all kinds of activity in Ny-Ålesund have seasonal variation. Due to absence of sunlight, cold temperatures and snow cover, the scientific fieldwork and excursions as well as building work are limited in the winter time. Therefore in December and January most of people staying in Ny-Ålesund overnight are employed by Kings Bay A/S only to maintain requisite services, and the population of the village decreases by times (Shears et al. 1998).

Thus the autocorrelation between source of pollution and atmospheric chemistry is present making the local pollution more important source in summer and long-range in winter and spring.

In accordance to the local activity trend, the aircraft traffic is also changing seasonally. Currently the flight schedule of Kings Bay A/S includes only 2 flights a week from the January to the end of April and 4 flights a week from the end of April to the end of September (source http://kingsbay.no/visitor_information/flight_schedule/).

The number of airplane and helicopter landings; diesel and petrol consumption in m^3; overnight stays and research days for the period from 2001 to 2013 are shown in Figure 9 (Kings Bay A/S's statistics).

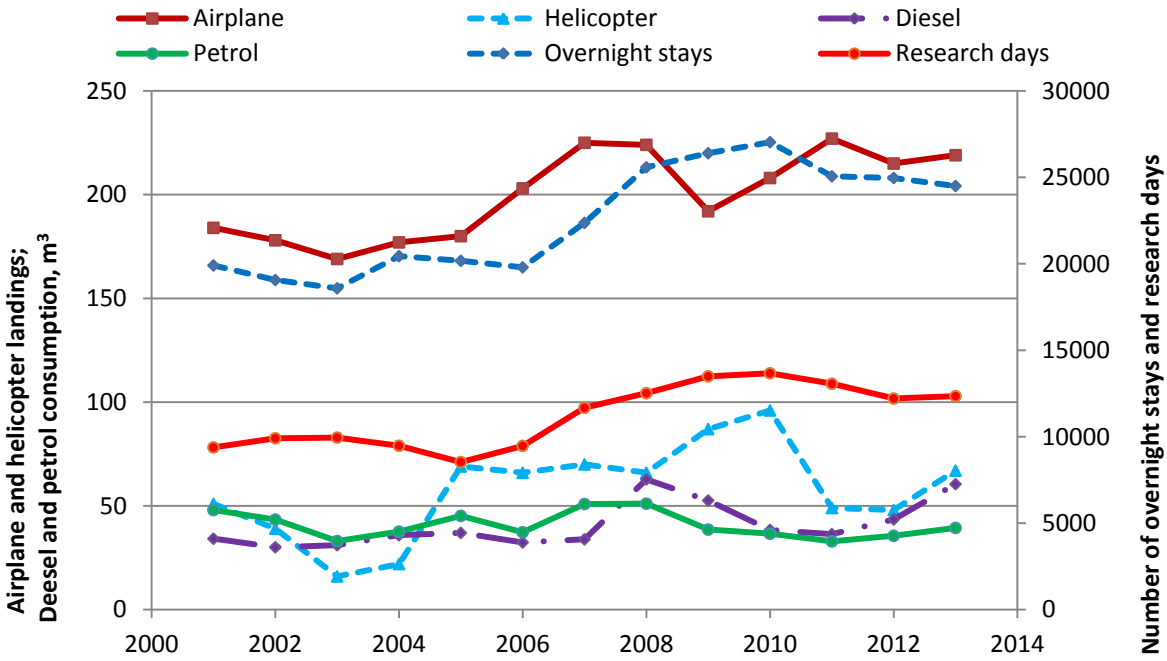

Figure 9 The number of airplane and helicopter landings; diesel and petrol consumption in m^3; overnight stays and research days (2001-2013)

The number of people staying overnight in Ny-Ålesund was increasing from 2003 then the steeper increase in 2006-2008 and the value fluctuating around 25000 for the last 5 years can be observed. The number of research days shows similar trend but the value is around half of the total overnight stays for all years. In general, there are no precautionary

limits set for the amount of people staying in Ny-Ålesund, and it depends on the planned construction and maintenance work in Ny-Ålesund and research projects. The number of helicopter landings in 2010 (96) was six times higher than in 2003 and was the largest for the period from 1996 to 2012. In 2011 it decreased significantly again from 96 to 49 (Sander et al. 2006, Kings Bay A/S's statistics).

The dependence of different parameters from the number of overnight stays for the period from 2001 to 2013 shows that the correlation exists only between number of overnight stays airplane landings, diesel consumption for vehicles and helicopter landings with the correlation coefficient R^2=0.4977, 0.4533 and 0.426, respectively, while petrol usage and diesel for power plant do not correlate with number of overnight stays at all (R^2=0.011 and 0.0093, separately). This means that the latter values are independent on number of people staying in the village. For the power plant it can be explained by seasonal pattern of fuel consumption and the trend of petrol consumption illustrates that it is changing slightly due to individual usage for motorboats and snowmobiles during the leisure time.

The consumption of diesel for cars and machines is determined by the activities taking place. One can see in Figure 10 that the elevated amount of fuel was utilised during summer 2008. The value reveals a large building work with extensive use of vehicles (Kings Bay A/S's statistics). The amount of diesel was twice higher than one used for construction activity in 2005 (Sander et al. 2006, Kings Bay A/S's statistics). In general, the monthly mean curve of the fuel consumption reflects seasonality of the diesel vehicle usage in the village.

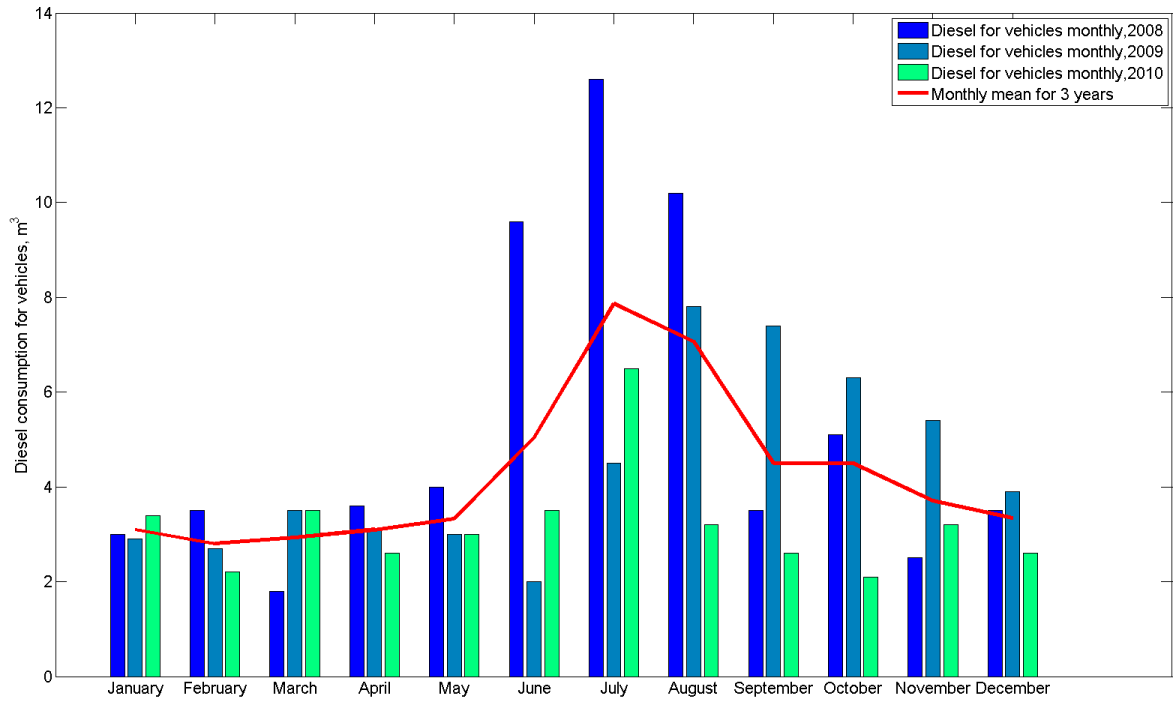

Figure 10 Monthly values of diesel consumption for vehicles for three years (2008-2010)

The combustion of petrol, which is mostly utilised by snowmobiles and motor boats in Ny-Ålesund, is a source of volatile organic compounds and CO (Shears et al. 1998). According to the "Environmental Impact Assessment of the Research Activities in Ny-Ålesund 2006", there were approximately 49 snowmobiles and 19 small open motorboats in 2005. The two-peak shape of the monthly mean curve of the petrol consumption in Figure 11 corresponds to the spring snowmobile season and summertime when motorboats are very often in use (Kings Bay A/S's statistics). This correlates also with the data represented in (Sander et al. 2006). However, one can see that the petrol use in 2008 seems to be very different to other years.

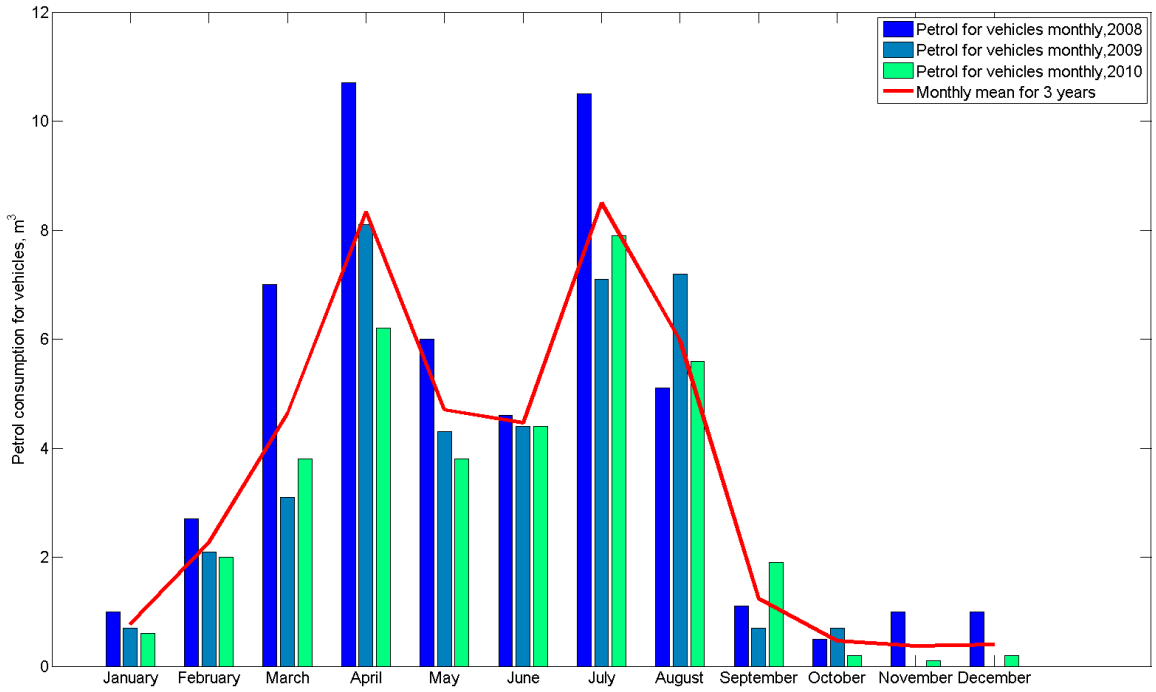

Figure 11 Monthly values of petrol consumption for vehicles for three years (2008-2010)

In the EIA 1998 the combustion of diesel fuel at the power station was stated as a major local source of PAHs, BC, NO_x, SO_2 and CO_2 (Shears et al. 1998). The installation of the cleaning module to reduce emissions of NO_x and SO_2 was recommended both in the EIA 1998 and the EIA 2006 (Sander et al. 2006; Shears et al. 1998) but has thus far not happened. When the local influence will be reduced it may lead to misinterpretations in the research if we don't know how often the local pollution disturbs the background monitoring results now without cleaning.

The energy consumption slightly increased comparing to one mentioned in the EIA 1998 (100 m^3 per month in winter and 60 m^3 in summer), and the mean value for winter and for summer 2008-2010 was approximately 110m^3 and 70m^3, respectively. The reason for this is a new energy demanding marine laboratory opened in June 2005. One can see in Figure 12 that the monthly trend of diesel consumption for the power plant shows that despite the winter minimum of human activity in Ny-Ålesund, the energy need is the highest in order to maintain the temperature inside the houses on an appropriate level (Kings Bay A/S's statistics).

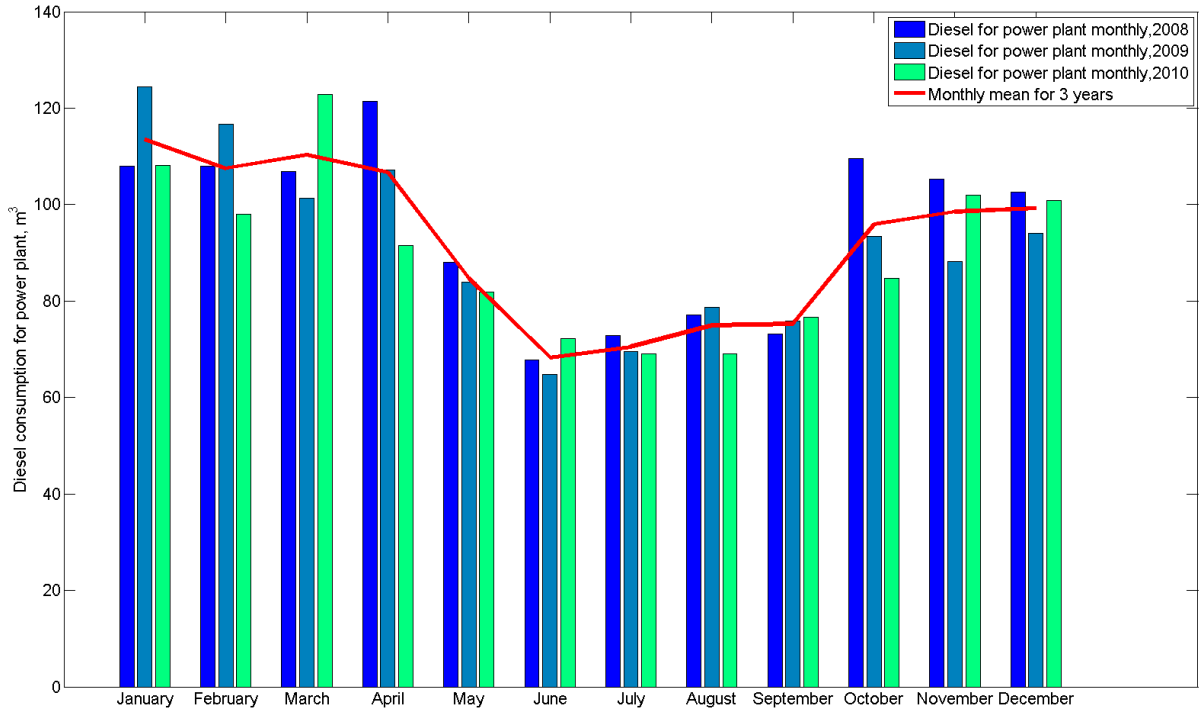

Figure 12 Monthly values of diesel consumption for the power plant for three years (2008-2010)

The power station located in the north of the settlement is the biggest source of NO_x in Ny-Ålesund. Therefore when measured wind in Ny-Ålesund contained prevailing N-component (e.g. N and NNW-direction) and values of the nitrous compounds were higher it could be an evidence of local impact of the power station (Beine et al. 1996).

According to the calculation of fuel consumption in Ny-Ålesund in 2002 presented in the EIA 2006, the power station is the main local fuel consumer and the second largest consumer is shipping (Sander et al. 2006).

From the number of landings of cruise tourists on Svalbard shown in Figure 13 one can see that among all destinations around Svalbard Ny-Ålesund is the most attractive for tourists nowadays (Ingerø 2010).

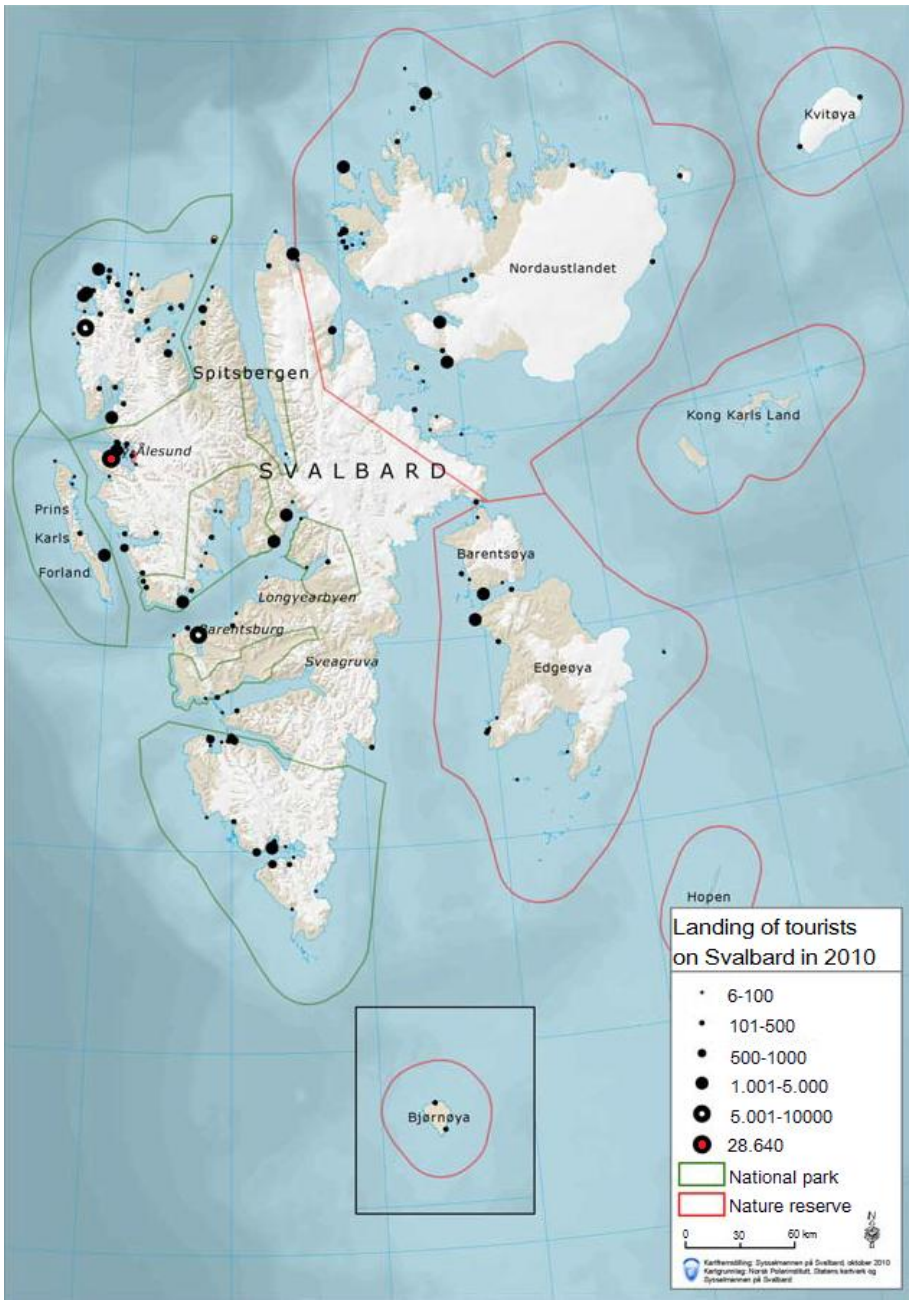

Figure 13 Landing of cruise tourists on Svalbard 2010 (Ingerø 2010)

Despite the situation may change after the ban of crude oil usage in Ny-Ålesund in 2015 the influence of the ship traffic in Ny-Ålesund on the atmospheric data quality is, indeed, a relevant topic of research. Several articles have touched on this problem. Two examples are given below.

Despite the limited number of samples the electron microscopy study of the chemical composition of aerosol particles collected at Zeppelin Mountain revealed that the soot internally mixed with secondary aerosol was observed during the field campaign in July and August 2007 exclusively when cruise ships were present around Ny-Ålesund (Weinbruch et

al. 2012).

The most resent paper based on long-term monitoring results brought out that the ships emissions raised the total summer mean concentrations of SO_2, 60 nm particles and EBC measured at the Zeppelin station by 15, 18 and 11 %, severally (Eckhardt et al. 2013).

Moreover, the intensification of the big vessels traffic is problematic because they produce enormous amount of emissions of most pollutants such as SO_2, NO_x, volatile organic compounds (VOCs) and BC comparing to the power plant. For example, the rate of cruise ship emissions per hour is more than 25 times higher for NO_x and more than 40 times higher for SO_2. The small ships emissions rate is comparable to the power plant (Sander et al. 2006; Shears et al. 1998).

The border of 200 passengers over board (pax) to assess the size of the ship has been chosen by the Kings Bay A/S because only vessels that have less than 200 passengers may circumnavigate Svalbard (Ingerø 2010). The number of calls by cruise ships with >200 pax varies from year to year with an average value of 32 per year according to the data for the time period from 2004 to 2013 (Kings Bay AS' statistics).

The data for 3 years (2008, 2009 and 2010) received from Kings Bay AS have been used for assessment of ship traffic influence on values of SO_2 and NO_x. One can see in Figure 14 that the total number of passengers on ships visiting Ny-Ålesund was approximately the same during summer 2008 (total 27379), summer 2009 (total 30647) and summer 2010 (total 30377), however, some ships have been anchored and some have come directly to the Ny-Ålesund harbour (Kings Bay A/S's statistics).

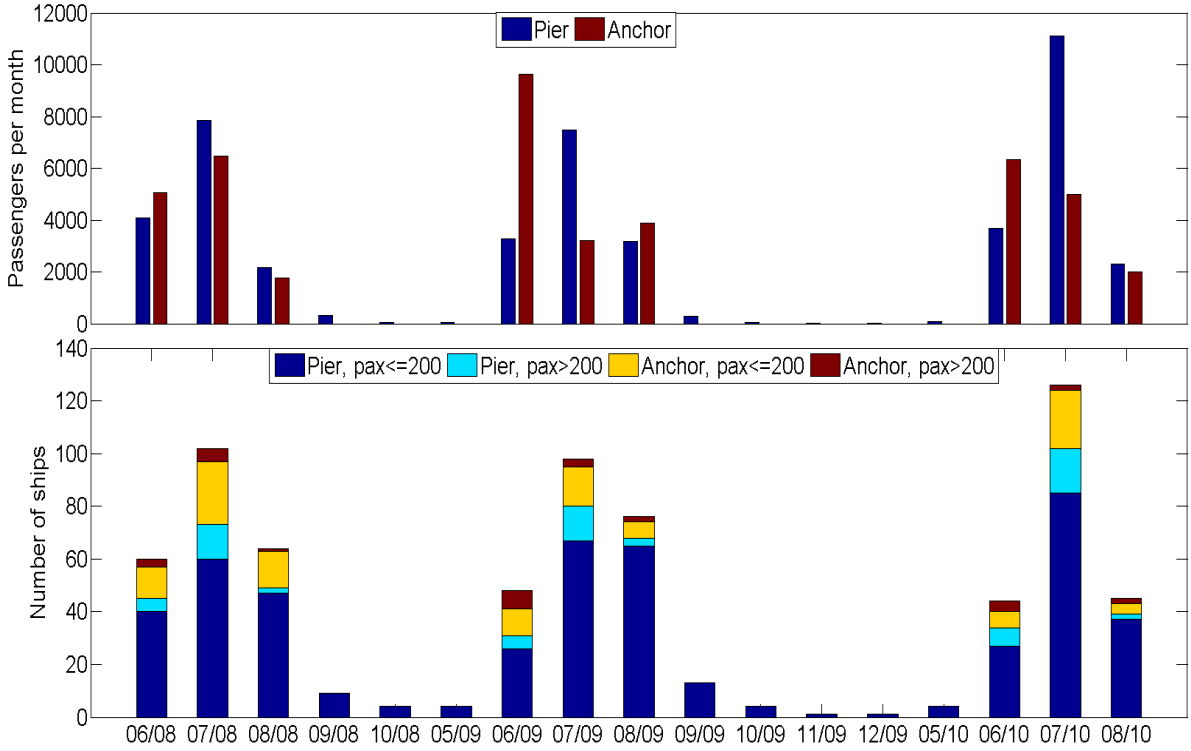

Figure 14 Number of passengers per month and ships attached to pier and anchored

Most of ships have less than 200pax. The number of big ships (pax >200) is highest in July and lowest in August for summer 2008, 2009 and 2010.

The data about exact location of anchored ships and meteorological data from these places were absent but the possible influence of the anchored ships on air quality measured results should be taken into consideration as well.

The data show that the ship traffic usually begins in May and stops in December. However, rapid increase in amount of ships is observed every year during June, July and August. Big ship with pax >200 appear only during summer months. Therefore the measurement results in Ny-Ålesund can be influenced by this source of pollution more frequent during summertime.

2 Atmospheric stability, turbulence and local pollution

In order to find out what are favourable conditions for the influence of local pollution cases on ground level measurements in Ny-Ålesund and at the Zeppelin mountain station, the example of plume geometry and evolution in time and space should be described.

The power plant as well as an individual ship stack can be considered as an elevated continuous point source. A typical geometry of the plume from such source and pollution dispersion are shown in Figure 15.

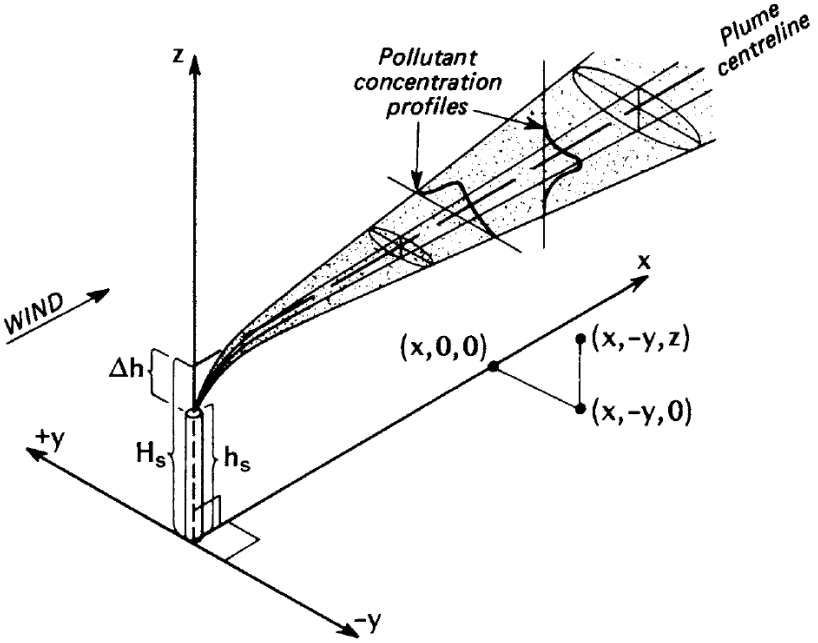

Figure 15 Example of plume spreading from an elevated point source (Oke 2002)

The effective stack height (H_s) there consists of the stack height (h_s) and the additional height of the plume rise (Δh) (Oke 2002):

$$H_s = h_s + \Delta h \tag{30}$$

The ground-level concentrations of pollutants downwind near the point of release are inversely proportional to h_s. The Δh depends on the outflow velocity and the temperature of the released gases as well as prevailing meteorological conditions such as wind speed and lapse rate.

One can see in Figure 16 widely used curves showing Pasqill's turbulent types as a function of the Monin-Obukhov stability length L and the aerodynamic roughness length z_0 (Hanna, Briggs, and Hosker 1982; Lyons and Scott 1990).

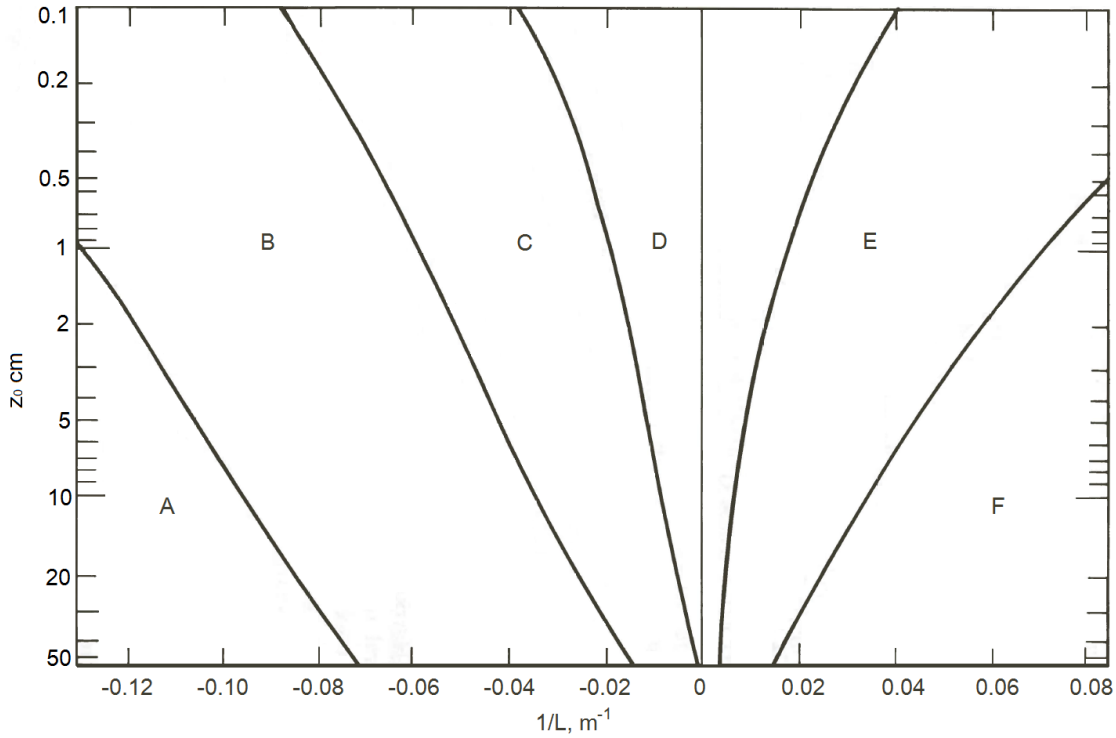

Figure 16 Pasqill's turbulent types as a function of the Monin-Obukhov stability length and the aerodynamic roughness length (A, extremely unstable conditions; B, moderately unstable conditions; C, slightly unstable conditions; D, neutral conditions (applicable to heavy overcast day or night); E, slightly stable condition; F, moderately stable conditions) (Lyons and Scott 1990).

The calculation of the Monin-Obukhov stability length L and the aerodynamic roughness length z_0 is shown further in this chapter.

A buoyant plume raises vertically under the calm winds conditions (Lyons and Scott 1990)

$$\Delta h = 5.3{F_0}^{1/2}s^{-3/8} - 6R_0, \tag{31}$$

where the environmental stability is

$$s = \frac{g}{\mathrm{T}_e}\left(\frac{d\mathrm{T}_e}{dz} + 0.0098\mathrm{C}^{\circ}/\mathrm{m}\right), \tag{32}$$

and initial buoyancy flux is

$$F_0 = \frac{g}{\mathrm{T}_{p0}}\left(\mathrm{T}_{p0} - \mathrm{T}_{e0}\right)w_0{R_0}^2 \tag{33}$$

w_0 and R_0 are the initial plume vertical speed at stack exit and plume radius in a plane perpendicular to the plume axis, respectively; $g = 9.81 m/s^2$ in equations 3 and 4 is the gravitational acceleration. Indexes e, p and 0 are environment, plume and initial values.

The formula for the final rise of a buoyant bent-over plume when the plume rise is

limited by ambient stability is following (Hanna et al. 1982)

$$\Delta h = 2.6 \left(\frac{F_0}{us}\right)^{1/3}, \tag{34}$$

where the wind speed u is the average value between the heights hs and hs + Δh which can be estimated from a measured wind speed at 10 m (u_{10}) and the parameter *p* from the Table 1

$$u(z) = u_{10} \left(\frac{z}{10}\right)^{p} \tag{35}$$

Table 1 Parameter p for estimating the wind speed as a function of stability (see Figure 16) and formulas for horizontal and vertical standard deviations of the pollutant distribution in the *y* and *z* directions σ_y *(x),* σ_z *(x)* where $10^2 < x < 10^4$ m is horizontal distance from the source

Stability class	p (rural area)	σ_y (m) (open-country conditions)	σ_z (m) (open-country conditions)
A	0.07	$0.22x(1+0.0001x)^{-1/2}$	$0.20x$
B	0.07	$0.16x(1+0.0001x)^{-1/2}$	$0.12x$
C	0.10	$0.11x(1+0.0001x)^{-1/2}$	$0.08x(1+0.0002x)^{-1/2}$
D	0.15	$0.08x(1+0.0001x)^{-1/2}$	$0.06x(1+0.0015x)^{-1/2}$
E	0.35	$0.06x(1+0.0001x)^{-1/2}$	$0.03x(1+0.0003x)^{-1}$
F	0.55	$0.04x(1+0.0001x)^{-1/2}$	$0.016x(1+0.0003x)^{-1}$

The buoyant, bent-over plume rise determined by ambient turbulence in nearly neutral conditions can be calculated as (Hanna et al. 1982)

$$\Delta h = 1.54 \left(\frac{F_0}{u{u_*}^2}\right)^{2/3} {h_s}^{1/3}, \tag{36}$$

where u_* is the friction velocity. The formula for calculation of u_* is shown is shown further in this chapter.

The plume-rise observations in unstable conditions are the least reliable due to rapid dilution.

However, following formula has been suggested by (Hanna et al. 1982)

$$\Delta h = 3 \left(\frac{F_0}{u}\right)^{3/5} H^{-2/5}, \tag{37}$$

where the surface buoyancy flux $H = \frac{g}{T}\frac{H_0}{\rho c_p}$ is proportional to the kinematic heat flux $\frac{H_0}{\rho c_p}$ (for further details see (Hanna et al. 1982))

Both vertical plume and bent-over plume can penetrate the inversion under certain conditions:

1) for vertical buoyant plume

$$z_{el} < 4.9{F_0}^{2/5}\left(\frac{g}{\theta_a}\Delta\theta_i\right)^{-3/5}, \quad (38)$$

where z_{el} is a height above the stack; $\Delta\theta_i$ is the jump in the potential temperature and $(g/\theta a \Delta \theta i$ is the inversion strength;

2) for bent-over plume

$$z_i < 2.5\left\{\frac{F_0}{[u(g/\theta_a)\Delta\theta_i]}\right\}^{1/2}, \quad (39)$$

where z_i is the inversion height.

The distribution of pollutant concentrations in Figure 15 is shown in the three-dimensional co-ordinate system and assumed to be the Gaussian both in the horizontal and vertical. Despite this is a simplification and the instant plume edges are wandering, it is allowable approximation because the time averaging (over time periods longer than 10 minutes) makes the shape of the plume evener and the concentration distribution closer to normal. The breadth of the plume is increasing and the relative concentration is decreasing downwind of the source (Oke 2002; Seinfeld and Pandis 2006).

Using the effective stack height H_s (m) one can calculate the concentration of pollution χ in kgm^{-3} (μgm^{-3}) at any point in a plume (Oke 2002)

$$\chi_{(x,y,z,H)} = \frac{X}{2\pi\sigma_y\sigma_z\bar{u}} exp\left[-\frac{y^2}{2{\sigma_y}^2}\right] \times \left[exp\left(-\frac{(z-H_s)^2}{2{\sigma_z}^2}\right) + exp\left(-\frac{(z+H_s)^2}{2{\sigma_z}^2}\right)\right] \quad (40)$$

where, X-rate of emission from the source (kgs^{-1}), σ_y, σ_z,—horizontal and vertical standard deviations of the pollutant distribution in the *y* and *z* directions (m) (see Table 1), $\bar{u}$—mean horizontal wind speed through the depth of the plume (ms^{-1}).

The rate of emissions from different activities at Ny-Ålesund is shown in Table 2 (calculated using data from Table 4 in Shears et al. 1998)

Table 2 Emissions from different activities at Ny-Ålesund (calculated from Shears et al. 1998)

	SO_2-S,·10^{-5} kgs^{-1}	NO_x,·10^{-5} kgs^{-1}
Diesel generators	9.72	111.11
Central heating	6.39	5.56
Snowmobiles and small boats	0	0.14
Diesel cars and heavy equipment	1.67	17.78
Small ships	6.94	83.33
Cruise ships	722.22	3888.89

The values at ground-level (i.e. *z*=0) can be calculated using following equation

$$\chi_{(x,y,0,H)} = \frac{X}{2\pi\sigma_y\sigma_z\bar{u}} exp\left[-\left(\frac{y^2}{2{\sigma_y}^2} + \frac{{H_s}^2}{2{\sigma_z}^2}\right)\right] \quad (41)$$

and compared with the monitor values available from the project Local Air Quality Monitoring 2008-2010 in Ny-Ålesund.

The Gaussian plume model is valid for simulation of the continuous emissions of inert nearly weightless pollutants (gases and particles with diameter< 20 μm) from a point source consist over distances from a few hundred metres to 10 km downwind from the source (Oke 2002). These conditions imply following limitations (Lyons and Scott 1990):

1) all of the material emitted is present in the plume (continuity is kept) which is far from reality due to various chemical reactions which can occur inside the plume, and moreover, multiple sources located in close vicinity, e.g. cruise ships and power plant, may lead to cumulative pollution and the production of secondary pollutants downwind (Oke 2002);

2) the assumption of constant wind speed with height that can cause a significant error in presence of strong wind shear often observed in the Arctic under stable conditions (Mäkiranta et al. 2011);

3) the assumption of constant wind direction at the surface in the xy-plane which often cannot be applied due to presence of sea breeze in the vicinity of the shore, mountainous landscape in Ny-Ålesund leading to channelling of the wind and katabatic winds from glaciers; besides even over a comparatively short periods of an hour or more the wind direction variations may be 30–45° from the mean wind direction (Oke 2002);

4) the dispersion parameters σ_y and σ_z are dependent of z and aerodynamic roughness length z_0 which in turn depends on the terrain type (the characteristic numbers for Ny-Ålesund could be different depending on the season from z_0=0.0002 (snow-covered flat plain) to z_0=0.03 (tundra) (Wallace and Hobbs 2006));

5) to represent the change of wind direction with height above the first 30m of the atmosphere the Ekman spiral vertical profile shown in Figure 17 should be used instead of logarithmic wind profile (Lyons and Scott 1990).

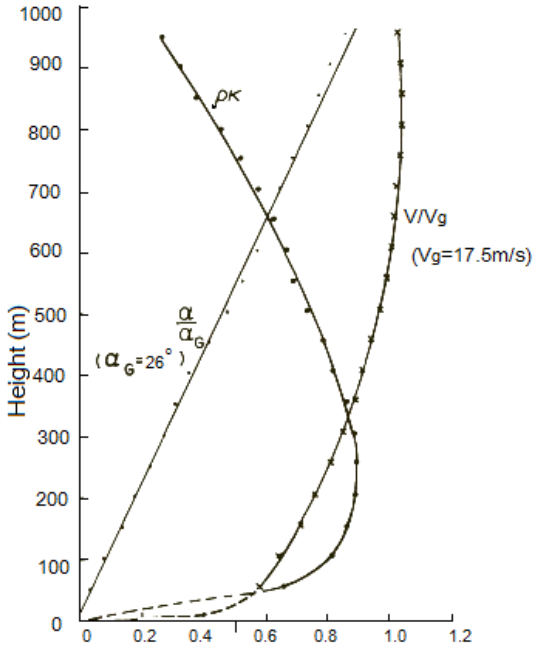

Figure 17 The Leipzig vertical profile of wind and eddy viscosity (Lyons and Scott 1990)

The resultant horizontal wind speed V, the geostrophic wind speed V_g, the change of wind direction from the surface value *a*, the geostrophic direction a_g, the exchange coefficient $A = \rho K$, the relative wind profile u/u_g and specific volume a/a_g are the values shown in Figure 17.

The general form of the wind profile with height can be described by following equations

$$\overline{u}(z) = \overline{u}_g(1 - e^{-az}\cos az) \tag{42}$$

$$\overline{v}(z) = \overline{u}_g\, e^{-az}\sin az \tag{43}$$

where geostrophic wind can be determined from

$$\overline{u}_g = \frac{-1}{f\rho}\frac{\partial p}{\partial y} \tag{44}$$

and parameter a depends on the Coriolis parameter f and a molecular kinematic viscosity K_M (in order of m^2/s) as

$$a = \left(\frac{f}{2K_M}\right)^{1/2} \tag{45}$$

where $f = 2\Omega \sin\varphi$ is the is the Coriolis parameter ($\Omega = \frac{2\pi}{24\cdot 60\cdot 60} = 7.272 \cdot 10^{-5}$ rad/sec is the angular velocity of rotation of the Earth and φ=78.55 is the latitude of Ny-Ålesund).

The northerly flow regime both at Zeppelin and Ny-Ålesund is thought to have higher possibility to bring the local pollution from the power plant or from the harbour, however, the

influence of wind direction turning with height has not yet been discussed (Beine et al. 2001).

One can see that effective stack height calculation and the concentration of pollutants can be very complicated especially taking into account the specific meteorological conditions in the Arctic and possible presence of several sources of pollution located in the same place. Hence this can be done in further work and the result of the modelling can be compared with the measured value.

However, knowing that the planetary boundary layer (PBL) stratification and the turbulence intensity (by analogy with the turbulence types shown in Figure 16) determine the effectiveness of local dispersion one can access and investigate the stability of the atmosphere and make some considerations about possibility of influence of local pollution on Zeppelin station (Beine et al. 2001).

In the previous studies of influence of local pollution on Zeppelin measurements the static stability index has been suggested as the quantity of the PBL stratification and the effect of low wind speed on pollution concentration has been noted as well, however, no joint characteristic taking into consideration both these values has not been proposed (Beine et al. 1996; Eckhardt et al. 2013).

The static stability index S_z (by analogy with the the environmental stability s from equation 32) can be estimated by equation (Beine et al., 1996)

$$S_z = \frac{1}{\theta}\frac{d\theta}{dz} = \frac{1}{T}(\Gamma_d - \Gamma) \tag{46}$$

where θ is the potential temperature, T is the temperature, z is altitude, Γ_d and Γ are the dry adiabatic and measured lapse rate, respectively.

The temperature an air parcel would have if it were brought down to a sea-level pressure adiabatically from its primary position is called potential temperature θ (Arya 1999). In turn potential temperature can be determined from (Seinfeld and Pandis 2006)

$$\theta = T\left(\frac{p_0}{\mathrm{p}}\right)^{R/c_p M_{air}} = T\left(\frac{p_0}{\mathrm{p}}\right)^{k} \tag{47}$$

where p_0 and p are pressure at the surface and at the altitude z, respectively; R is the is the gas constant of air; c_p is the specific heat capacity of air with the constant pressure, M_{air} is molecular weight of dry air, $k = R/c_p M_{air} \cong 0{,}286$.

Local pollution cases in Ny-Ålesund usually occur when wind speed (average 2 ms^{-1}) and atmospheric stability are low (S_z=0,02-0,16 and average 0,08) during periods of surface inversion (Beine et al., 1996). Such conditions prevent dispersion, and therefore local pollution is generally characterized by higher levels of compounds than long-range transport.

This was concluded also during Environmental impact assessment of Ny-Ålesund (Shears et al., 1998).

However, the stability index S_z alone cannot be an appropriate measure of turbulence, because it contain no information on the mechanical wind generated turbulence (Arya 1999). In general the higher wind speed the higher is the momentum flux and thus turbulent eddy diffusion is pronounced. Besides, there is negative interdependence between the concentration of pollutants per unit volume of air passing the stack exit per unit time and the wind speed (Oke 2002).Therefore the parameter including both buoyancy and mechanical production of turbulence is needed. The Richardson number widely used in the micrometeorology is therefore an appropriate characteristic.

The Richardson bulk number Ri_B and gradient Richardson number Ri_m are the approximations used in this study.

The gradient Richardson number can be calculated as (Arya 1999)

$$Ri_m = \frac{g}{T_0}\frac{\overline{\Delta\theta} z_m}{\overline{\Delta u}^2}\ln\left(\frac{z_2}{z_1}\right), \tag{48}$$

where T_0 is the mean temperature for the heights z_1 and z_2; $z_m = (z_1 \cdot z_2)^{1/2}$ is the geometric mean height; $\overline{\Delta\theta}$ and $\overline{\Delta u}$ are the potential temperature and the wind speed differences between two heights.

Friction velocity and friction temperature can be calculated as

$$u_* = \frac{k\overline{\Delta u}}{[\varphi_m(z_m/L)\ln(z_2/z_1)]}, \tag{49}$$

$$\theta_* = \frac{k\overline{\Delta\theta}}{[\varphi_h(z_m/L)\ln(z_2/z_1)]}, \tag{50}$$

where $k = 0.4$ is von Karman's constant and u_* is the friction velocity and the stability dependent functions φ_m and φ_h are following (Arya 1999; Mäkiranta 2009):

$$\varphi_m{}^2 = \varphi_h = (1 - 16\zeta)^{-1/2} \quad \text{for } \zeta<0; \tag{51}$$

$$\varphi_m = \varphi_h = 1 + 5\zeta \quad \text{for } 0\leq\zeta<1; \tag{52}$$

$$\varphi_m = \varphi_h = 1 + 0.7\zeta + 0.75\zeta(6 - 0.35\zeta)exp(-0.35\zeta) \quad \text{for } \zeta>1; \tag{53}$$

where $\zeta = \frac{z_m}{L}$ is the stability parameter.

The kinematic surface stress and the kinematic heat flux can be calculated as following

$$\frac{\tau_0}{\rho} = u_*{}^2 \tag{54}$$

$$\frac{H_0}{\rho c_p} = -\theta_* u_* \tag{55}$$

The gradient Richardson number is related to the Monin-Obukhov stability length L in following way

$$\frac{z_m}{L} = Ri_m\,, \qquad \text{for } \mathrm{Ri_m}<0; \tag{56}$$

$$\frac{z_m}{L} = \frac{Ri_m}{(1-5Ri_m)}\,, \qquad \text{for } 0\leq \mathrm{Ri_m}<0.2 \tag{57}$$

From these values the Monin-Obukhov stability length L can be determined as

$$L = \frac{{u_*}^2}{k(g/\mathrm{T_0})\theta_*} \tag{58}$$

or $$L = \frac{z_m}{Ri_m}\,, \qquad \text{for } \mathrm{Ri_m}<0; \tag{59}$$

and $$L = \frac{z_{m(1-5Ri_m)}}{Ri_m}\,, \qquad \text{for } 0<\mathrm{Ri_m}<0.2 \tag{60}$$

The adopted integrated forms of equations for the very stable boundary layer can be used (Mäkiranta 2009)

$$\psi_m = \psi_h = -0.7\zeta + 0.75\left(\zeta - \frac{5}{0.35}\right)exp(0.35\zeta) + \frac{3.75}{0.35} \tag{61}$$

while for unstable conditions

$$\psi_m = 2\ln\left[\frac{1+X}{2}\right] + \ln\left[\frac{1+X^2}{2}\right] + \frac{\pi}{2} - 2\tan^{-1}X \tag{62}$$

and $$\psi_h = 2\ln\left[\frac{1+Y}{2}\right] \tag{63}$$

where $\mathrm{X} = {\varphi_\mathrm{m}}^{-1} = (1-16\zeta)^{1/4}$ and $Y = {\varphi_\mathrm{h}}^{-1} = (1-16\zeta)^{1/2}$.

Introducing ψ_m into the logarithmic wind profile equation, the surface roughness calculation for non-neutral conditions can be corrected as (Mäkiranta 2009)

$$z_0 = \frac{z}{\exp\left(\frac{kU}{u_*}+\psi_m\right)} \tag{64}$$

The alternative version is the for the dynamic stability calculation is the bulk Richardson number used for the assessment of the profile measurements (Wallace and Hobbs 2006)

$$Ri_B = \frac{g}{\overline{\mathrm{T}_v}}\frac{\overline{\Delta\theta}_v\Delta z}{(\Delta U)^2+(\Delta V)^2}, \tag{65}$$

where $\overline{\mathrm{T}_v}$ is the average virtual potential temperature across the whole layer and ΔU and ΔV are the virtual potential temperature and the wind speed differences between two heights, Δz is the heights difference. In the absence of the humidity data the average temperature $\overline{\mathrm{T}}$ across whole layer and the potential temperature difference between two heights $\overline{\Delta\theta}$ are used instead of the $\overline{\mathrm{T}_v}$ and $\overline{\Delta\theta}_v$.

The equation 65 is used for because (Arya 1999) suggested that the gradient Richardson number is better to use when the ratio between two measurement heights is within 2-4. Otherwise the Ri_B has been used.

3 Analysis of the meteorological data

The description of the meteorological data available for the local pollution analysis is given below.

3.1 In situ meteorological data from Ny-Ålesund

The various measured meteorological parameters from different stations are available for Ny-Ålesund. In the thesis the data from stations located close to the monitors that measured NO_x and SO_2 in the village and to the Zeppelin station have been chosen and compared in order to investigate the micrometeorological features of the area crucial for understanding how local pollution may spread. The available meteorological data is shown in Table 3.

Table 3 Available meteorological data

№	Station name	Coordinates	Maintenance	Parameters*	Period
1	Monitor (Nordpolhotellet)	34m a.s.l. 78.9247 11.9262	Norsk institutt for luftforskning (NILU)	t_{air2m}, rH, U, Dir, p	03.09.2008 12:00-24.08.2010 12:00 (hourly data, 4% of data is missing)
2	Ny-Ålesund WMO station	8m a.s.l. 78.9230 N 11.9333 E	Norwegian Meteorological Institute (eKlima.no)	t_{air2m}, U_{10}, Dir, p	01.01.2008 00:00-31.12.2010 23:00 (hourly data, 2.5% of data is missing)
3	AWI station	11m a.s.l. 78.9231 N 11.9223 E	Alfred Wegener Institute for Polar and Marine Research	2m,10m: t_{air}, U, Dir	01.01.2008 01:00-31.12.2010 23:00 (hourly data, 11% and 0.2% of data is missing for 2m and 10m, respectively)
				Radiosonde soundings: h, t_{air}, U, Dir, p, rH	01.01.2008 10:49-30.04.2011 11:04 (daily data)
				Sunshine duration	01.01.2008 00:00-31.12.2010 23:00:00 (hourly data)
4	The Amundsen-Nobile Climate Change Tower (CCT)	50 m a.s.l. 78.9222 N 11.8689 E	The National Research Council of Italy (CNR)	3, 4.8, 10.3 and 33.4m: t_{air}, U, Dir	05.10.2009 00:30-31.12.2010 23:30 (hourly data, 2.3% of data is missing)
5	Zeppelin	474m a.s.l. 78.9073 N 11.8859 E	NILU	t_{air}, rH, U, Dir, p	01.07.2008 00:00-01.01.2011 00:00 (hourly data, 7% of data is missing)

* t_{air}-air temperature, °C, rH-relative humidity, %, U-wind speed, m/s, Dir-wind direction, °,

p-atmospheric pressure at measurement level, hPa, h-sounding height, sunshine duration-min

The Ny-Ålesund WMO station data were taken from e-klima.no portal from the web-page http://sharki.oslo.dnmi.no/portal/page?_pageid=73,39035,73_39049&_dad=portal&_schema=PORTAL.

The AWI local meteorological data (station 3) with 1-min measurement interval have been hourly averaged in order to comply with the data from the Monitor. A detailed description of the meteorological sensors used at the AWI station is given in the (Maturilli, Herber, and König-Langlo 2013). The AWI 10m and 2m measurements have been used to calculate the Richardson gradient number. The radiosonde data have been used to investigate the wind and temperature variation with height. The sunshine duration data was used to examine the influence of insolation on new particle formation process and results of aerosol measurements at the Zeppelin station.

The investigations of the planetary boundary (PBL) layer height estimations, temperature and heat fluxes, annual wind distribution and radiation budget are provided by the CCT station. The description of the instruments used at the station is given in p.38 of the CNR report about research activity in Ny-Ålesund 2011-2012 (Ciciotti et al. 2013). Despite the Table 3 shows that CCT measurements cover only part of the period of interest, the potential of using them for future local pollution analysis is explored in this study. The Richardson gradient number has been calculated for the 10.3 and 3m heights and compared it with the Ri_m from the AWI measurements.

The meteorological equipment used at the Zeppelin station is described in the (Beine et al. 2001).

The location of the measurement listed in the Table 3 stations is shown in Figure 18, and a closer view of the three station in Ny-Ålesund is given in Figure 19.

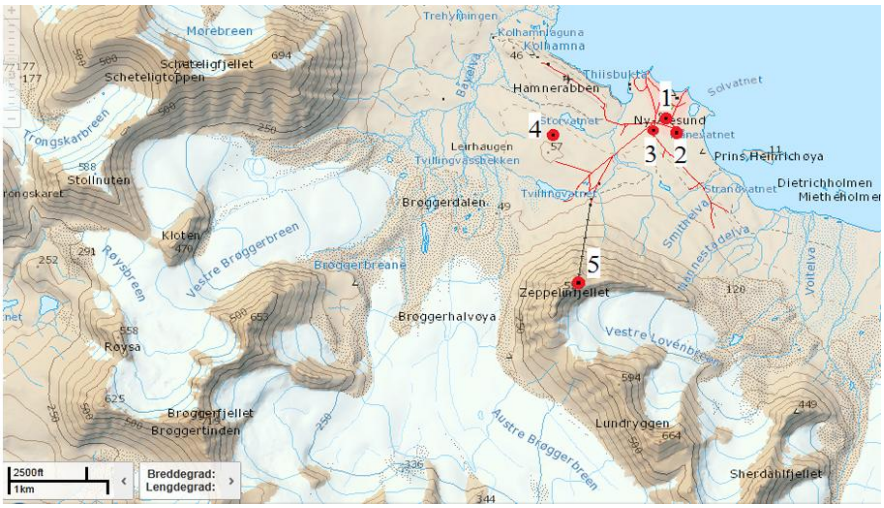

Figure 18 The meteorological stations in Ny-Ålesund

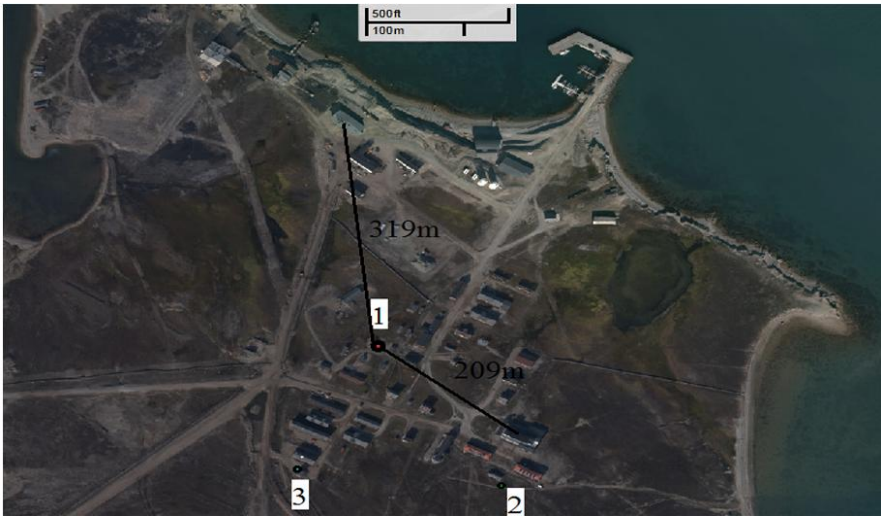

Figure 19 The meteorological stations and power plant and kitchen

The measured distances 209m and 319m in the Figure 19 correspond to the Ny-Ålesund's kitchen and power plant, respectively, which are two fixed sources of particles and gases. The station (1) was surrounded by small houses therefore shadowing affects on the wind measurements may result, however, the data from this station have been used when available for analysis of hourly monitor SO_2 and NO_x measurements because these sensors were placed together.

The wind roses from the monitor, WMO and AWI stations are shown in Figures 20, 21 and 22. All three wind roses show similar seasonal patterns characteristic for the wind climate in Kongsfjorden where the prevailing large scale easterly winds are altered by the mechanical channelling along the fjord, the flow from large glaciers on the south east side of the fjord and the thermal land-sea breeze circulation. The sea breeze is from north-northwest

(300°-330°), while the strongest winds aligned with the valley axis are from SE (Beine et al. 2001; Esau and Repina 2012).

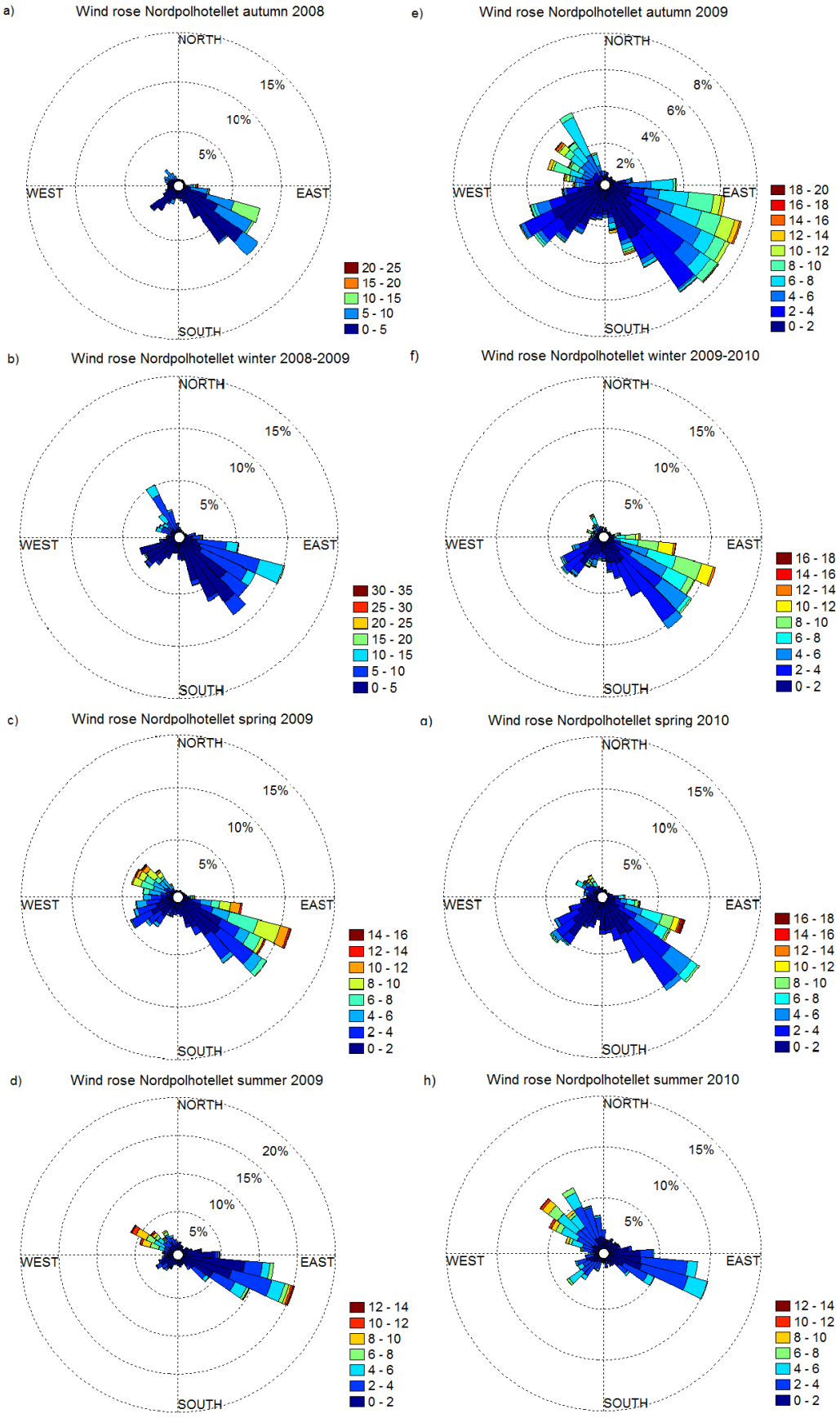

Figure 20 Wind roses monitor (Nordpolhotellet). Colours indicate wind speed (m/s)

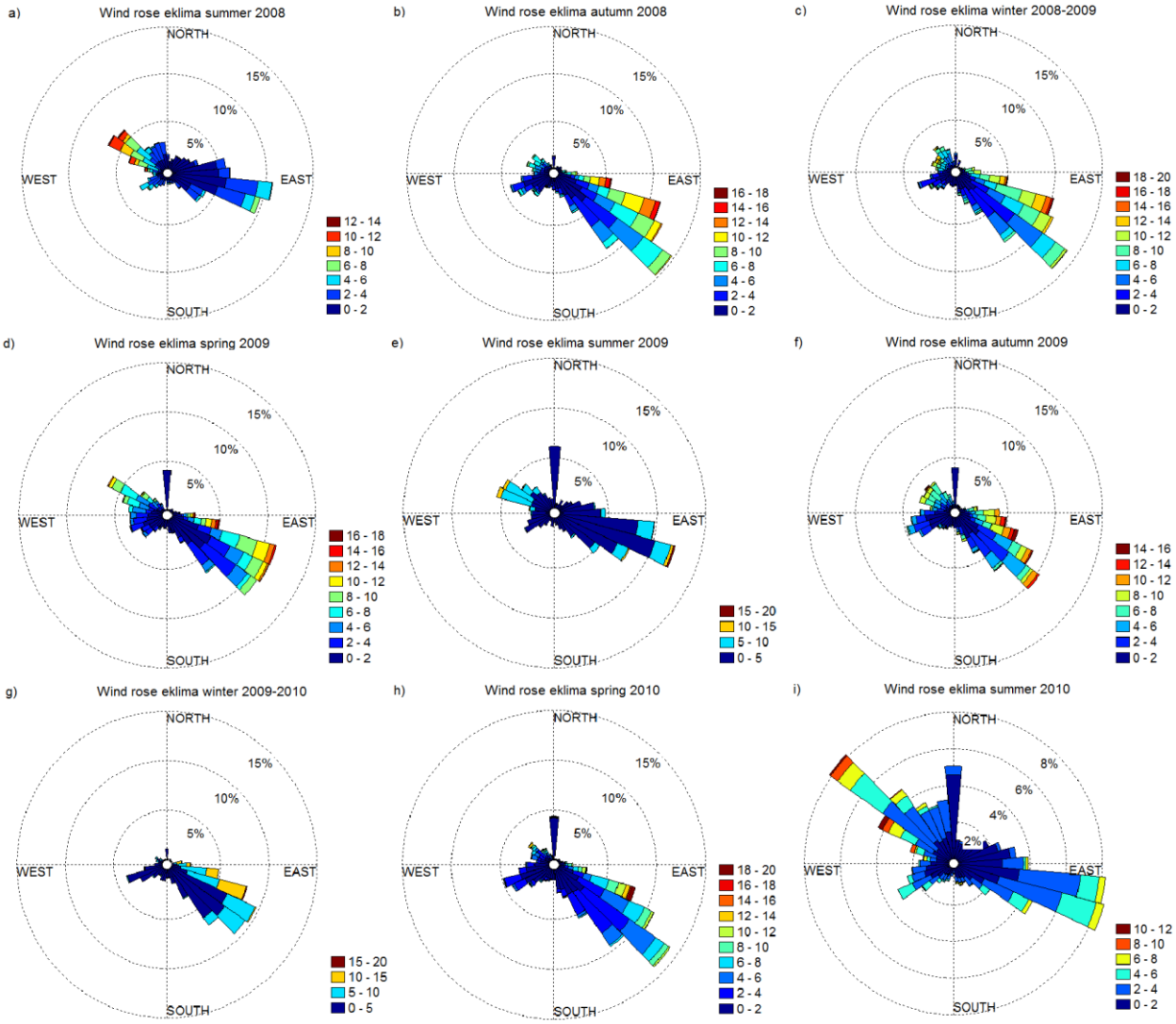

Figure 21 Wind roses Norwegian meteorological institute. Colours indicate wind speed (m/s)

From Figure 22 one can see that during summer time unstable conditions in the atmosphere are prevalent (Ri<0), while stable conditions are usual for winter and spring time (Ri>0). Autumn is a period of transition between the these two distinct seasons.

Similarity of the wind roses from the village locations allow to replace missing meteorological data from the Monitor with data from the WMO and AWI stations.

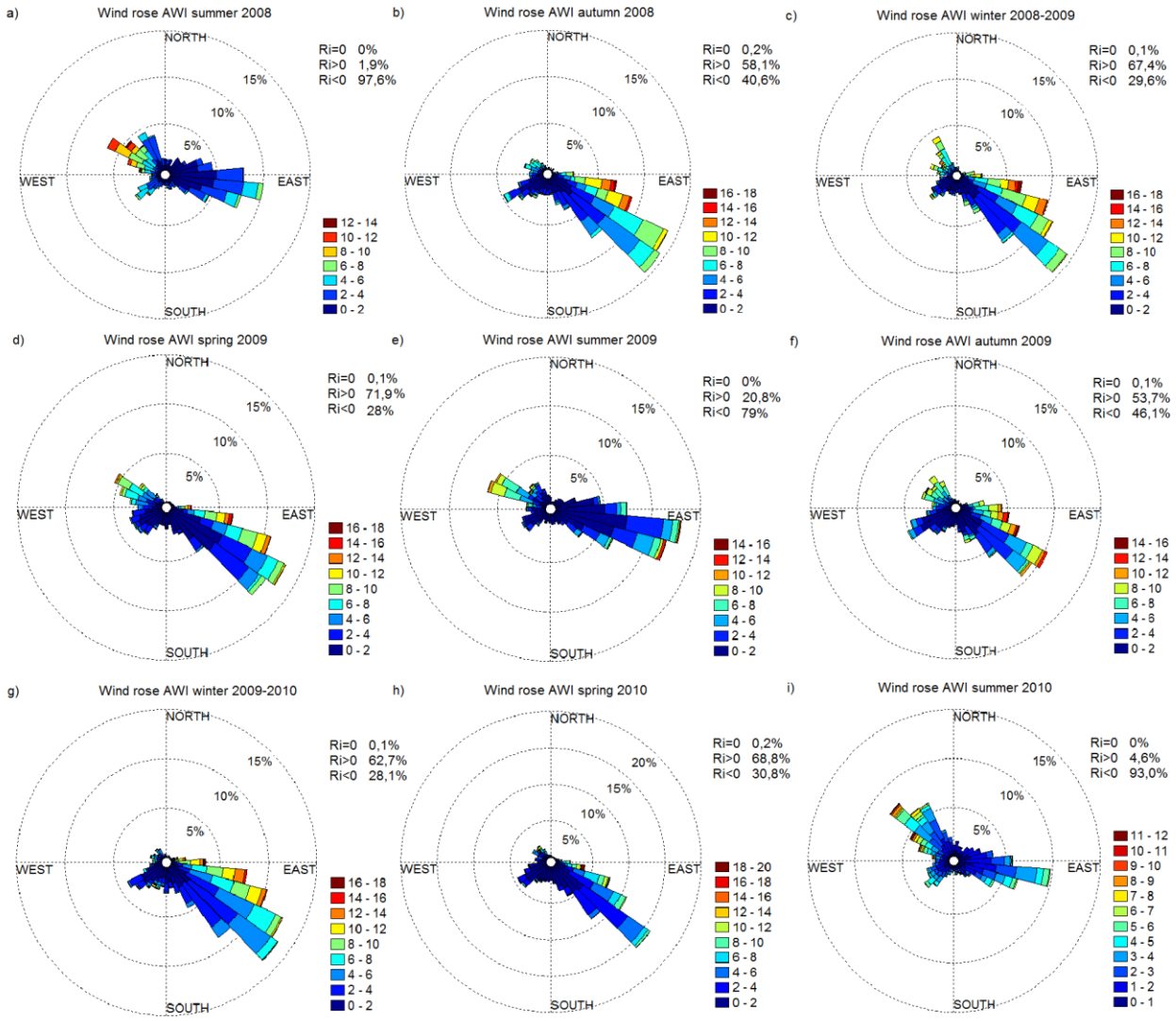

Figure 22 Wind roses AWI (10m). Colours indicate wind speed (m/s). Percentage of Ri=0, Ri>0 and Ri<0 is calculated for every season separately

The wind roses for the CCT station are shown in Figure 23. One can see that there is constant significant south-west component of wind which was not so pronounced in the roses from the monitor, WMO and AWI stations. If one recall the Figure 18 it becomes evident that this is the wind from Brøggerdalen formed by two flows from the nearest glaciers Vestre Brøggerbreen and Austre Brøggerbreen. From Figure 23 it is clear that the wind speed for SW directions is rarely higher than 6 m/s which is consistent with expected speeds of katabatic flows for Svalbard glaciers (Esau and Repina 2012). The wind roses consistent with previous results from the CCT station (Ciciotti et al. 2013, page 43).

The influence of the katabatic flow can be revealed also from the comparison of gradient Richardson number calculated from the CCT and AWI data for the same measurement period. The results show that stable stratification (Ri_m>0) occurs at the CCT

station and at the AWI station in 89% and in 52% of time, respectively. The cold air from the glacier near the CCT station prevent mixing while in the village sea-land breeze and large scale circulation produce more mixing. The seasonality in Richardson number value was not observed in CCT data and the atmospheric conditions were stable most of the time. Only during the summer 2010 the percentage of negative Richardson number increased because the NW sea breeze was observed more often than in previous periods.

Thus the usage of the CCT data with positive Ri_m values for the local pollution assessment at the Zeppelin station would lead to the misleading conclusion that Zeppelin is unaffected by the flow below.

However, for the particular hours when Ri_m at CCT were negative (6% of the data) the same result was received for AWI station. From this it is concluded that when unstable conditions occur at the CCT the same is valid for the village.

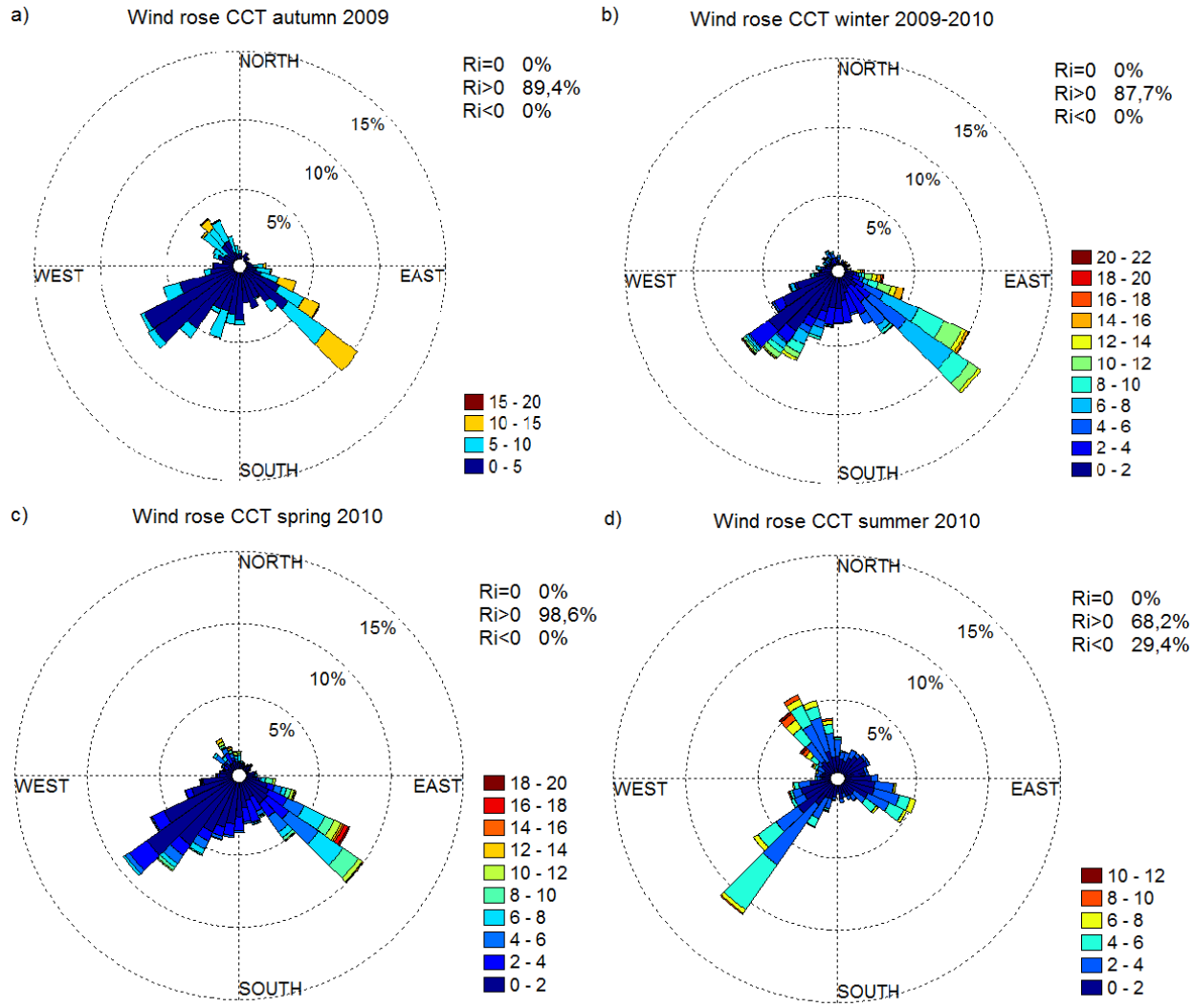

Figure 23 Wind roses CCT (10.3m). Colours indicate wind speed (m/s). Percentage of

Ri=0, Ri>0 and Ri<0 is calculated for every season separately

One can see from the Figure 24 that the meteorological conditions at Zeppelin mountain have significant differences with conditions in Ny-Ålesund. Because of local topography west and east wind are very rare at the station. This shadowing effect of the mountain has already been noticed in previous research papers (Beine et al. 1996; Eneroth et al. 2007; Heintzenberg and Leck 1994).

The prevailing wind directions at the Zeppelin station is S, SSE, and to a lesser extent NNW. However, despite less abundance the last one plays key role in assessing influence of local pollution from Ny-Ålesund on Zeppelin measurements.

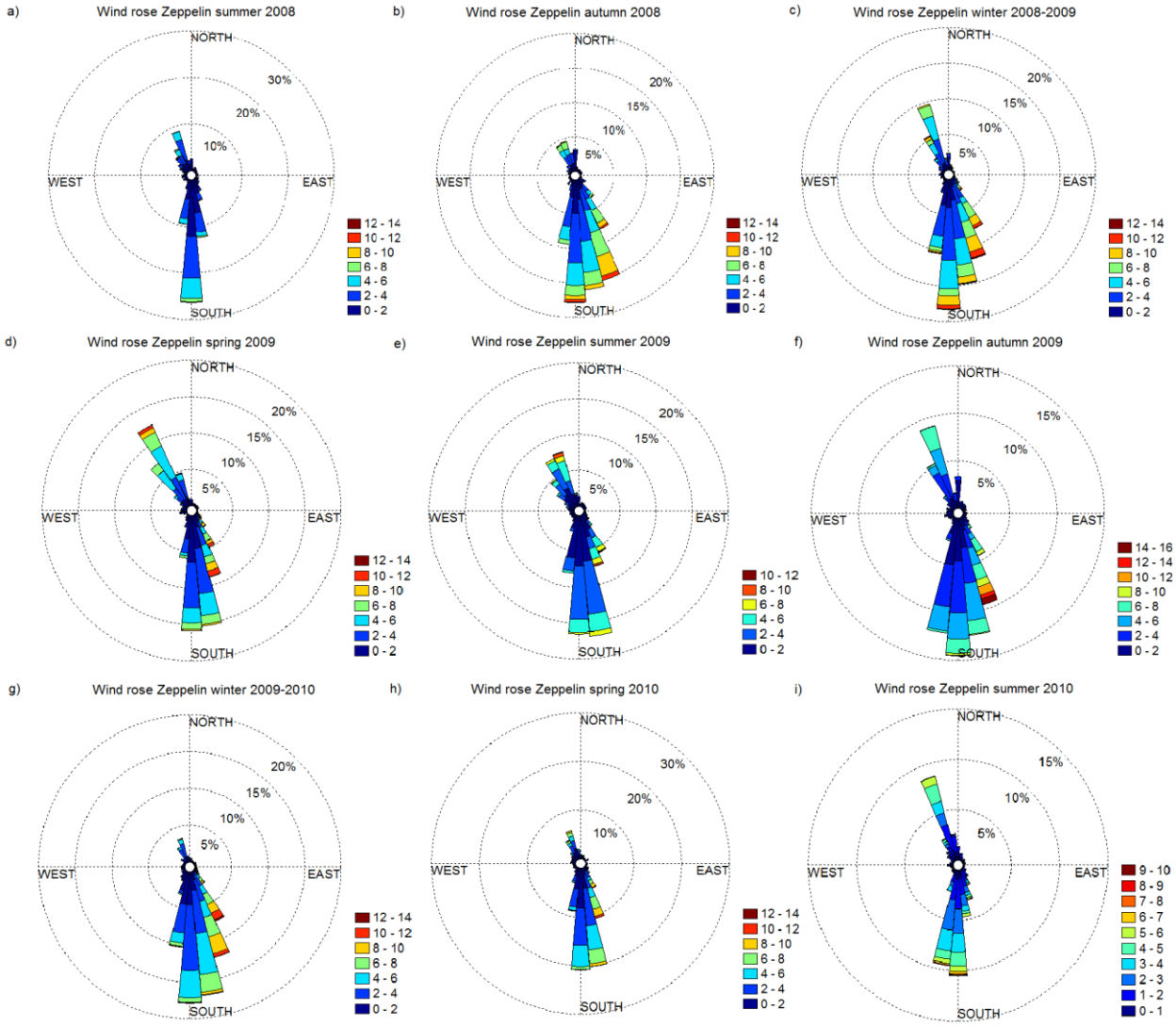

Figure 24 Wind roses Zeppelin. Colours indicate wind speed (m/s)

The Doppler sodar measurements stated previously that the 120° and 320° wind direction measured in the fjord correspond to 180° and 350° at Zeppelin (Beine et al. 2001). Also during that measurement campaign was concluded that the Zeppelin station may observe

N-flow when the wind in Ny-Ålesund is from SE (Beine et al. 2001). However, during such event the upward contamination spreading from the village is unrealistic due to the wind shear accompanied by the inversion.

Therefore one concludes that only when both Ny-Ålesund and the Zeppelin station observe northerly flow there is risk that the Zeppelin station could be influenced by the polluted air from the village (Beine et al. 2001).

3.2 Comparison with results from Weather Research and Forecasting model

The atmosphere and surface conditions on Svalbard have been simulated with the Weather Research and Forecasting model (WRF version 3.4) by Kjetil Schanke Aas at the University of Oslo. The model running was a part of his PhD studies. The description of the model is given in his paper submitted to the Journal of Applied Meteorology and Climatology (Aas et al. n.d.). The dataset from the WRF model for the Ny-Alesund area is available for the period from the 1st of July 2008 to the 15th of March 2009. The variables are following: potential temperature T_{pot} (K), temperature at 2m height T_{2m} (K); latitude and longitude of the grid points, land-sea flag for every grid point (0=sea point,1=land point); surface elevation (m); east-west wind component U (m/s) and north-south wind component V (m/s) for different heights; U at 10m height (m/s) and V at 10m height (m/s); vertical wind speed W (m/s); pressure (Pa). Using these variables the Richardson bulk number calculation and the wind roses for the grid points of interest have been produced.

The grid shown in Figure 25 is taken from the model. It includes the location of the Zeppelin station and the village and consists of 4x5 cells 1x1km each.

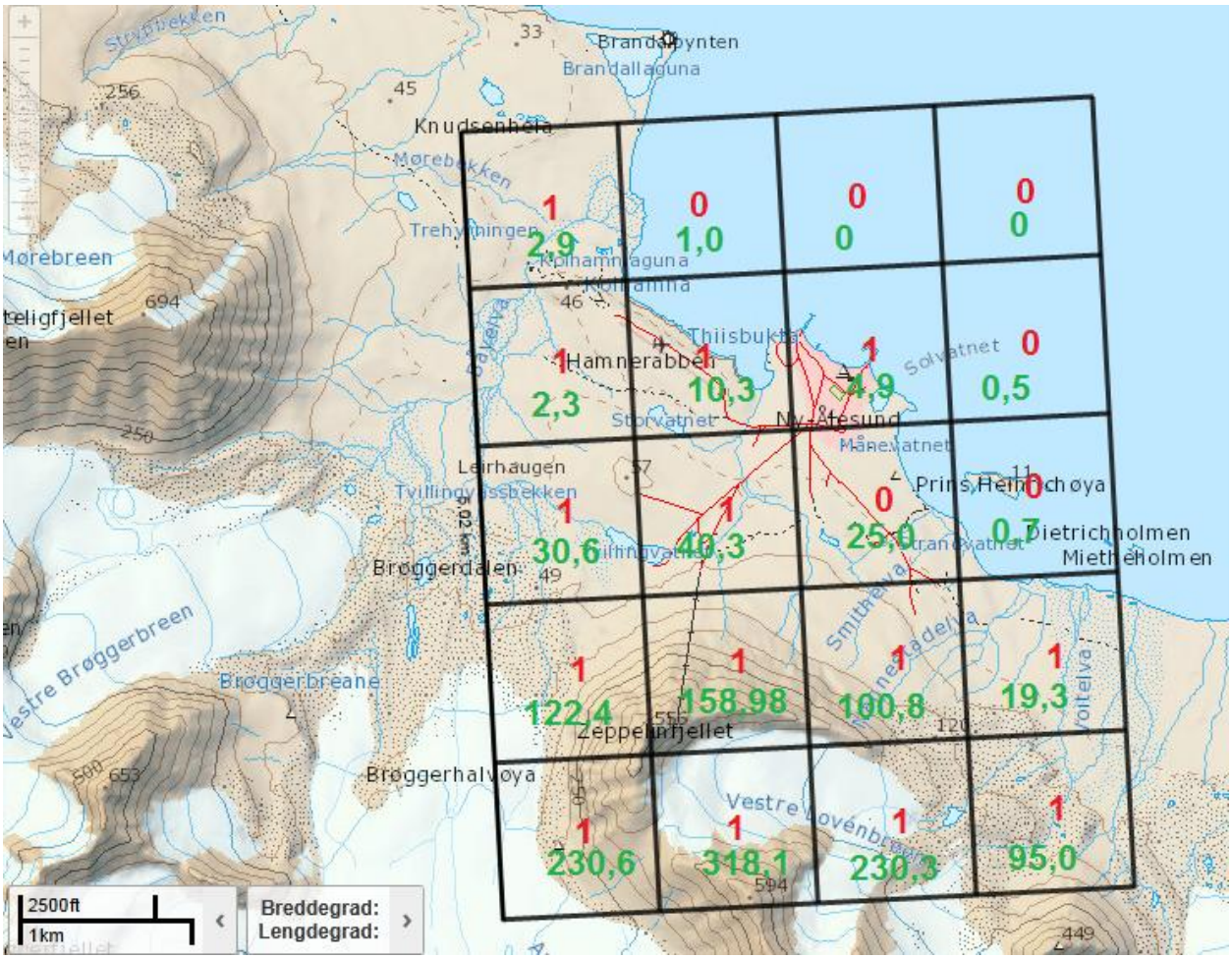

Figure 25 The modelled grid (red numbers state the land-sea modelled cells (1-land and 0-sea) and green numbers point to the average grid cells height in m).

All modelled values are averaged for the whole grid cell. To compare with measurement results from the AWI station or from the Zeppelin station we choose cell by first identifying the closest land points with code 1 in red colour in the Figure 25 and then choosing the surface elevation which will be the most representative for the stations level (see Table 3).

Such consideration leads to taking modelled results from the cells 2,1 and 3,4 (counting from the left lower corner in horizontal and then in vertical direction) for comparison with Zeppelin station and AWI meteorology data, respectively. However, such algorithm of cell selection neither allows to take the closest point for comparison (from the Figure 18 it would be points 2,2 and 3,3, correspondingly), nor reflects in detail local topography because, for example, the highest elevation in the modelled territory (318,1m in the Figure 25) in cell 2,1 is composed from height of the northern peak of the mountain Lundryggen with the highest point of 594 m in the Figure and the glacier Vestre Lovenbreen.

Thus one can see that despite very high resolution of this WRF model it is still coarse when seeking to study local scale features.

This is also well seen from the wind roses for the modelled grid points 3,4 and 2,1 chosen to represent area close to the village and to the Zeppelin, respectively, which are shown in Figures 26 and 27. The wind direction deviates for both points for all seasons and, as in previous research result of WRF usage for PBL modelling on Svalbard, the surface wind speeds in Kongsfjorden are overrated by WRF (Dütsch and Hole 2012)

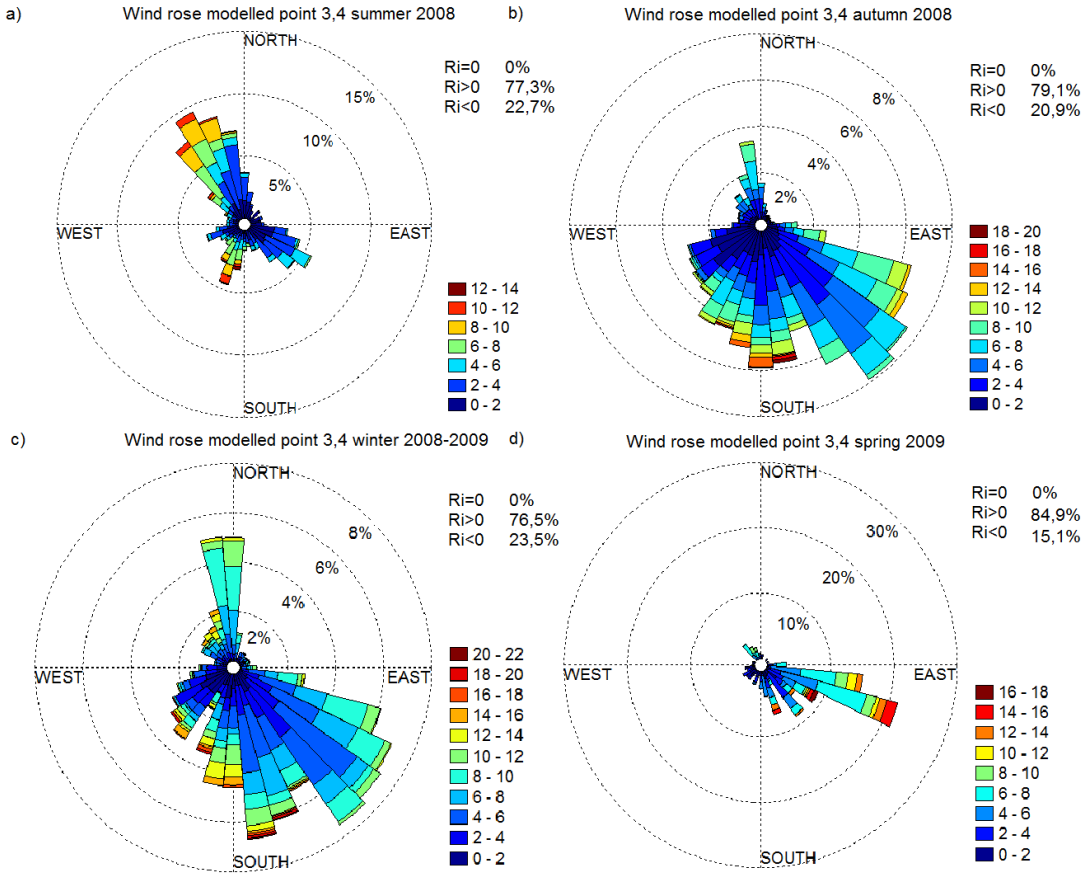

Figure 26 Wind roses modelled for grid point 3,4 (10m height). Colours indicate wind speed (m/s). Percentage of Ri=0, Ri>0 and Ri<0 is calculated for every season separately

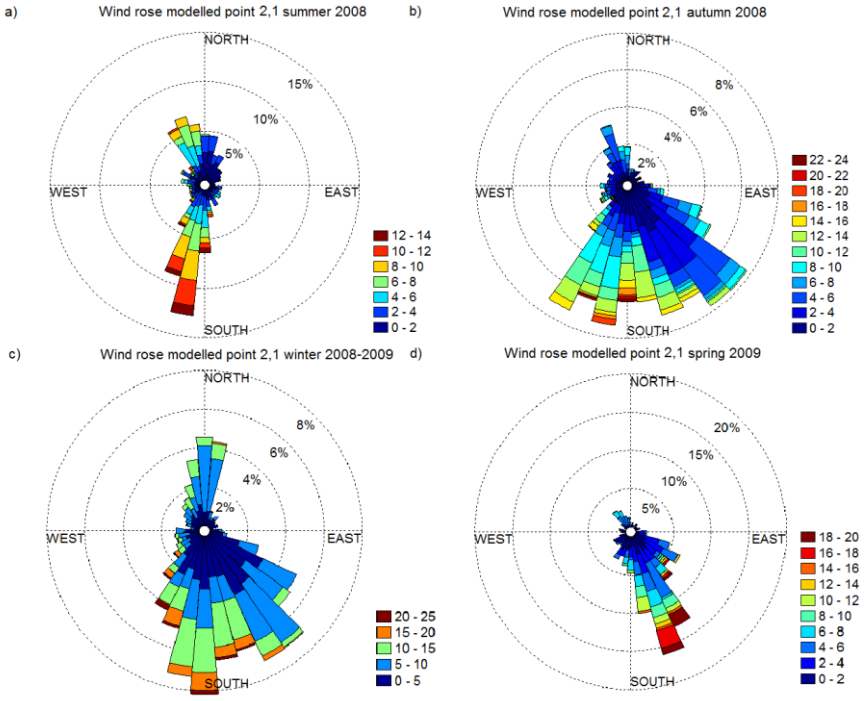

Figure 27 Wind roses modelled for grid point 2,1 (10m height). Colours indicate wind speed (m/s)

Thus this WRF modelled results cannot be used directly for the local pollution assessment due to ambigous wind speed and direction estimats. It appears that a model with finer resolution is needed. The wind climate in Kongsfjorden and different wind driving mechanisms have been also assessed in the paper (Esau and Repina 2012) where the simulations were performed with the real surface topography at resolution of about 60 m for non-stratified boundary layer. Therefore in the future work applicability of this model for the local pollution assessment should be investigated.

Result from the Ri_B calculation for the lowest layer for point 3,4 has been compared with Ri_m received from AWI observations. The model and measurements coincide for 47% of the negative Richardson bulk number measurement cases while for the positive values the coincidence is 77%. Thus when the model shows that the stratification is stable (Ri>0), it is quite probable to occur in reality.

4 Analysis of hourly monitor data from the station located in "Hyttebyen" in Ny-Ålesund

4.1 Method description

The data were measured during the period from 14.07.2008 00:00 to 24.08.2010 12:00. The measured components are presented in Table 4.

Table 4 Components measured by monitor in Ny-Ålesund

Components	Measurement equipment	Units
NO, NO_2, NO_x	Chemiluminescence NO_x analyzer (model 200E)	$\mu g/m^3$
SO_2	UV Fluorescence SO_2 analyzer (model 100E)	$\mu g/m^3$

The NO_x analyzer measures the amount of chemiluminescence emitted when NO in the gas sample is exposed to ozone and calculates the concentration of nitrogen oxide reacted using the detected amount of light. After that a catalytic-reactive converter turns all NO_2 in the sample gas into NO, which is then measured using the process described above. The sum of NO measurements is reported as NO_x. NO_2 is calculated as the difference between NO_x and the original NO in the sample gas (Teledyne Advanced Pollution Instrumentation 2010).

The SO_2 analyzer measures the amount of fluorescence given off from exposure of SO_2 in the gas sample by ultraviolet light in the instrument's sample chamber. The measurement result is used to calculate the amount of SO_2 present in the sample. (Teledyne Advanced Pollution Instrumentation 2011)

Both analyzers are equipped with microprocessors, and the software compensates the temperature and pressure changes. For both instruments lower detectable limit (LDL) is 0.4 ppb. The results are given in the Appendix 1.

4.2 Monitor measurements results

Figure 28 shows the seasonal mean concentrations of NO_x and SO_2 in ng/m^3 (instead of $\mu g/m^3$ to display all variables at the same graph) averaged for 8 wind directions and wind roses for the corresponding time of year composed using the monitor meteorological data. There was no meteorological data from the monitor for summer 2008 and for November 2008 therefore data from the WMO station has been used for these periods. When at the WMO station wind direction was not defined AWI measurement result for 10m height has been used.

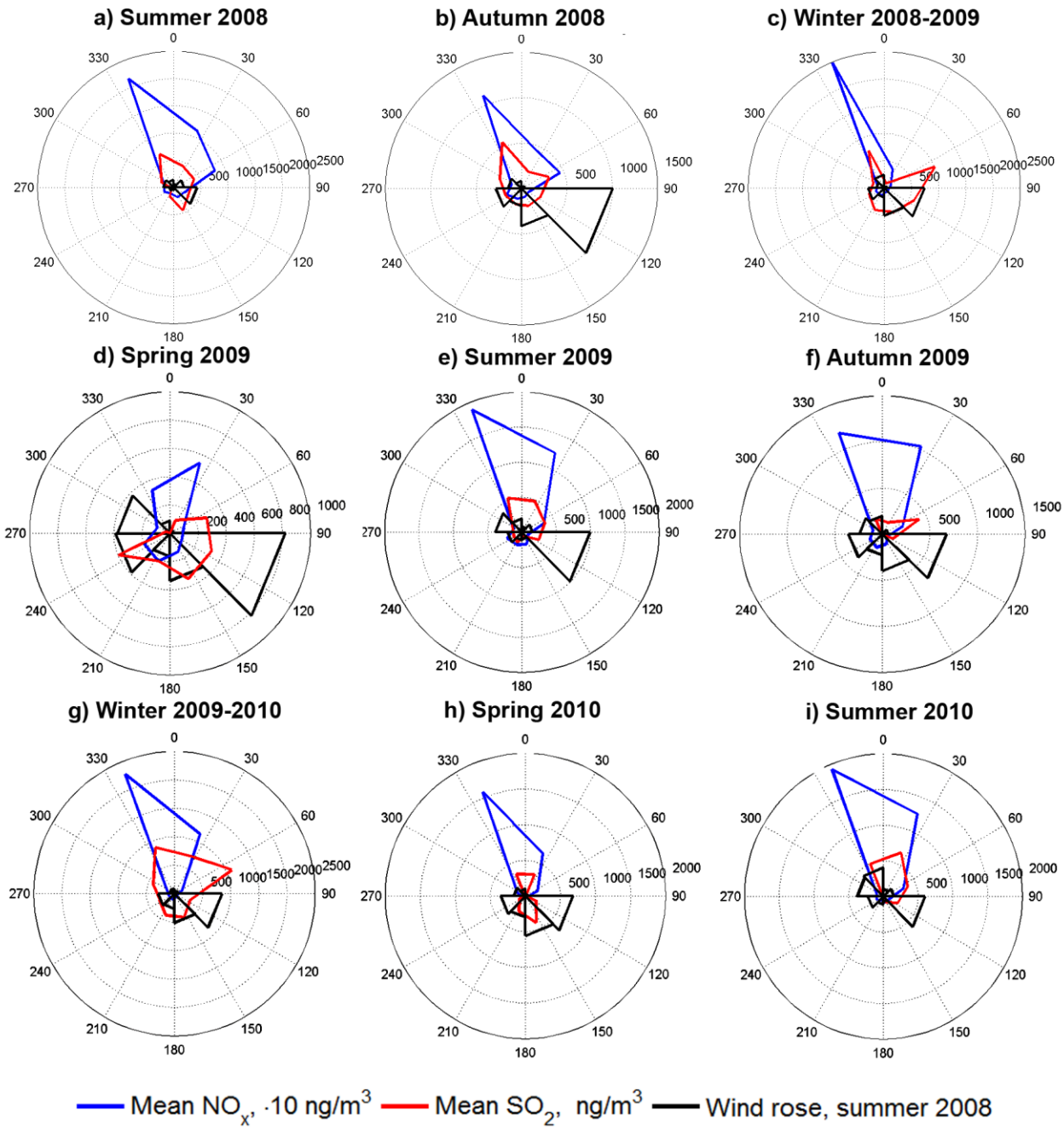

Figure 28 The seasonal mean concentrations of NO_x and SO_2 averaged for 8 wind directions and wind roses for the corresponding time of year

Air coming from NW direction has higher values of NO_x regardless of season. The only exception is spring 2009 (Figure 28d)) when the highest mean concentration occurs from the NE direction. The highest mean concentration observed when wind was from northerly direction is consistent with the influence of local pollution sources on NO_x measurements described in the first part of the thesis.

Summertime northerly direction of the highest concentration of SO_2 also contribute to the hypothesis of impact of local pollution sources on sulphur dioxide measurements.

However, during winter time both years the highest average values of SO_2 were measured when wind direction was easterly. This likely the result of long-range transport of pollution to Ny-Ålesund.

Plots in Figure 28 show clear seasonality of concentration both SO_2 and NO_x. Average values of compounds measured by monitor increase every summer and winter and decrease every autumn and spring. The possible reasons for these features are summertime ship traffic as an additional seasonal source of pollution in Ny-Ålesund and wintertime long-range transport detected by the monitor.

4.3 Local ship traffic influence on the hourly monitor measurements

The peaks of nitrogen oxides and sulphur dioxide have been found using the peak height criteria and compared with data from the cruise call list. The values higher than the sum of two standard deviations and median value of measured compounds have been assigned as the peaks, which correspond to concentrations higher than 20.46 $\mu g/m^3$ and 1.69 $\mu g/m^3$ for NO_x and SO_2, respectively.

The time interval from arrival to two hours after the departure time stated in the cruise call list was compared with the time of NO_x and SO_2 concentration peaks in the monitor data. Such timing has been chosen because it should be enough for ship plume to reach monitor in Ny-Ålesund even if the wind speed would be very low. The same period has been chosen in (Eckhardt et al. 2013).

The results of analysis are shown in Figures 29 and 30.

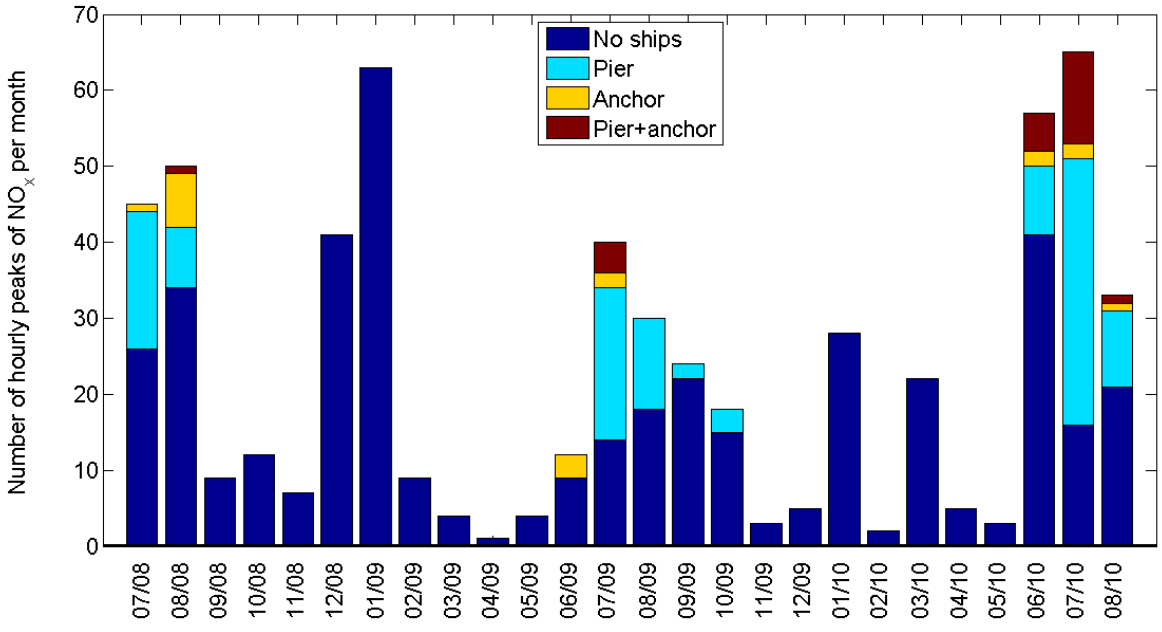

Figure 29 Number of hourly peaks of NO_x concentration per month vs data from the cruise

calls list

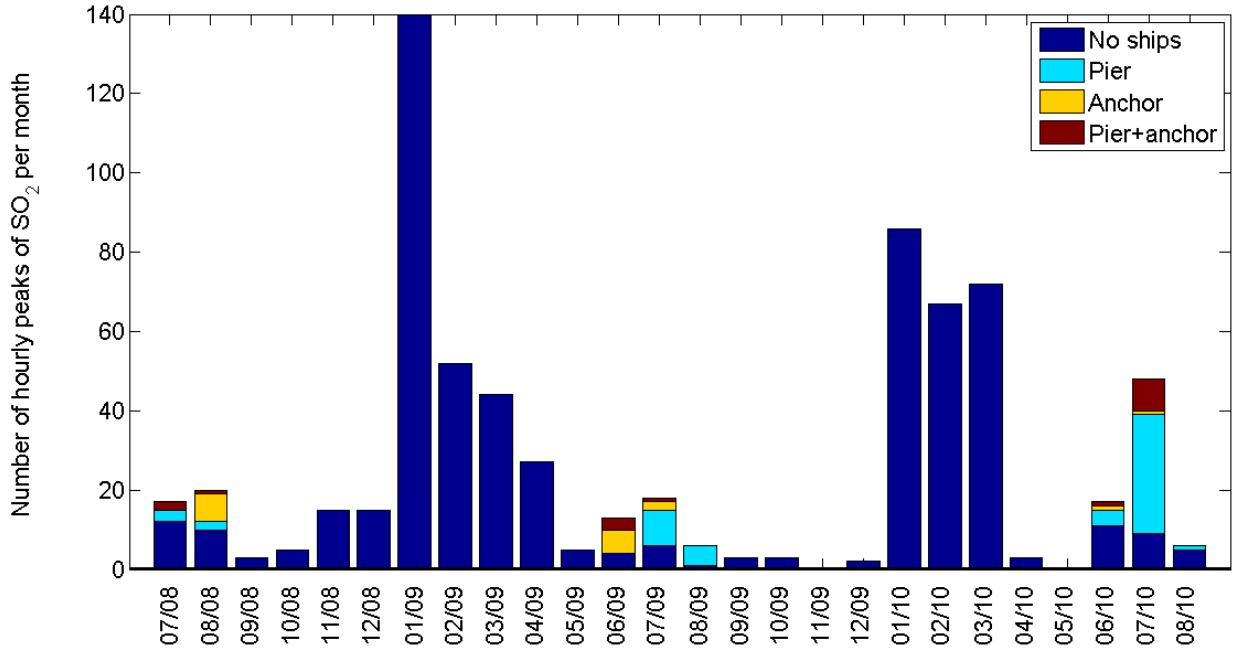

Figure 30 Number of hourly peaks of SO_2 concentration per month vs data from the cruise calls list

One can see from the Figures 29 and 30 that frequency of peak occurrence shows seasonal variation. Very low amount peaks of both compounds is detected in autumn, while the number of peaks rise dramatically in winter and spring time. For NO_x this noticeable increase is observed in December 2008, January 2009 and 2010 and in March 2010; for SO_2 it is well seen for the period from January to April 2009 and from January to March 2010.

The percentage of peaks for the winter and spring coinciding with northerly winds (from sectors 300º-330º,330º-360º,1º-30º) is shown in Table 5. There only data for spring and winter time have been used here, firstly, due to more frequently observed stable stratification the emissions from the power plant will be detected by the monitor almost immediately in absence of mixing when the wind will be northerly; secondly, during summertime there are non-stationary local sources with unknown location, for example, anchored cruise ships, and therefore the northerly wind in the village is not a good indicator of local influence.

Table 5 The percentage of peaks for the winter and spring coinciding with northerly winds

	Winter 2008-2009			Spring 2009			Winter 2009-2010			Spring 2010		
	Dec	Jan	Feb	Mar	Apr	May	Dec	Jan	Feb	Mar	Apr	May
NO_x	47.2	60.8	19.6	7	8.6	19.7	16.5	54.6	1.3	65.6	16.3	21.5
SO_2	40	30.7	9.6	2.3	0	20	0	16.3	0	5.6	0	0

The Table 5 reveals the difference between SO_2 and NO_x peaks origin. For example, the highest number of peaks during January 2009 can be seen both in Figures 30 and 31. However, from Table 5 one can see that the number of NO_x peaks with northerly winds was two times higher than SO_2 during that period. The same situation can be observed for January and March 2010.

In general, NO_x shows higher percentage of peaks for the winter and spring coinciding with northerly winds thus the power plant located northerly from the monitor is very likely to be the biggest source of NO_x in Ny-Ålesund. It is also the time with the highest diesel consumption for power plant as was shown in Figure 12.

On the other hand, according to the Table 5 SO_2 during winter and spring time is very likely to have long-range origin. This is discussed later in detail in the chapter 6 of the thesis. The following pattern of SO_2 peaks distribution during winter and spring time in absence of ship traffic corroborates the previous findings about the Arctic haze described in the first chapter.

However, as one can see the summertime local pollution from ships traffic adds significantly to the number of peaks and therefore to the monthly concentration of both NO_x and SO_2 if one compares with the lowest autumn values. Especially it is affecting the nitrogen oxides concentration. According to these graphs the highest influence on concentration from ships emissions was during summer 2010, particularly in July 2010. It correlates very well with the maximum number of ships and passengers for all three years (Figure 14).
Nevertheless, in order to assess the influence of local pollution on measurements at the Zeppelin station, one should analyze measurements directly from there because even during summer time the stratification of boundary layer and wind direction difference may prevent the impact of ship and power plant plumes on the measurements on the mountain station. Such indicator for pollution on Zeppelin station used in the thesis are aerosol particle number measurements.

5 Analysis of the aerosol measurements from the Zeppelin station

According to the classification presented in (Seinfeld and Pandis 2006) the submicron aerosol particles lifetime is related to the aerosol particle modes as shown in Table 6.

Table 6 Aerosol mode distribution and lifetime for submicron aerosol particles

Mode	Size (nm)	Lifetime in lower atmosphere
Nucleation mode	1-25	Minutes to hours
Aitken mode	25-100	Days
Accumulation mode	100-1000	Two-three weeks

The fresh aerosols consist of the nucleation mode particles formed by the nucleation from the gas phase. These ultrafine particles are growing primarily due to condensation of sulphuric acid which is a product of reactions described in chapter 1 of the thesis (Seinfeld and Pandis 2006). Therefore the amount of particles of this mode is dependent on the presence of the atmospheric water and the nucleation mode particle precursor gases SO_2 and NO_x.

5.1 Method description

The integral aerosol number density and size distribution are measured by Stockholm University at the Zeppelin mountain.

The data used in the thesis contains measurements from two Condensation Particle Counters (CPC). In the instruments the supersaturated vapour is condensed onto the particles resulting to the particle growth into bigger droplets which are detected and counted by an optical detector. (TSI 2002a, 2002b)

The models TSI CPC 3025 and TSI CPC 3010 have minimum detectable particle sizes 50% of 3nm particles and 50% of 10nm particles, respectively (TSI 2002a, 2002b). Thus the difference between total numbers of particles detected by the two instruments gives a measure of nucleation mode particles within the size range 3 to 10nm.

According to the data from the experimental studies from the cruise ship emission, the smaller-sized particle mode is centred at d=20nm while the combustion particle mode is centred at modal diameters range from 50nm for raw emissions and 100 nm for a plume age of 1 hour (Petzold et al. 2008). The latter sizes are much larger than the numbers shown in the Table 6 for nucleation mode. Due to this difference between theory and result from practical studies the measured values for all three sizes of interest (3-10nm, 20nm and 50-100nm) are compared.

In order to assess the influence of local pollution on the measurements at the Zeppelin

station the following procedures for peak detection that has been applied:

1) Comparison of time when Richardson gradient number calculated from AWI measurements was negative or equal to zero with time of NO_x and SO_2 monitor peaks in the village. During these hours there was possibility for upward spreading of pollution from the village. The time interval included 4 additional hours possibly needed for pollution to reach the Zeppelin station in case of very low wind speeds;

2) Comparison of the filtered results from step one with time of aerosol peak measured at the Zeppelin station. The values higher than the sum of two standard deviations and median value of measured particle concentrations have been assigned as peaks. The concentration peaks of aerosol particles with sizes from 3nm to 10nm; particles with d≈20nm and from 50nm to 100nm have been used separately in order to compare with the fresh aerosol (nucleation mode) size from Table 6 (Seinfeld and Pandis 2006)and the cruise ship exhaust sizes described in (Petzold et al. 2008), respectively.

3) Then the result from step 2 was sorted according to the prevailing wind direction at the Zeppelin station during the time of aerosol peaks. When northerly winds (from sectors 300º-330º,330º-360º,1º-30º) were observed at the station it is assumed that the station could be affected by local pollution from the village.

4) As far as daily data from the Zeppelin filter samples are used for different research projects, the possible hours of local pollution influence received from previous steps are presented in terms of days of impact.

5.2 Results

One can see from the seasonal mean particle concentration shown in Figure 31 all three sizes groups have maximum mean seasonal concentration is during summertime.

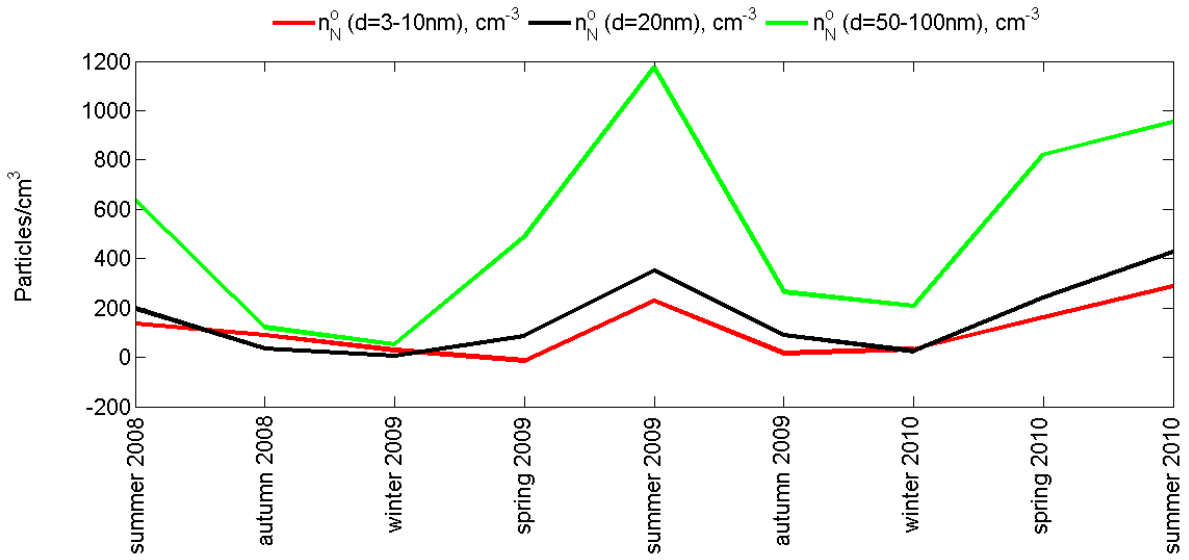

Figure 31 Seasonal mean particle concentration for sizes from 3nm to 10nm; particles with d≈20nm and from 50nm to 100nm

During that time the photochemical activity increases and insolation effectively provokes new particle formation with the peak of process in June (Tunved, Ström, and Krejci 2013).

However, for Arctic haze time the nucleation mode mean diameter is also 50nm because the growth rates during the winter and spring are multiple times lower than during the summer resulting to favourable conditions for the long-range transport (Seinfeld and Pandis 2006).

The result of the assessment of local pollution influence on the Zeppelin station measurements is shown in Table 7.

Table 7 Days of possible local pollution influence on Zeppelin station measurements

Compound	Days of possible pollution defined using different particle sizes		
	d=3nm-10nm	d≈20nm	d=50nm-100nm
NO_x (In total 16 days for d=3nm-10nm; 13 days for d≈20nm; 10 days for d=50nm-100nm)	18.07.2008 30.07.2008 31.07.2008 16.08.2008 20.06.2009 14.08.2009 16.08.2009 19.08.2009 25.08.2009 04.09.2009 11.06.2010 28.07.2010 29.07.2010 31.07.2010 10.08.2010 23.08.2010	31.07.2008 16.08.2008 05.07.2009 13.07.2009 14.08.2009 16.08.2009 19.08.2009 25.08.2009 04.09.2009 05.09.2009 29.07.2010 31.07.2010 23.08.2010	31.07.2008 01.08.2008 16.08.2008 20.06.2009 25.06.2009 05.07.2009 07.07.2009 29.07.2009 31.07.2009 05.08.2009
SO_2 (In total 10 days for d=3nm-10nm; 9 days for d≈20nm; 7 days for d=50nm-100nm)	31.07.2008 16.08.2008 20.06.2009 30.06.2009 14.08.2009 25.08.2009 29.07.2010 31.07.2010 10.08.2010 23.08.2010	31.07.2008 16.08.2008 30.06.2009 05.07.2009 13.07.2009 14.08.2009 25.08.2009 29.07.2010 31.07.2010	31.07.2008 01.08.2008 16.08.2008 20.06.2009 21.06.2009 30.06.2009 05.07.2009

As one can see from the Table 7 the percentage of days with possible pollution at the Zeppelin station is very low: 4.1%, 3.3% and 2.6% from 389 days when northerly wind was measured at the Zeppelin station for NO_x pollution calculated using d=3nm-10nm, d≈20nm and d=50nm-100nm aerosol peaks; 2.6%, 2.4%, 1.8% and from 389 days when northerly

wind was measured at the Zeppelin station for SO_2 pollution calculated using d=3nm-10nm, d≈20nm and d=50nm-100nm aerosol peaks.

The results from Table 7 are visualized in Figure 32 and 33.

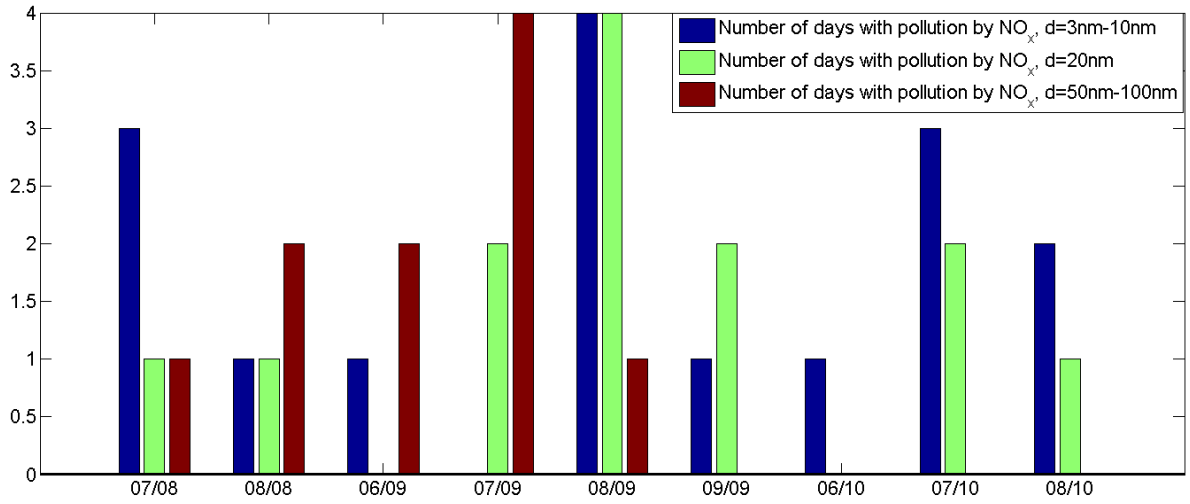

Figure 32 Number of days of possible local pollution influence on Zeppelin station measurements per month (filtered for NO_x)

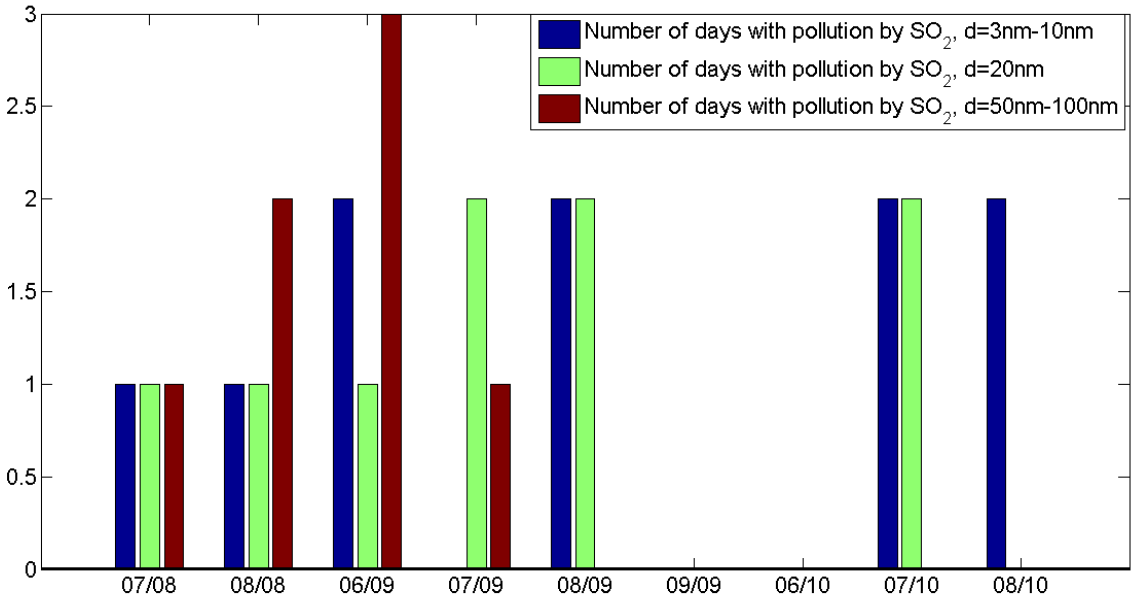

Figure 33 Number of days of possible local pollution influence on Zeppelin station measurements per month (filtered for SO_2)

Figure 32 and 33 show that most of days of possible pollution at the Zeppelin station are during summertime except two days in September 2009. This is due to the fact that the atmosphere is unstably stratified in summer more often than in winter therefore possibility for local pollution to reach the mountain increases. Limited number of peaks in June and July

2010 comparing with summer 2009 could be due to frequent absence of AWI and Zeppelin meteorological data in some particular days during these months.

One can see in the Figure 34 that the aerosol size distribution is dependent on time of day. During the 31st of July 2008 the concentration begins to rise after 13:30 and then decreases again at 17:30.

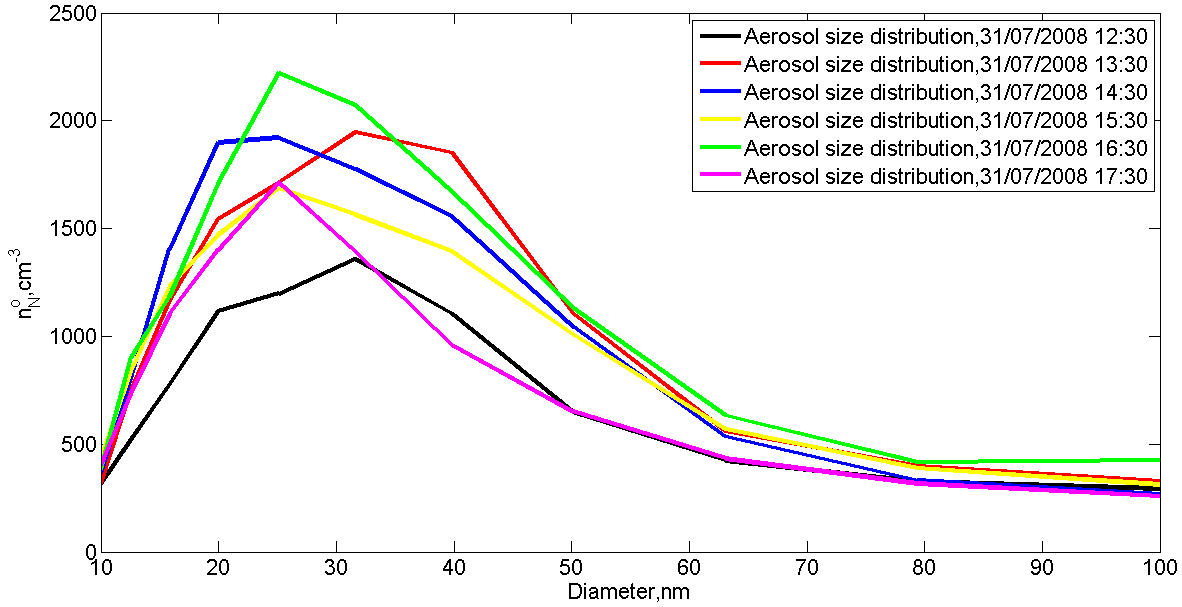

Figure 34 Submicron aerosol size distribution for the 31st of July 2008

In order to check the influence of the sunshine on new particle formation the AWI record of sunshine duration in minutes per hour was compared with the filtered results for different diameters. The values when sunshine duration was higher than 30minutes per hour were filtered out. The 50-100nm diameter results for both NO_x and SO_2 values appeared to be the least influenced by the sunshine duration. Furthermore, the Zeppelin station is located in 2km distance from the harbour thus it will take some time for the plume to reach the station therefore it probably could be wise to use this number characteristic for the 1hour aged plume for further control of local pollution at the Zeppelin station.

Days when measurements of all three sizes coincided with both SO_2 and NO_x peaks of pollution in the village are 31.07.2008 and 16.08.2008. These two cases are described in detail further.

The time series of SO_2, NO_x and particle concentration, number of passengers (anchor and pier), wind measurements from the WMO station and the Zeppelin station are represented in Figure 35.

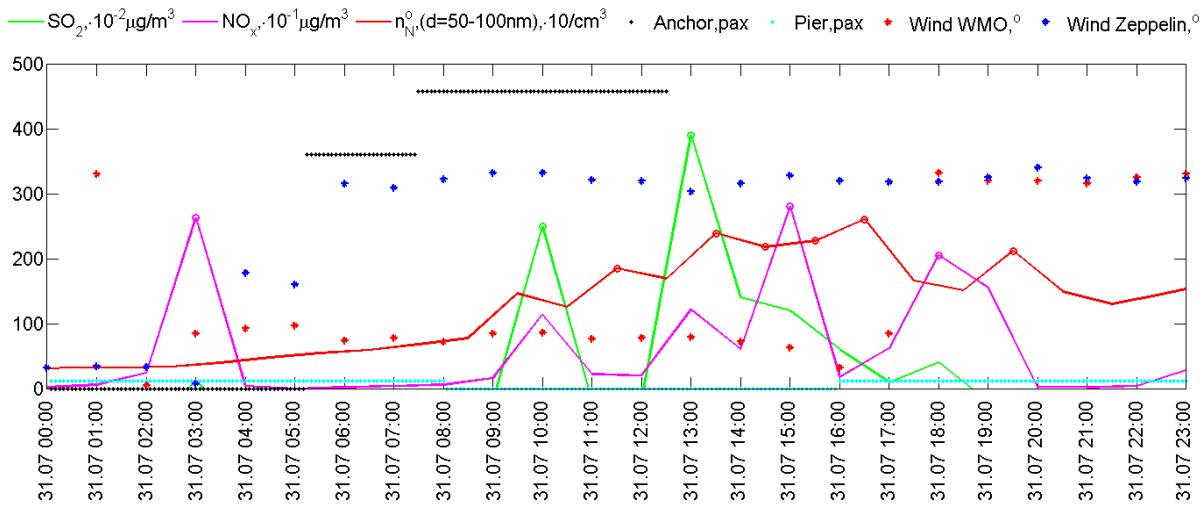

Figure 35 Time series of SO_2, NO_x and particle concentration, number of passengers (anchor and pier), wind measurements from the WMO station and the Zeppelin station 31.07.2008

As one can see, contrary to the supposition mentioned in the chapter 3.1 that the Zeppelin station could be influenced by local pollution only when there is northerly wind both at the station and in Ny-Ålesund, different wind directions in the village and at the Zeppelin station do not serve as a guarantee of air cleanness at the station and the pollution at the mountain from local sources is still possible. Firstly, because even in the absence of northerly wind the monitor still detected elevated concentrations of both NO_x and SO_2 what says about ship traffic around fjord, for example excursions, or local air circulation system development (Oke 2002). Secondly, in the graph the large amount of passengers on the anchored ships (over 400 pax here) suggests the high emission rate from these big cruise ships. Additionally to this the source is at height (the emission is from the ship stack) and the plume can reach the northerly wind flow on the altitude of the Zeppelin mountain and be transported to the station. As already been seen from comparison of Ri_m calculated using data from AWI and from CCT in the chapter 3.1 even on land the Richardson number varies significantly from one place to another and the difference between different parts of the fjord can be more dramatic thus the unknown location of the anchored ships and therefore the atmospheric stability at the point of emission adds further uncertainty.

The Figures 36 and 37 based on data from radiosonde launched by AWI at 16:51 31.07.2008 show that the wind is turning with height dramatically.

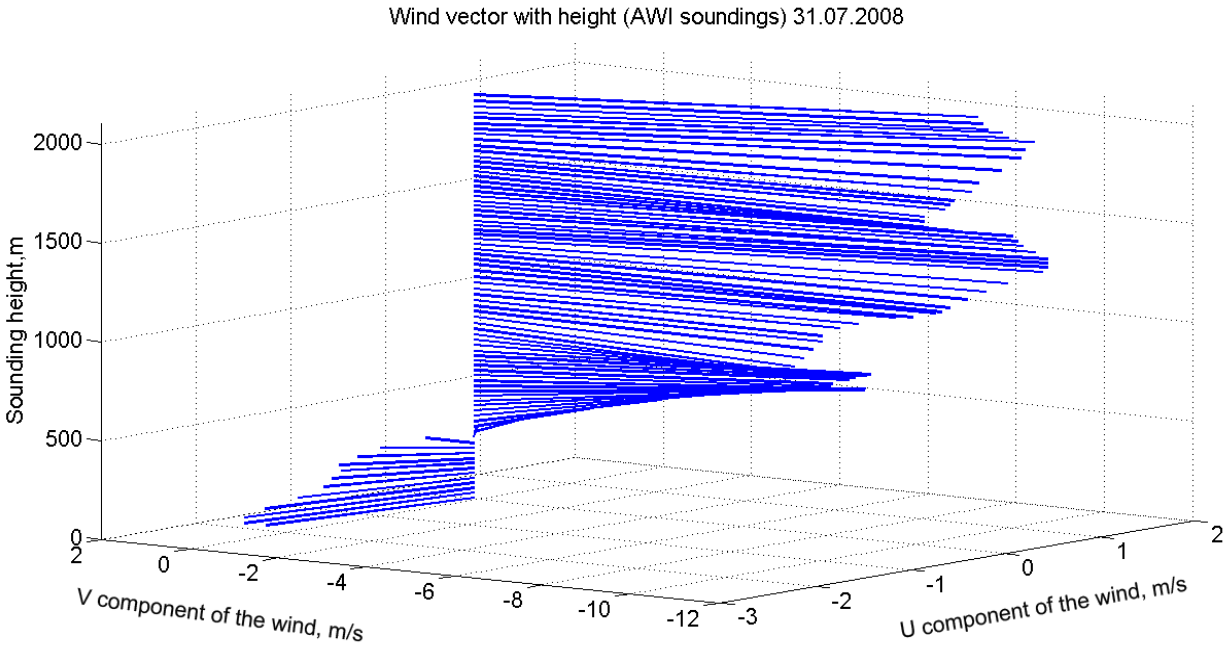

Figures 36 Wind velocity distribution with height 31.07.2008. U component of wind is positive toward the east, V component is positive toward the north

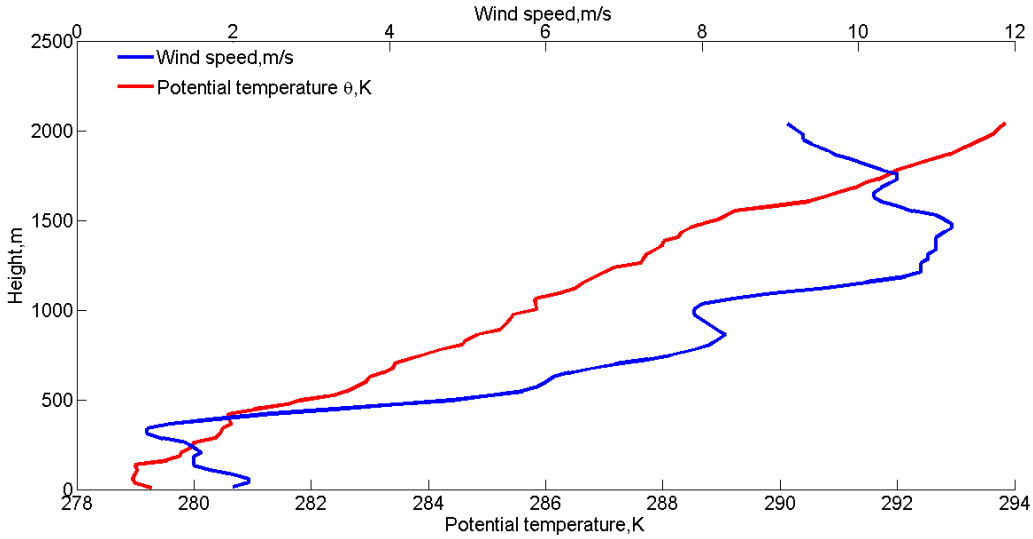

Figures 37 Wind speed and potential temperature distribution with height 31.07.2008

The most important aspect is that the level where the wind changes direction is just below the Zeppelin station. Furthermore, the wind is changing during the day and as one can see from the Figure 35 at 18:00 wind in the village approached the same direction as at the Zeppelin station. Thus without hourly data about vertical atmospheric stratification dynamics it is difficult to say whether there was pollution during such a day or not. Probably some of the equations from the chapter 2 later could help to build up the model to include plume

height in such assessment solving ambiguity with influence of elevated sources on the measurements at the station.

The second day when all particle sizes showed peaks both for NO_x and SO_2 is 16.08.2008. The time series of SO_2, NO_x and particle concentration, number of passengers (anchor and pier), wind measurements from the WMO station and the Zeppelin station for this day are shown in Figure 38.

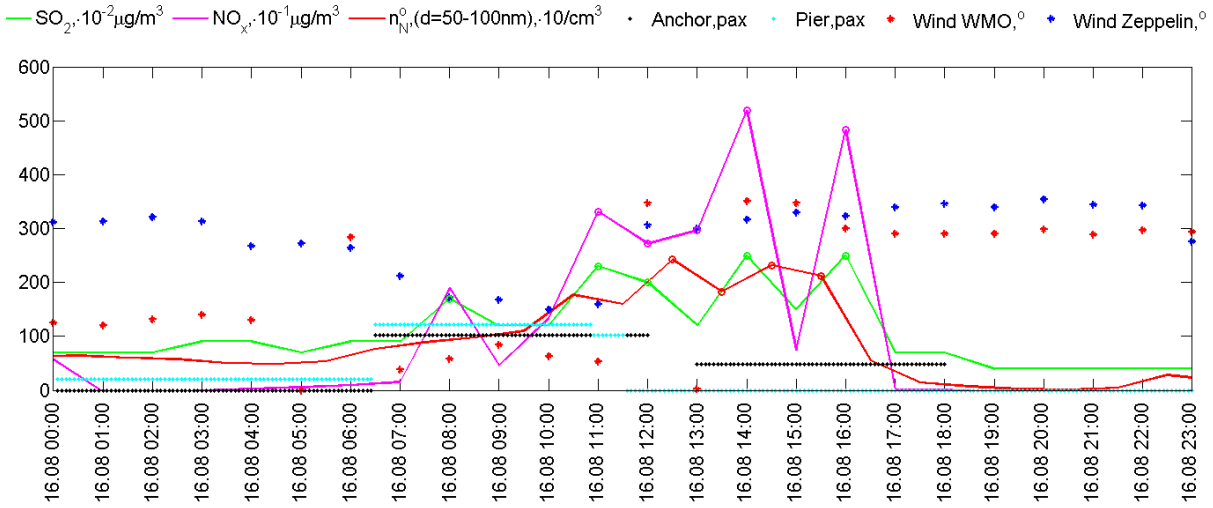

Figure 38 Time series of SO_2, NO_x and particle concentration, number of passengers (anchor and pier), wind measurements from the WMO station and the Zeppelin station 16.08.2008

The wind direction at the Zeppelin and in the village was similar from 12:00 to 16:00, and both stations probably received the same polluted air from the NW. Here ships attached to pier can also play role in the local emissions. Therefore the source location is in vicinity of the point for which Richardson number was calculated and the statement about local pollution influence on the Zeppelin station and on the Ny-Ålesund measurements during this day is more certain.

The wind velocity distribution with height (Figure 39) and wind speed and potential temperature distribution with height (Figure 40) are based on measurement result from radiosonde launching at 10:35 16.08.2008.

Figure 39 shows that significant change of the wind direction was observed only at height above 700m.

The Figure 40 also shows no significant change in wind as well as no abrupt temperature inversions in the level below 500m. However, all peaks in the village occured later during that day therefore with only one radiosonde launching a day it is hard to make

any presice conclusion about atmospheric statification during the whole day.

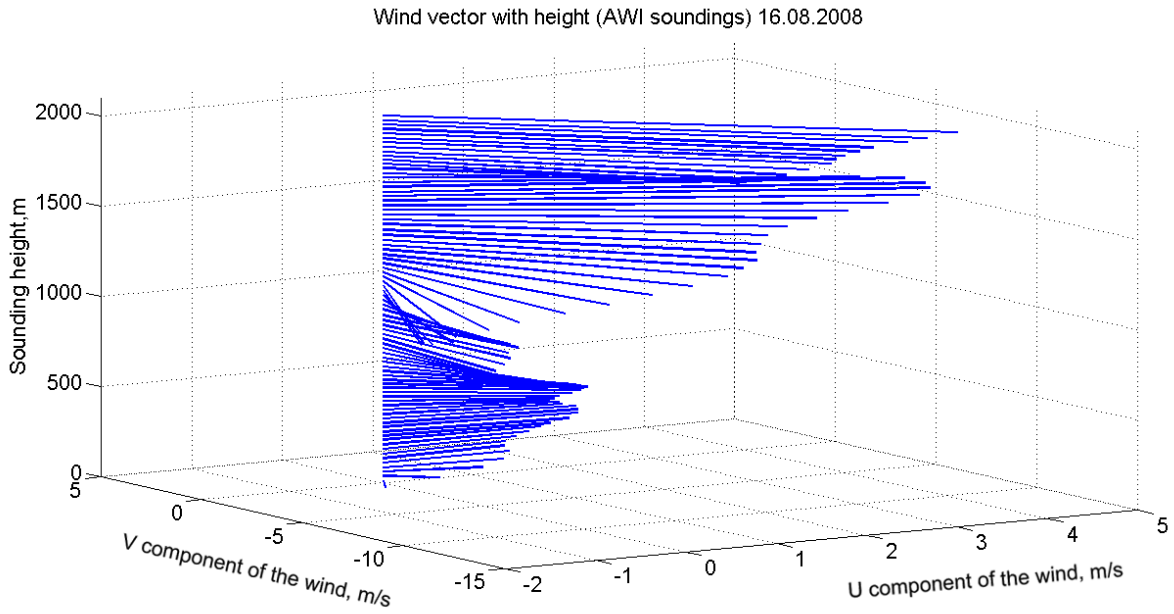

Figures 39 Wind velocity distribution with height 16.08.2008. U component of wind is positive toward the east, V component is positive toward the north

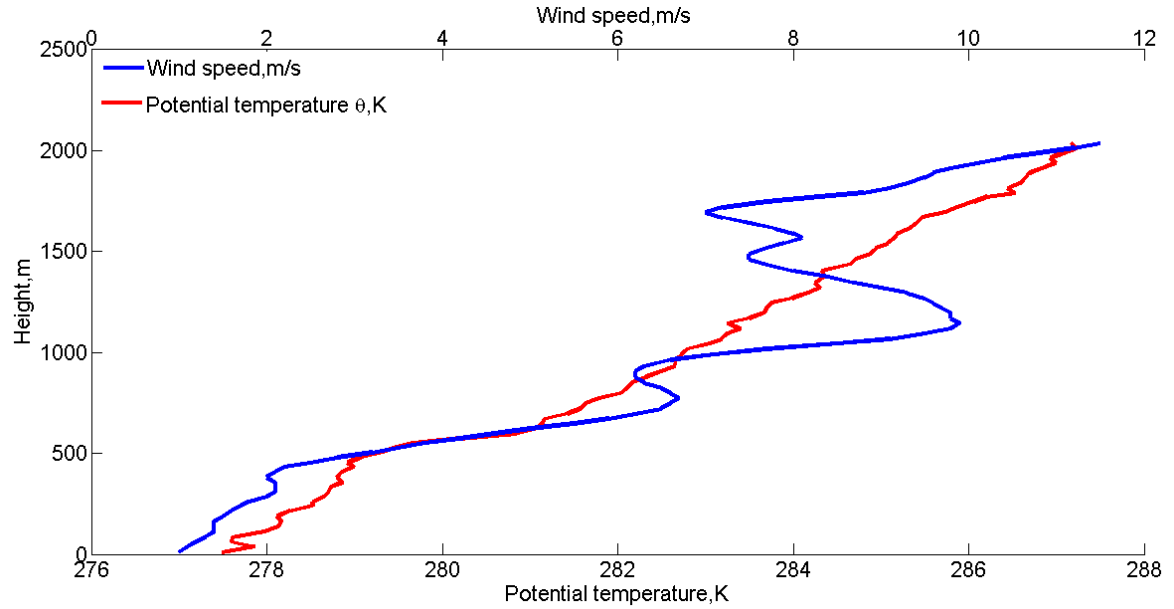

Figures 40 Wind speed and potential temperature distribution with height 16.08.2008

Thus taking into account the two case studies described above one can determine main uncertainties which add to complexity of the problem of the assessment of local pollution influence on the measurement in the village and at the Zeppelin station. First of all, it is the natural inconstancy of the wind flow in Ny-Ålesund both in horizontal and in vertical

direction, difference in atmospheric stability from one location to another, the diurnal variability of the aerosol particle concentration depending on the sunshine duration. In addition to this natural factors there is uncertainty regarding to the exact ship location, the stack height and characteristics of emitted gases. In addition to this the missing meteorological data during summer time like it happened in June and July 2010 restrict any assessment and changes the total statistics of influence as it was shown in Figures 32 and 33.

Therefore despite the few occasions with possible pollution we have been able to find in this study we still have too little information to be absolutely sure that the number is so low in reality.

However, in view of the defined days of possible influence of local pollution listed in Table 7, the daily filter samples from the long-term EMEP monitoring programme are analyzed in the next chapter in order to assess the influence of local pollution on these important measurements carried out at the Zeppelin station.

6 Analysis of daily data from filter samples collected at the Zeppelin station and in Ny-Ålesund

The knowledge about chemical properties of measured compounds and FLEXTRA trajectory model have been applied in order to distinguish long-range origin of pollution and local impact on filter samples measurements.

The trajectories from the web-site http://www.nilu.no/projects/ccc/trajectories/ were used for the identification of sources of long-range transport. Plots of trajectories (drawn for 6:00, 12:00, 18:00 and 00:00 every day) are available for all period of interest except several discrete dates.

The trajectory errors in FLEXTRA are on the order of 20% of the travelled distance and the performance varies with the meteorological conditions. Detailed information about this kinematic trajectory model is available online in the FLEXTRA Trajectory Model Version 3.0 User Guide on the web-site http://zardoz.nilu.no/~andreas/flextra/flextra3.html#tth_chAp1.

The daily filter samples data have been compared with the days of possible local pollution influence on Zeppelin station measurements defined in the previous chapter.

6.1 Method description

The data from filter samples is received from NILU. The quality control of the data was provided by the NILU's staff.

The measurements from filter samples available are presented in Table 8.

Table 8 Components measured in impregnated filter samples

Components	Sampling methods in field	Units
$SO_2(g)$	KOH impregnated filters	$\mu gS/m^3$
$HNO_3(g)$	Denuder	$\mu g\ N/\ m^3$
$NH_3(g)$	Denuder	$\mu g\ N/\ m^3$
$SO_4^{2-}(p)$	Aerosol filter	mg S/l
$NO_3^-(p)$	Aerosol filter after denuder	mg N/l
$NH_4^+(p)$	Aerosol filter after denuder	mg N/l
$Na^+(p)$, $Mg^{2+}(p)$, $Ca^{2+}(p)$	Aerosol filter	mg /l
$HNO_3(g)+NO_3^-(p)$,	Filter pack	$\mu g\ N/\ m^3$
$NH_3(g)+ NH_4^+ (p)$	Filter pack	$\mu g\ N/\ m^3$

*g-for gases, p-for particles

There are two different sets of data from the filters from the Zeppelin station and from

the monitor station. The results are shown in the Appendix 2. For these two measurement series every sample started at 7 o'clock and ended at 7 o'clock the next day.

The monitor station was located in the centre of Ny-Ålesund for the period from 20.07.2008 to 01.01.2010. There were missing data for the period from 01.09.2008 to 18.10.2008 and several discrete days almost every month. Measurement results from the Zeppelin station are available for the period from 01.07.2008 to 01.10.2010.

The detailed description of used equipment and methods of chemical analysis is given in EMEP manual for sampling and chemical analysis, 1996, available in the web-site http://www.nilu.no/projects/CCC/manual/.

As far as the "Cooperative programme for monitoring and evaluation of long-range transmission of air pollutants in Europe" (EMEP) is an extensive long-term monitoring project dozens of researchers are involved in analysis of the result of this data and variety of papers and report is produced, in the thesis only results which are related to the topic of local pollution in Ny-Ålesund and comparison of the measurement samples from the village and from the Zeppelin station are discussed.

6.2 General trends of monthly means of measured filter compounds

During periods of building high concentration of Ca^{2+} and comparatively low concentration of other marine ions could occur due to construction dust (EMEP, 1996). Comparing Figure 10 where the monthly diesel consumption for vehicles were shown with Figure 41 given below the previous assumption about usage of the cars in the building work in July 2008 is supported. Calcium ions can be an indicator for such type of local pollution.

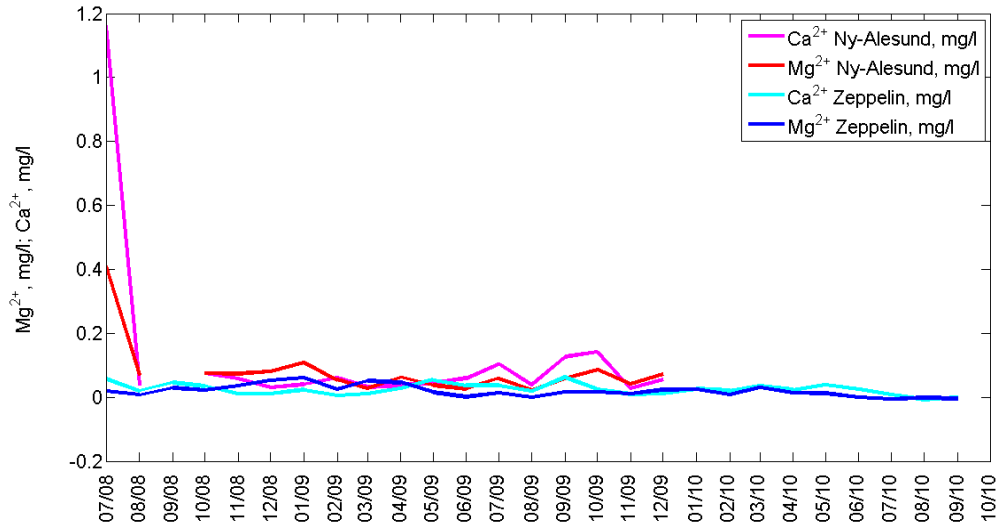

Figure 41 Monthly mean of Ca^{2+} and Mg^{2+} in Ny-Ålesund and at the Zeppelin station

There are two different ways of description of results for sulphate measurements:

- sulphate, mg S/l, not corrected
- sulphate, mg S/l, corrected for seaspray.

High concentrations of such ions as Na^+, Cl^-, Mg^{2+} (sea-salt constituents) are the signals of marine nature of the air and also can be used for determination of part of sulphate concentration which is due to marine sea-spray aerosols. (EMEP, 1996).

The non-sea-salt sulphate thus is determined by correction of total measured sulphate for sea salt which has been done according to the non-sea salt sulphate correction algorithm defined in (WMO, 2004) based on the constant sodium and sulphate ion content in the ocean.

The Figure 42 shows that the level of sodium ion Na^+ is lower than at Zeppelin. The station appears to escapes much of the impact of the sea spray at the mountain ridge location.

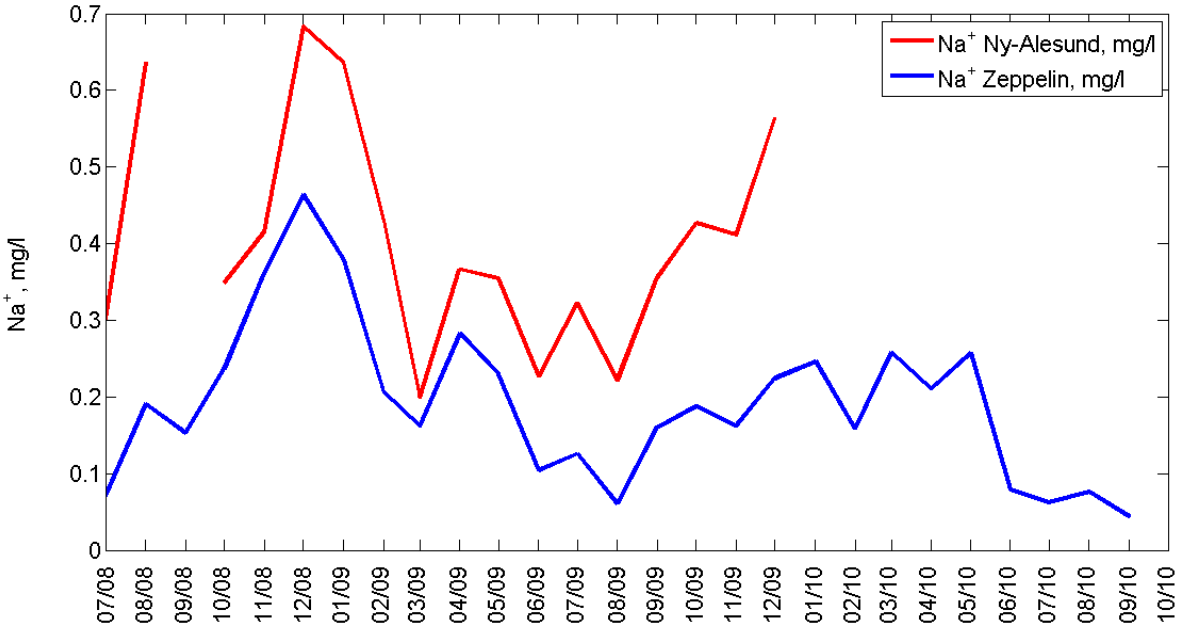

Figure 42 Monthly mean of Na^+ in Ny-Ålesund and at the Zeppelin station

The monthly mean of the total and non-sea salt sulphate concentration in Ny-Ålesund and at the Zeppelin station is shown in Figure 43. The distribution of sulphate concentration is very typical for Arctic location with high values in winter and spring when the Arctic haze (chapter 1) takes is prevalent.

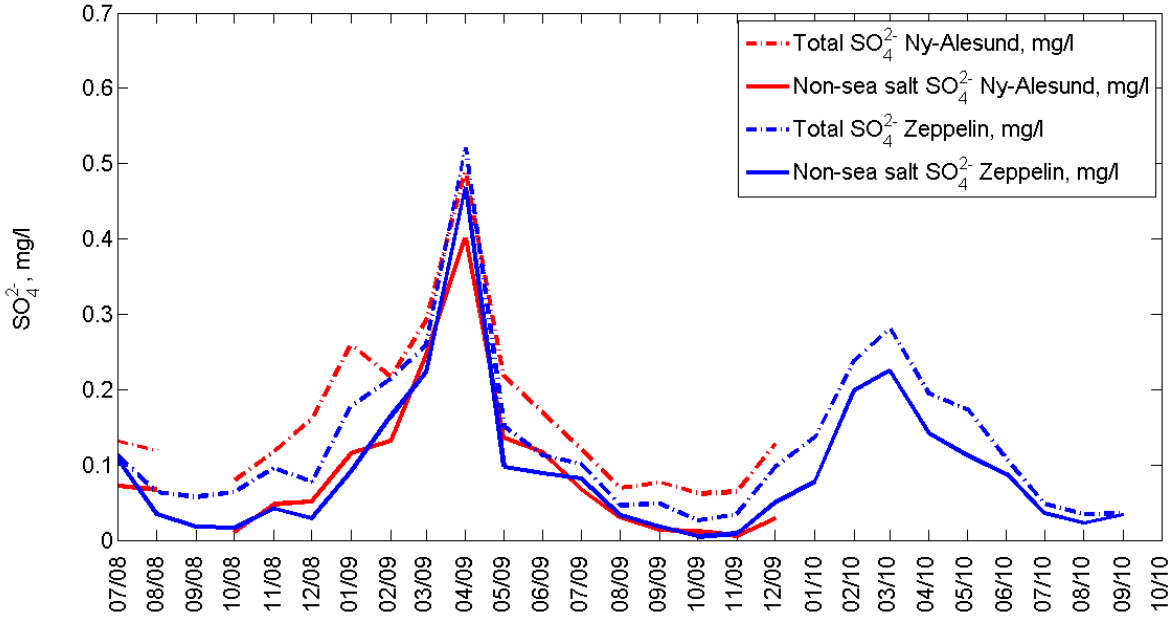

Figure 43 The total and sea salt corrected monthly mean concentrations of sulphate measured at Zeppelin and in Ny-Ålesund

Figure 44 shows seasonal mean particle concentration for sizes with d≈200nm typical for the accumulation mode during the Arctic haze time where the sulphate presents 40% of the total mass in long-range transported polar aerosol (Seinfeld and Pandis 2006). The aerosol data used in chapter 5 are displayed here to depict the connection between two different datasets. One can see that the highest mean particle concentrations are observed in spring 2009 and 2010 correlating very well with the theory described in chapter 1,with previous studies and with trend in Figure 43 (Tunved et al. 2013).

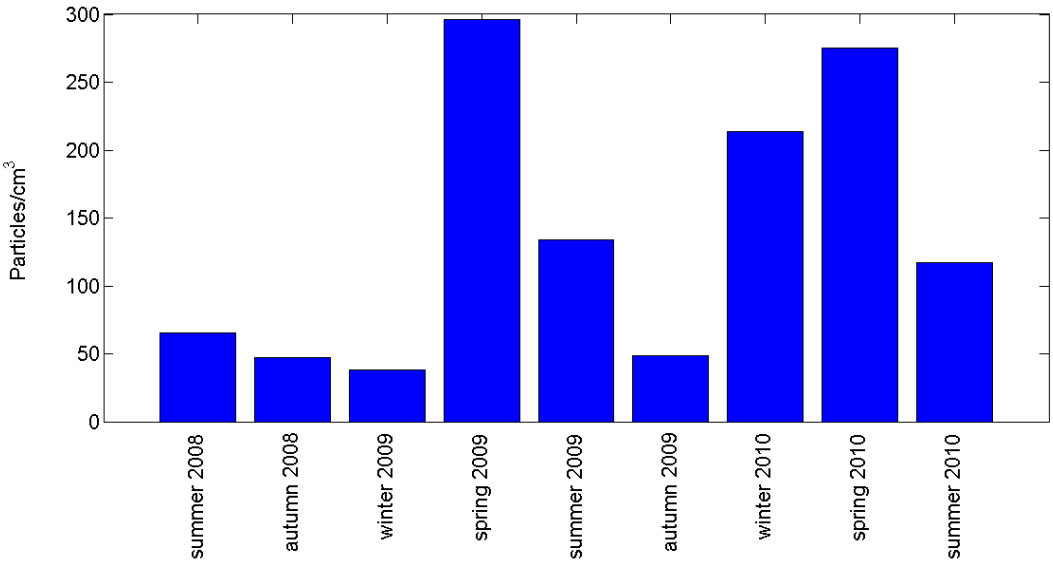

Figure 44 Seasonal mean particle concentration for sizes with d≈200nm

The highest sulphate concentration 1.13 μgS/m^3 was observed at the Zeppelin station 27.04.2009. The trajectories for this day shown in Figure 45 indicate that the air could be transported from Russia.

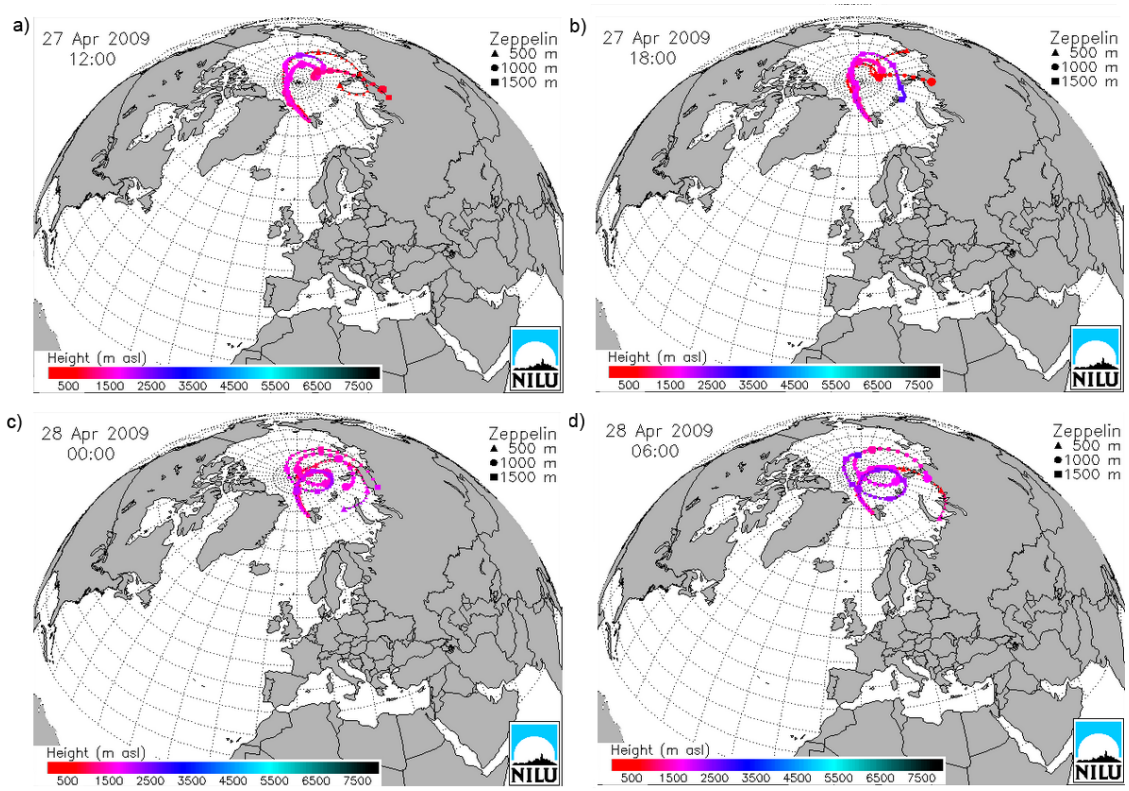

Figure 45 The trajectories for 27.09.2009, the day when the highest sulphate concentration was observed at the Zeppelin station

Monthly average SO_2 data from filters from Zeppelin and Ny-Ålesund presented in Figure 46 show minimum values in summer time and maximum in winter and spring.

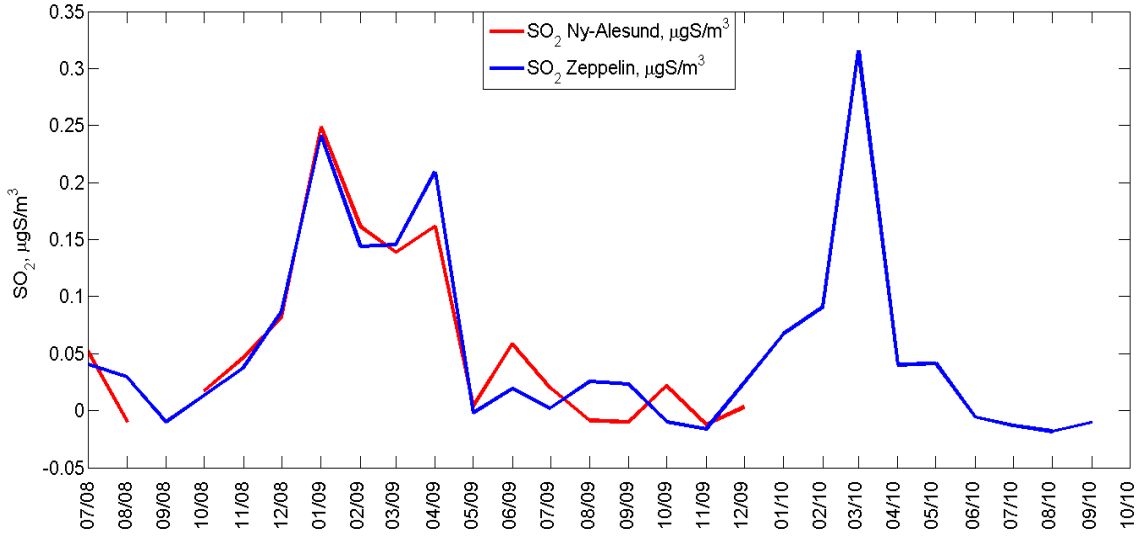

Figure 46 Monthly average SO_2 data from filters from Zeppelin and Ny-Ålesund

The distinct monthly peak in June 2009 in the data from Ny-Ålesund could be due to the ship traffic influence (Figure 30). However, there are no filter data from Ny-Ålesund for summer 2010 when the highest number of hourly SO_2 peaks for summer time was accompanied by presence of ships thus we cannot say precisely whether there is the strong influence of ships on filter samples.

The highest SO_2 concentration 2.5 μgS/m^3 was observed at the Zeppelin station 16.03.2010. The trajectories for this day shown in Figure 47 indicate that the air could be transported from Europe and European part of Russia.

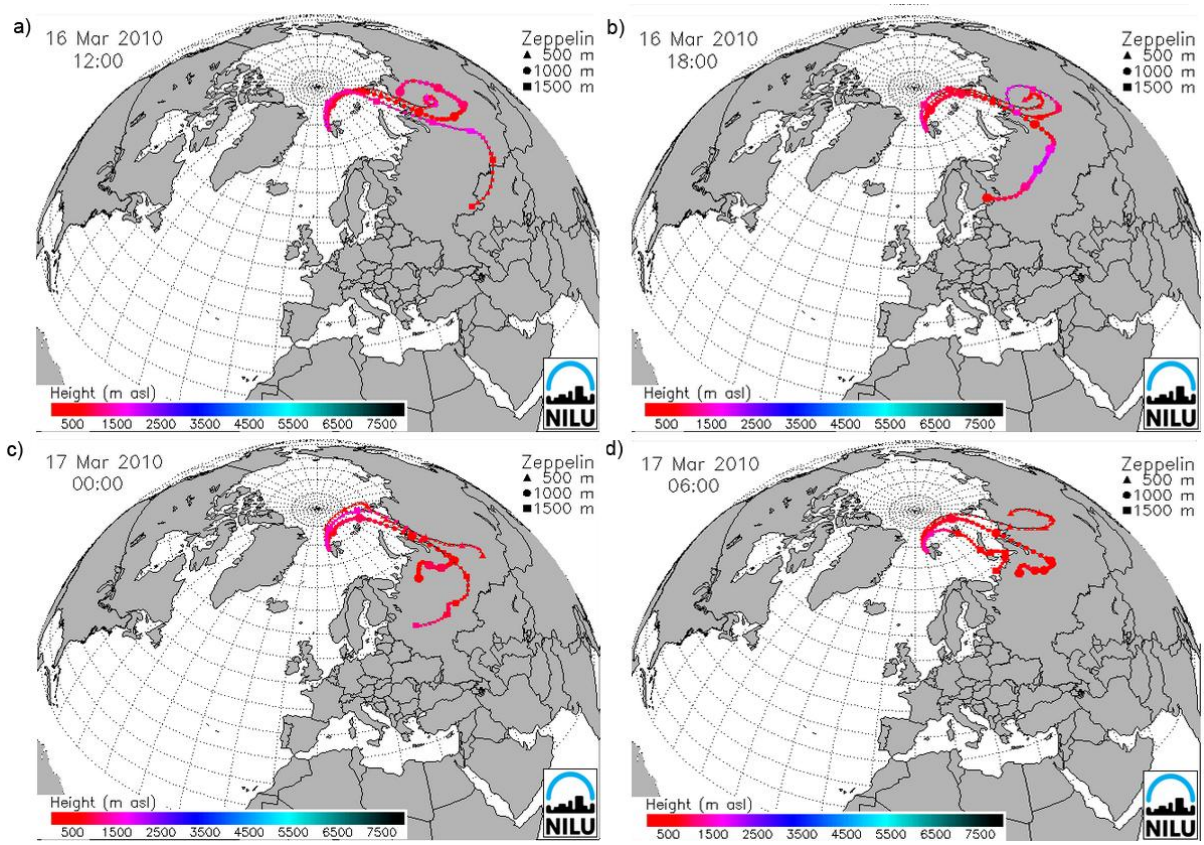

Figure 47 The trajectories for 16.03.2010, the day when the highest sulphur dioxide concentration was observed at the Zeppelin station

The highest concentrations of SO_2 were measured in filter samples during wintertime, however, according to measurement description in the EMEP manual "the absorption of sulfur dioxide is quantitative at a relative humidity above 30% at temperature down to -10^{o}C" (NILU 1996). Although the temperature dependence of efficiency is not so strong and the data for days with lower temperatures still can be used (Lewin and Zachau-Christiansen 1977), there were 5 days when the humidity was less than 30% . During these days (05.02.2009, 06.02.2009, 19.02.2010, 21.02.2010, 06.12.2010) the filter efficiency is strongly

reduced.

The gas-to-aerosol ratio can be overestimated on the impregnated filters and underestimated on the front filter while according to (Aas et al. 2012) the sum of nitrate (HNO_3 (g) + NO_3 (s)) and sum of ammonium (NH_3 (g) + NH_4^+(s)) in the filter pack measurements are unbiased thus they have been used in the thesis.

One can see from the Figure 48 that monthly average sum of nitrate and sum of ammonium concentration measured in Ny-Ålesund are extremely high for August, October, November and December 2009. According to NILU (personal communication), this could be due to the measurement error (contamination of the filters by manufacturer) during several days in these months.

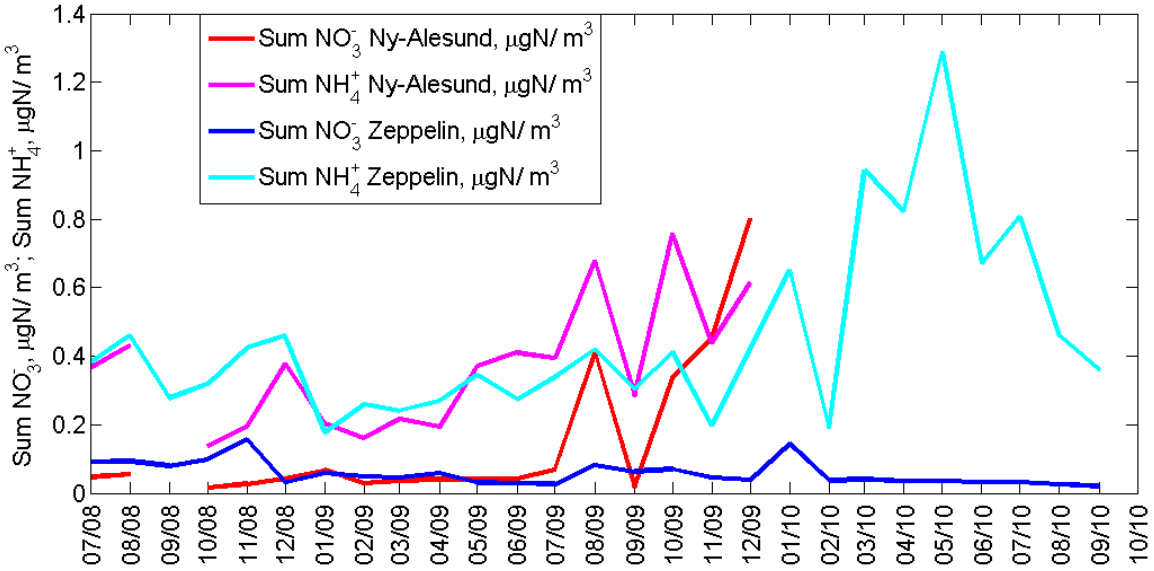

Figure 48 Monthly average NO_3^- and NH_4^+ concentration measured at filters at the Zeppelin station and in Ny-Ålesund

The distribution of monthly mean NH_4^+ data from the Zeppelin station shown in Figure 48 reveals that the influence of the summer time boreal fires plumes on ammonium concentration in Arctic mentioned in chapter 1 is less pronounced than impact of the spring agricultural fires in Eastern Europe. Many trajectories during spring and summertime 2010 were from this region. The influence of the agricultural burning biomass in the Russian Federation was observed previously during record smoke event in the European Arctic in May 2006 (Treffeisen et al. 2007)

The highest NH_4^+ concentration 2.44 µgN/m^3 was observed at the Zeppelin station 18.05.2010. The trajectories for this day shown in Figure 49 indicate that the air could be transported from Europe and European part of Russia.

In addition to NH_3 forest and agricultural fires are source of EBC and NO_x as was mentioned in chapter 1. Thus coincidence of the ship traffic maximum and summer time biomass burning could lead to misinterpretation of the data.

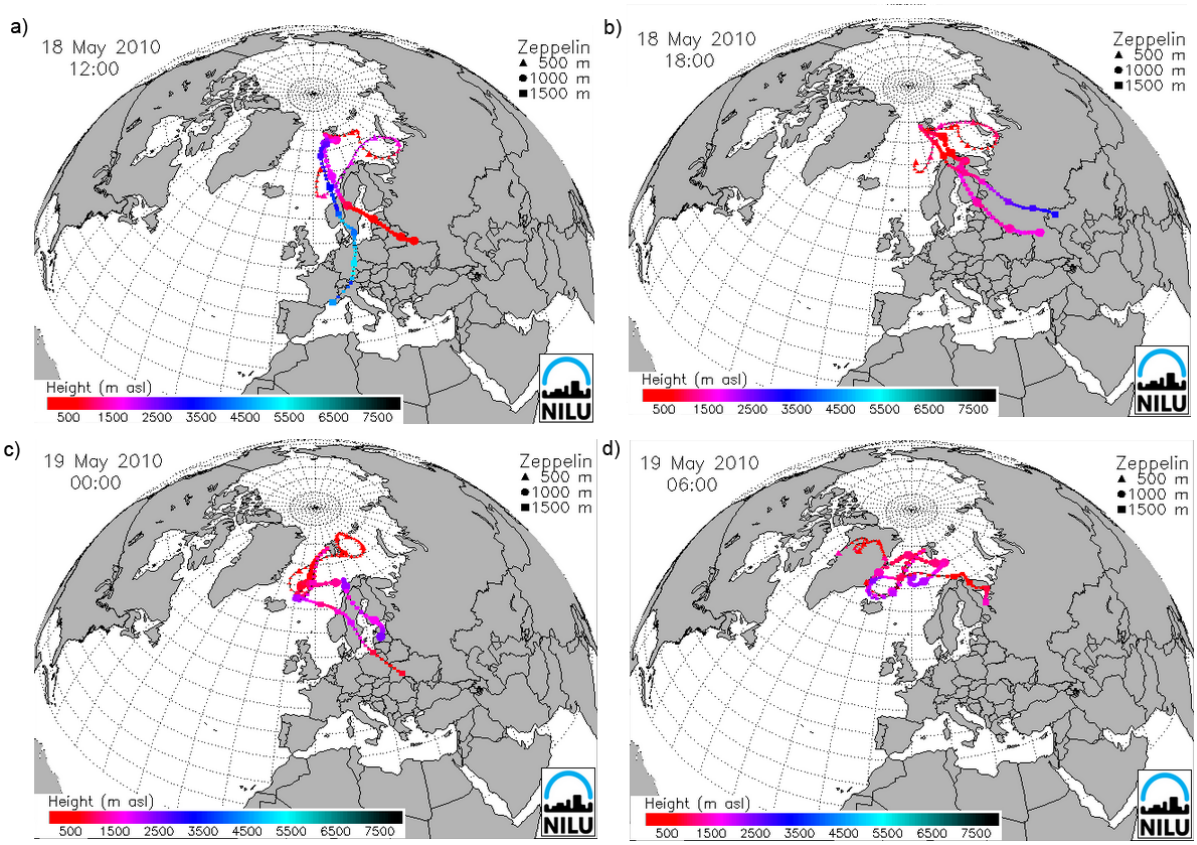

Figure 49 The trajectories for 18.05.2010, the day when the highest ammonia concentration was observed at the Zeppelin station

However, the characteristic sizes of particles described in the literature for smoke from forest fires are around 200 nm and 400 nm for fresh and long-range transported plume, respectively (Colarco et al. 2004; Müller et al. 2007). These numbers are much higher than the range of 3-100nm used in the chapter 5 for aerosol assessment thus one can distinguish between local pollution from ships and long range transport of biomass burning plume.

6.3 Comparison of daily data from filter samples in the Zeppelin station and in Ny-Ålesund

The comparison of days of possible impact from the local pollution defined in chapter 5 has been done for all days listed in Table 7.

Only for size 50-10nm there was coincidence between possible day of pollution filtered for SO_2 and aerosol and elevated concentration of SO_2 in the filter sample in Ny-Ålesund for 21.06.2009. For Zeppelin there was no evidence of influence on filter samples

concentration from local pollution.

One can see from Figure 50 that the concentration of aerosol at the Zeppelin station was elevated almost during the whole day 21.06.2009 which indicates that it probably was not connected with local pollution. However, peaks of SO_2 several times higher than the mean value of 1.69μg/m^3 occurred on the monitor only when at least one big ship or many smaller ones were at the pier. This means that if filter samples for EMEP monitoring would be placed in the village but not at the Zeppelin station they probably would be affected by local pollution.

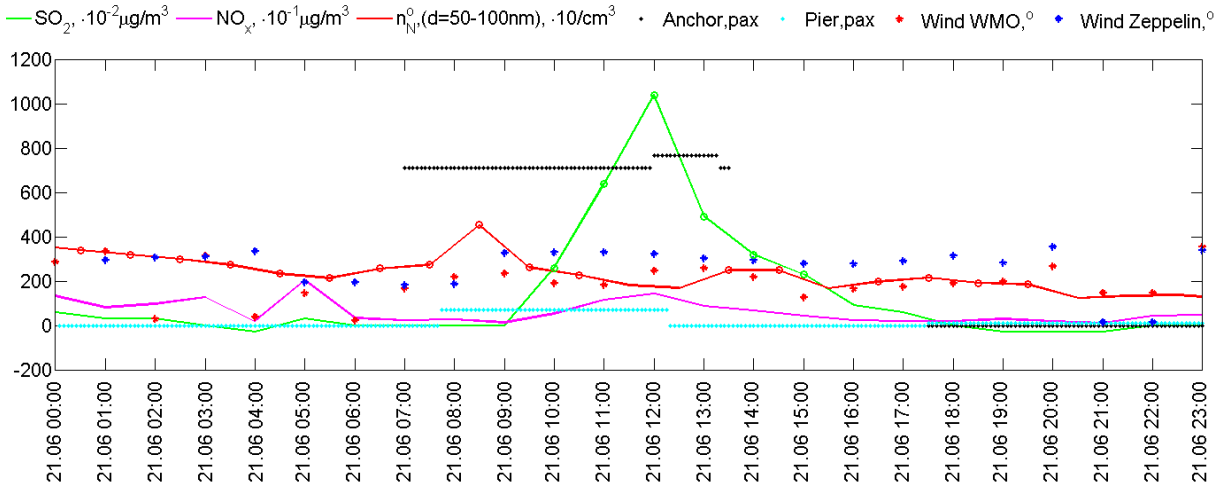

Figure 50 The day of possible influence of local pollution on the sulphur dioxide filter samples in the Ny-Ålesund

For sizes 50-10nm and 3-10nm there was coincidence between possible day of pollution for SO_2 and aerosol and elevated concentration of SO_4^{2-} in the filter sample in Ny-Ålesund for 20.06.2009. For Zeppelin there was no evidence of influence on filter samples concentration from local pollution. However, one can see from Figure 51 that the concentration of aerosol at the Zeppelin station was elevated during the whole day 20.06.2009. One can see in the Figure 52 that the FLEXTRA model shows trajectories over Atlantic during that day.

Thus, a possible explanation could be natural new particle formation observed at the Zeppelin station. While two distinct peaks of SO_2 and NO_x observed in the village may result, for example, from car traffic.

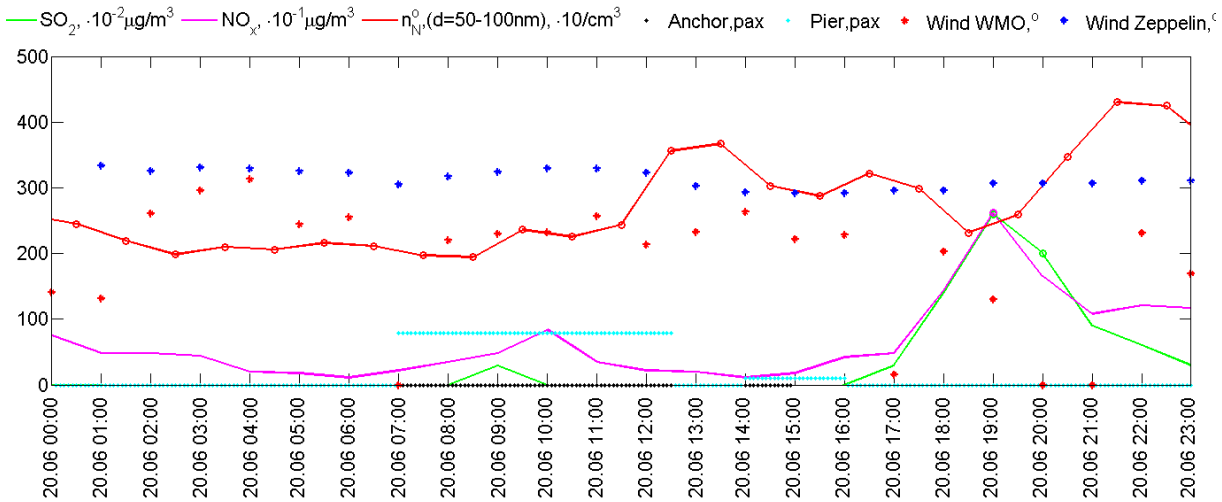

Figure 51 The day of possible influence of local pollution on the sulphate filter samples in the Ny-Ålesund

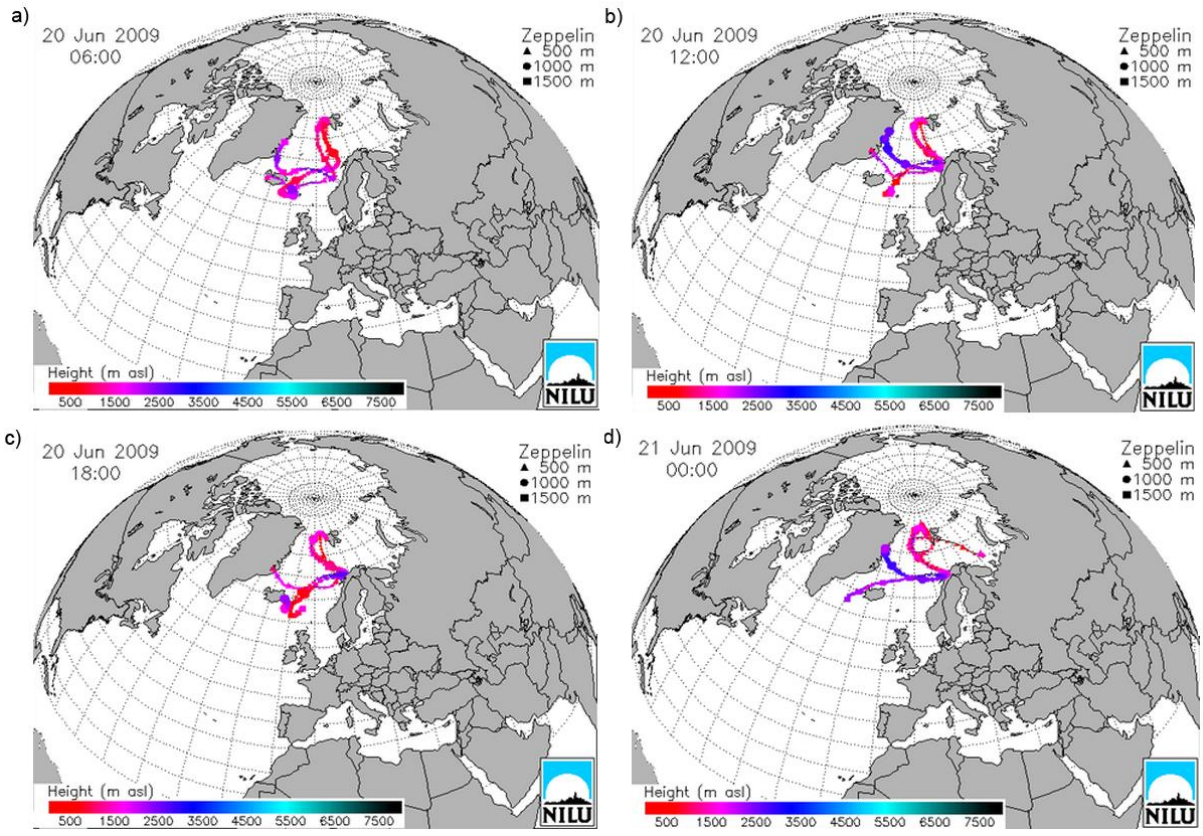

Figure 52 Trajectories for the 20th of June, 2009

No coincidence for sum of nitrate and days of possible pollution for NO_x defined in previous chapter has been found, neither in Ny-Ålesund nor at the Zeppelin station.

7 Discussion

1) The analysis of the aerosol peaks presented in the chapter 5 shows that the coincidence of intensive ship traffic and internal atmospheric characteristics in Ny-Ålesund such as wind and atmospheric stability described in chapter 3 create conditions where local pollution can be problematic. This is a particular trait during summertime (the majority of the peaks defined in Table 7 were during summertime). Furthermore, the influence of local pollution on the NO_x and SO_2 monitors concentration in the village was highest during summer 2010 as was suggested in the chapter 4.

However, in previous research and in chapter 5 it has been noted that the diurnal variability of the maximum concentration of particles with diameter less than 60 nm is observed during June, July and August (Tunved et al. 2013) in the afternoon. Thus there is autocorrelation with the diurnal cruise ship traffic maximum and maximum number of particles. Thus boundary layer nucleation events could have non-anthropogenic origin (for example result from the DMS oceanic emissions as was described in the chapter 1), or occur in the locally emitted fresh plume.

2) In this thesis emissions from elevated sources has been treated in an approximate manner. Despite the characteristics of such sources described in detail in the chapter 2 there is no information available at the moment about ships location, gases content and temperature and the stack height. Provided such values and information on atmospheric conditions it would be possible solve many ambiguities related to the spreading of cruise ship and power plant local pollution in Kongsfjorden.

3) The problem is complicated because of data measured in Ny-Ålesund and at the Zeppelin station (particle concentration and size distribution and hourly monitor peaks NO_x and SO_2) had different temporal resolution. The ambiguity is present in nature of measured chemical components as it was told in chapter 1 SO_2 and SO_4^{2-} can be both anthropogenic and natural origin and as one can see in Figure 51 using logically constructed filter described in chapter 5 during data processing it can be difficult to treat this properly. Thus may be the parametric controller used by (Heintzenberg and Leck 1994) to turn off the sampler when number concentration is rapidly increasing would solve the problem of local pollution. Similar to this controller could also set the mark about specific conditions such as, for example, sunshine duration and change in wind direction, but not switch the sampling completely though. It is less time consuming and would operate with real-time in situ parameters. For example, check after filtering for sunshine influence on new particle

formation gave astonishing result. For hours at Zeppelin with possible pollution from the village calculated in chapter 5 only 30% of hourly peaks of SO_2 and 48,5% % of hourly peaks of NO_x for diameter 50-100nm left after applying the criteria of sunshine duration less than 30minutes; for smaller diameters even less number of possible hours of pollution was left. This means that the total number of possible days of pollution shown in Table 7 would decrease significantly.

4) However, the most crucial problem is the days with absent meteorological data from Zeppelin because then nothing is known about the atmospheric structure and wind flow on the mountain. As one have seen from the Figures 20-24 the wind climate Ny-Ålesund is quite complex and even in the valley the data varies from one place to another. There were 6 more days of possible pollution with absent the meteorological data at Zeppelin station in June 2010 and 3 days in July 2010; 3 days in June 2010 and 2 days in July 2010 defined from aerosol filtering using NO_x and SO_2, respectively.

Conclusions

In the p.44 of the (Ciciotti et al. 2013) one can find the results of the convective PBL investigation where the case study for the 14th of June 2010 shows that the boundary layer height can reach up to 767m. This means that under such conditions and with presence of the north wind direction at the Zeppelin station the local pollution can reach the Zeppelin station. In the previously published substantiation report which was a long time an example for the further studies was stated that "the site is above any local inversion most of the time" and "the site should not be influenced by local pollution, on the other hand it should be accessible on a daily basis" (Braathen, Hov, and Stordal 1990). The convective PBL which can develop most effectively in the summer due to prevailing unstable conditions when the influence of the local pollution could be the most significant due to cruise ship traffic poses the treat to the goals stated when the Zeppelin station was constructed. This is why the Richardson number calculation and measurements of wind direction at the Zeppelin station are crucial parts of the stability and local pollution analysis.

Environmental and climatic effects of the emissions on Svalbard could be evaluated using dispersion modelling (Vestreng, 2009). However, the same technique can be implemented also in order to estimate influence of local pollution on measurements in the Ny-Ålesund and at the Zeppelin station. The dispersion model set for the plume from the power station would allow to estimate input from this local source to the measured concentration of pollutants under different atmospheric stability conditions.

Further the same model can be adapted for evaluation of ship traffic emissions impact and regional pollution assessment.

Clear seasonality of concentration both SO_2 and NO_x was revealed. Average values of compounds measured by monitor increase every summer and winter and decrease every autumn and spring. The possible reasons for these features are summertime ship traffic as an additional seasonal source of pollution in Ny-Ålesund and wintertime long-range transport detected by the monitor.

However, statistically influence of local pollution assumed to be brought to the monitor by northerly winds is very different for NO_x and SO_2. The correlation between days with detected NO_x pollution and number of days with wind direction from North per month is 0.7217. This means that air with elevated concentration of NO_x arrives at the monitor mainly with NW-N winds.

Nevertheless, for SO_2 the correlation is not significant 0.0282. This could either mean

that SO_2 is dominated by long-range transport, or that summer time sulphur dioxide measurements are affected by a local unknown source (e.g. anchored cruise ship).

Simultaneous summertime measurements of NO_x and submicron particles at the Zeppelin could be recommended in order to control the filter samples regarding the long-range transport of the NO_x, NH_3 and EC from boreal and agricultural fires. This could solve ambiguities and exclude influence of local pollution on these measurement results because characteristic diameter of aerosol from forest plume (200-400nm) does not intersect the diameter of aerosol from local pollution (50-100nm).

Due to local topography only NW-N winds could bring the pollution from the village to the station. However, in this thesis we find that less than 3% from 389 days when northerly wind was measured at the Zeppelin station there was possibility for NO_x local pollution to reach the station level. This value correspond to less than 1,5% from total period of interest. For SO_2 these values are even lower: less than 2% and from 389 days when northerly wind was measured at the Zeppelin and less than 1% of the total number of measurement days. All possible cases of pollution have been revealed for summer time due to prevailing unstable atmospheric conditions. These numbers have been received using the aerosol concentration data from the Zeppelin station which are, however, affected very much by natural processes of nucleation. The results from filter samples showed no influence of local pollution. Nevertheless, these were daily data while for preciseness of assessment more frequent measurements are needed.

Despite relative abundance of NW-N winds at the Zeppelin station it is very rarely can be influenced by the flow from the village due to complexity of underlying wind fields. The winds from the nearest glaciers are commonly observed at the CCT station. This katabatic flow from SW affects the atmospheric conditions and disconnect the place from the village by stable stratification of the surface layer. Thus even in presence of Northerly wind in the village it most probably would be turned before reaching the Zeppelin station.

In general, Zeppelin remains a highly valuable remote place for long-term monitoring of background air with minimal influence of local pollution sources. If it will be so with changing regulations is to be revealed setting up the dispersion model and checking all worst-case scenarios for cruise ships under different atmospheric conditions.

This work also uncovers important micrometeorological features of the area which are especially significant to take into account producing databases and combining measurement results from different scientific stations around Ny-Ålesund.

Acknowledgements

I would like to express my gratefulness to my supervisor at the University of Tromsø and Norwegian Polar Institute, Kim Holmén, for inspiring cooperation and bringing an opportunity to me to be involved in the useful applied research and work within interesting and inspiring scientific environment. I appreciate very much his patience and encouragement, useful suggestions on the paper and help in search for data sources for this project. His comments were extremely helpful for developing of my scientific cognition, critical way of thinking and for improving the quality of the work.

I am especially thankful to logistics provided by the Norwegian Polar Institute, particularly by my supervisor Kim Holmén. The acquiring data from international scientific stations is a complex process involving many people, facilities and supplies that would be impossible to combine without coordination from the Norwegian Polar Institute. Furthermore, the most effective way to teach the student is to show the subject in reality, and thanks to Kim, I was lucky to have a chance to be see the Arctic nature peculiarities, and uniqueness of the Ny-Ålesund station in particular, for myself.

In the thesis, I combine analysis of various chemical and meteorological data with the modelling results. I would like to thank the staff of the Norwegian Meteorological Institute for freely available data from the Ny-Ålesund WMO station on the web-site eKlima.no, Hans-Christen Hansson from the Stockholm University for the aerosol data from the Zeppelin station, Ove Hermansen and Are Bäcklund from the Norsk institutt for luftforskning (NILU) for the monitor meteorological data and chemical measurements from Ny-Ålesund and from the Zeppelin station, Marion Maturilli from the Alfred Wegener Institute for Polar and Marine Research for all the AWI data extensively utilized in my thesis and Mauro Mazzola from The National Research Council of Italy for the Amundsen-Nobile Climate Change Tower data.

Kjetil Schanke Aas from the University of Oslo deserves special gratitude for permission to use the results of his simulation performed using the high resolution Weather Research and Forecasting model and providing valuable comments concerning the model.

I also would like to acknowledge the staff of NILU for freely available air mass trajectories on the web-site http://www.nilu.no/projects/ccc/trajectories/ calculated using the FLEXTRA model developed by Andreas Stohl (NILU) in cooperation with Gerhard Wotawa og Petra Seibert (Institute of Meteorology and Geophysics, Wienna) and using meteorological data provided from ECMWF (European Centre for Medium Range Weather Forcast).

I would like to express my gratitude Jan Even Ø. Nilsen for a very intelligible and

useful Statistical analysis and presentation of geophysical data course at UNIS and specific comments related to my Master project and all teachers at UNIS who gave me good understanding of the polar meteorology processes through the course AGF 213.

At last but not the least I would like to thank my husband and my mom for endless patience and encouragement. Without them I would not be the person I am now.

Appendix 1 Hourly monitor data from Ny-Ålesund

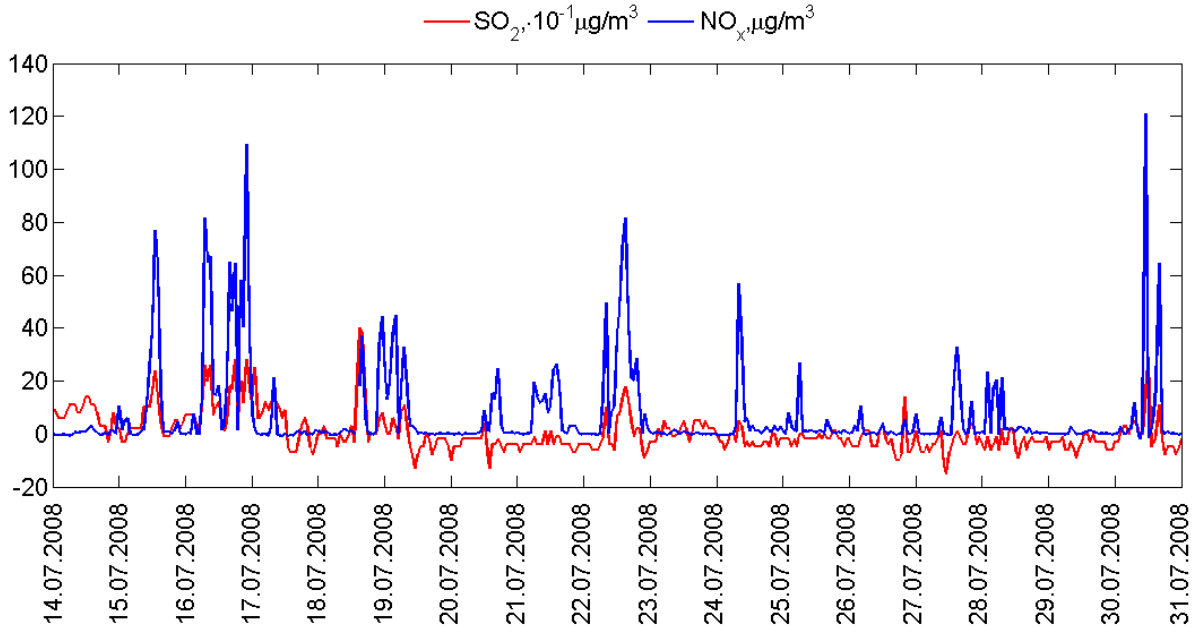

Figure 1 Hourly NO, NO_2, NO_x and SO_2 data from 14.07.2008 to 31.07.2008

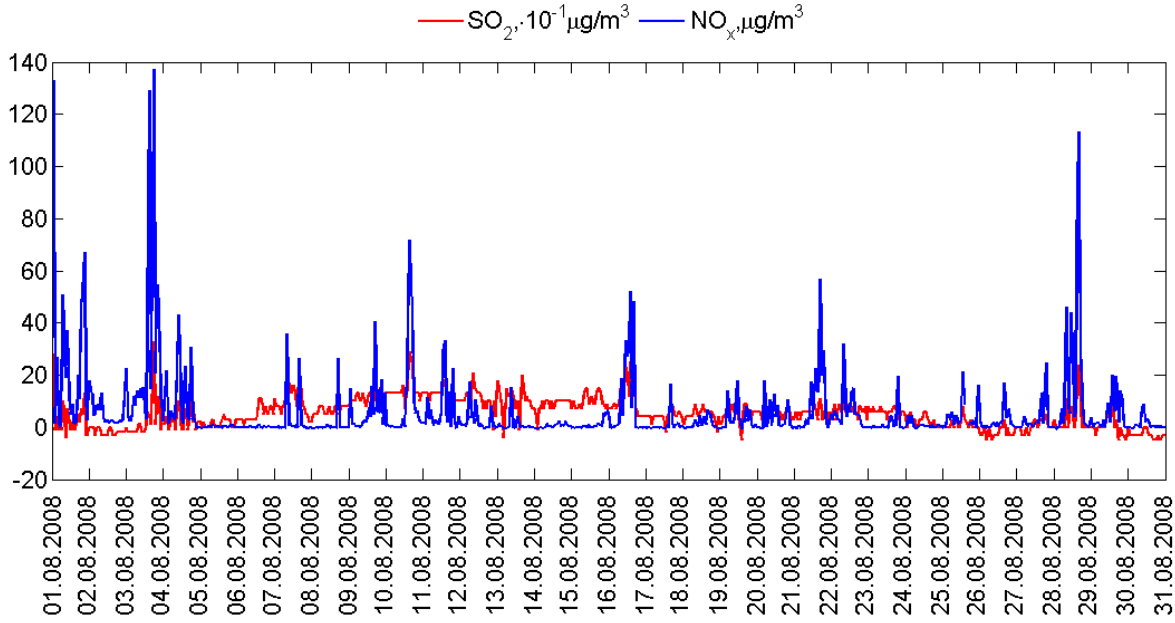

Figure 2 Hourly NO, NO_2, NO_x and SO_2 data from 01.08.2008 to 31.08.2008

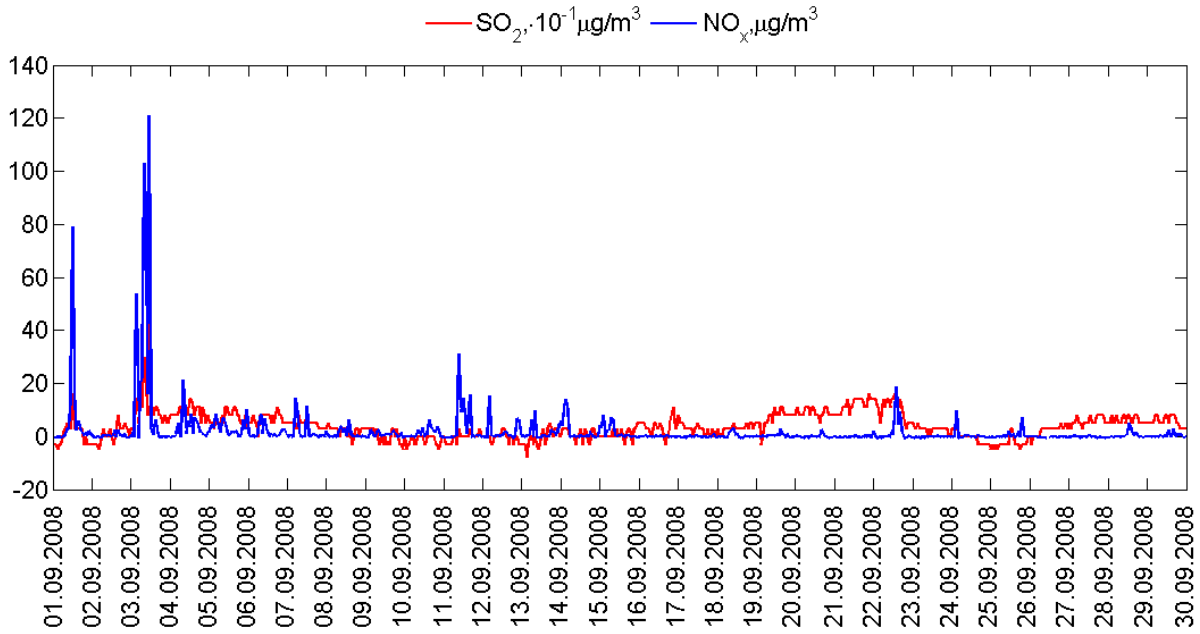

Figure 3 Hourly NO, NO_2, NO_x and SO_2 data from 01.09.2008 to 30.09.2008

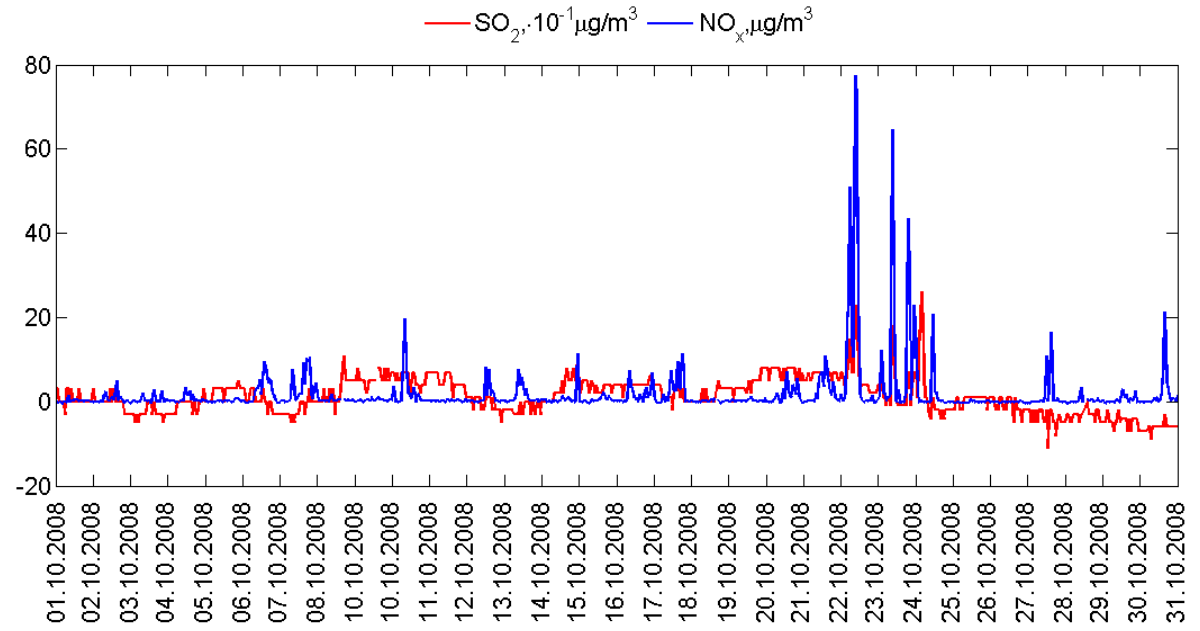

Figure 4 Hourly NO, NO_2, NO_x and SO_2 data from 01.10.2008 to 31.10.2008

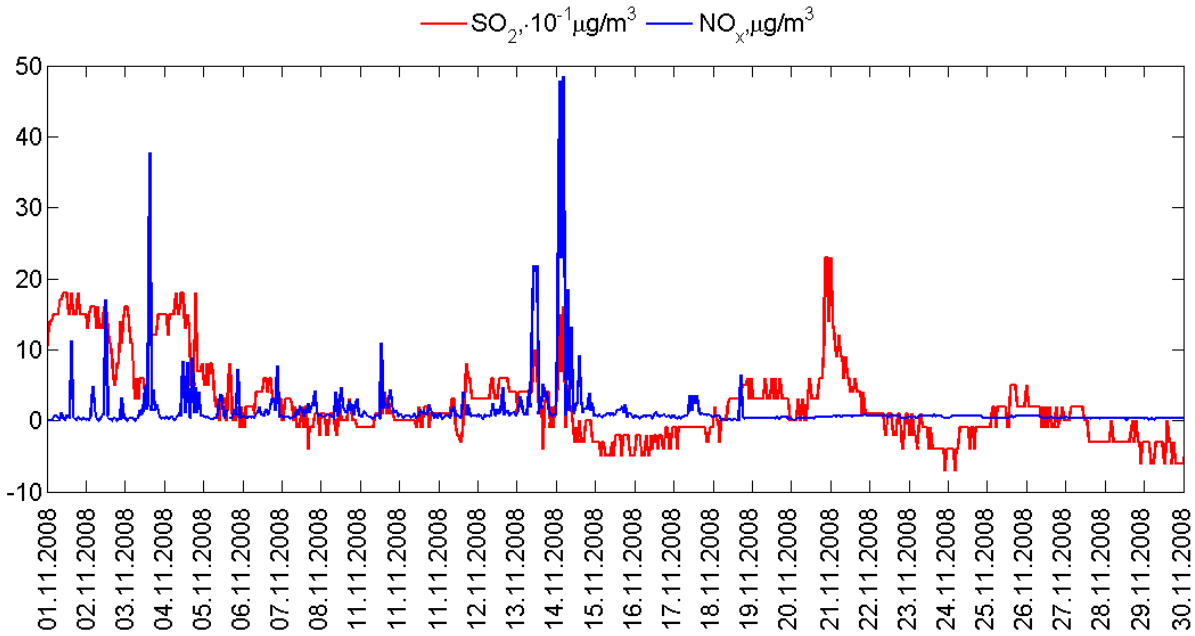

Figure 5 Hourly NO, NO_2, NO_x and SO_2 data from 01.11.2008 to 30.11.2008

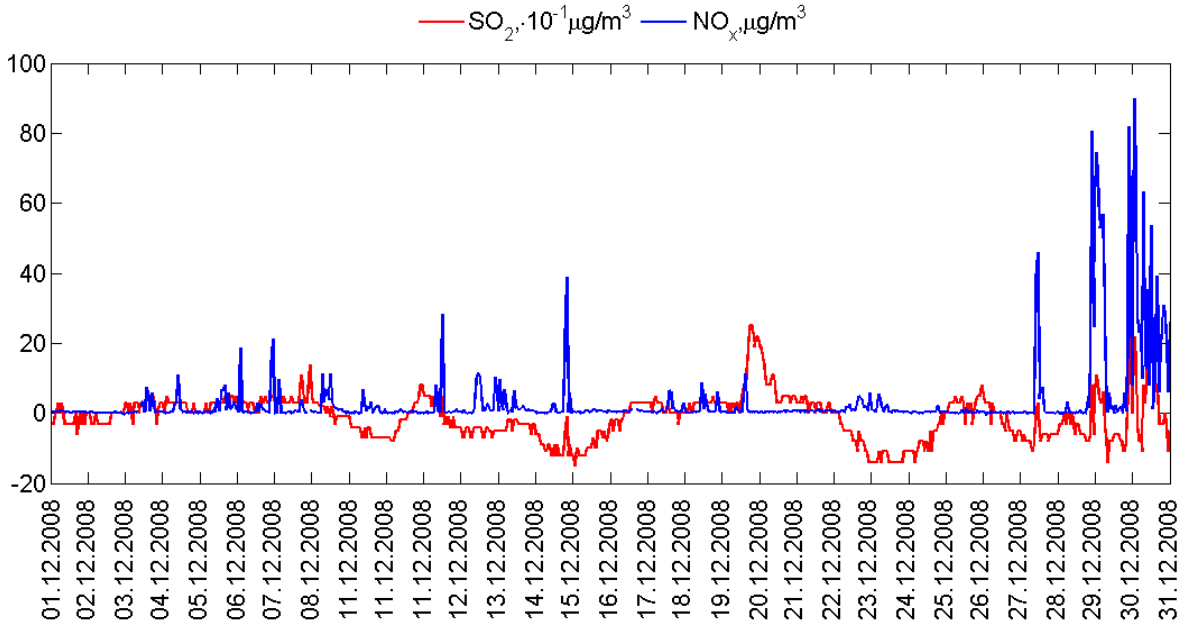

Figure 6 Hourly NO, NO_2, NO_x and SO_2 data from 01.12.2008 to 31.12.2008

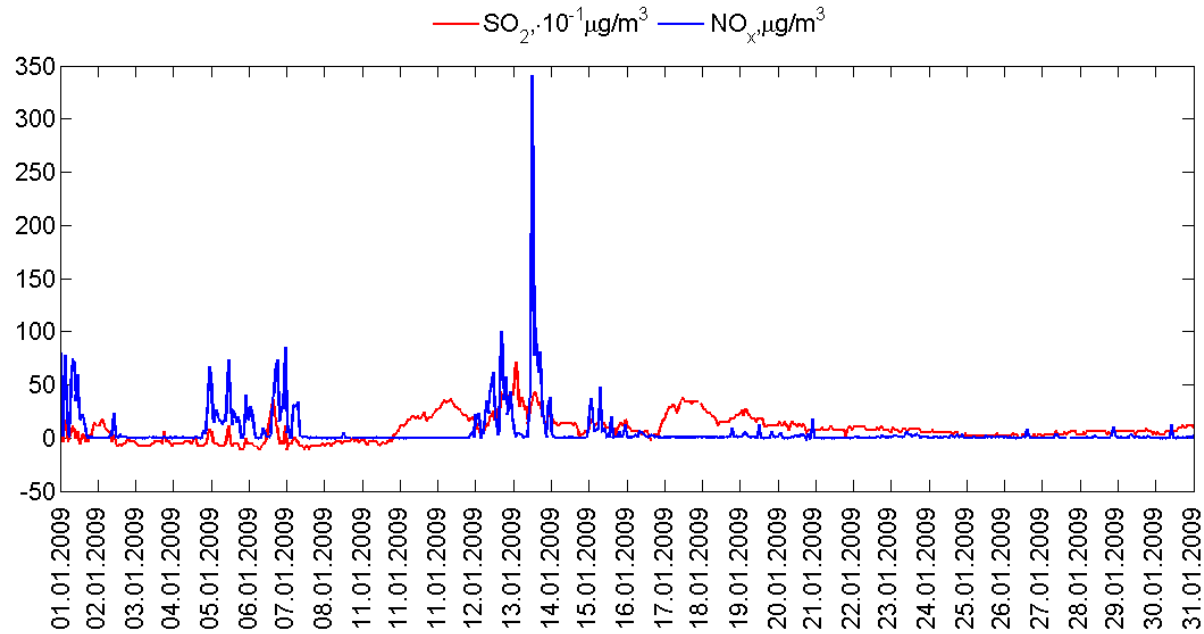

Figure 7 Hourly NO, NO_2, NO_x and SO_2 data from 01.01.2009 to 31.01.2009

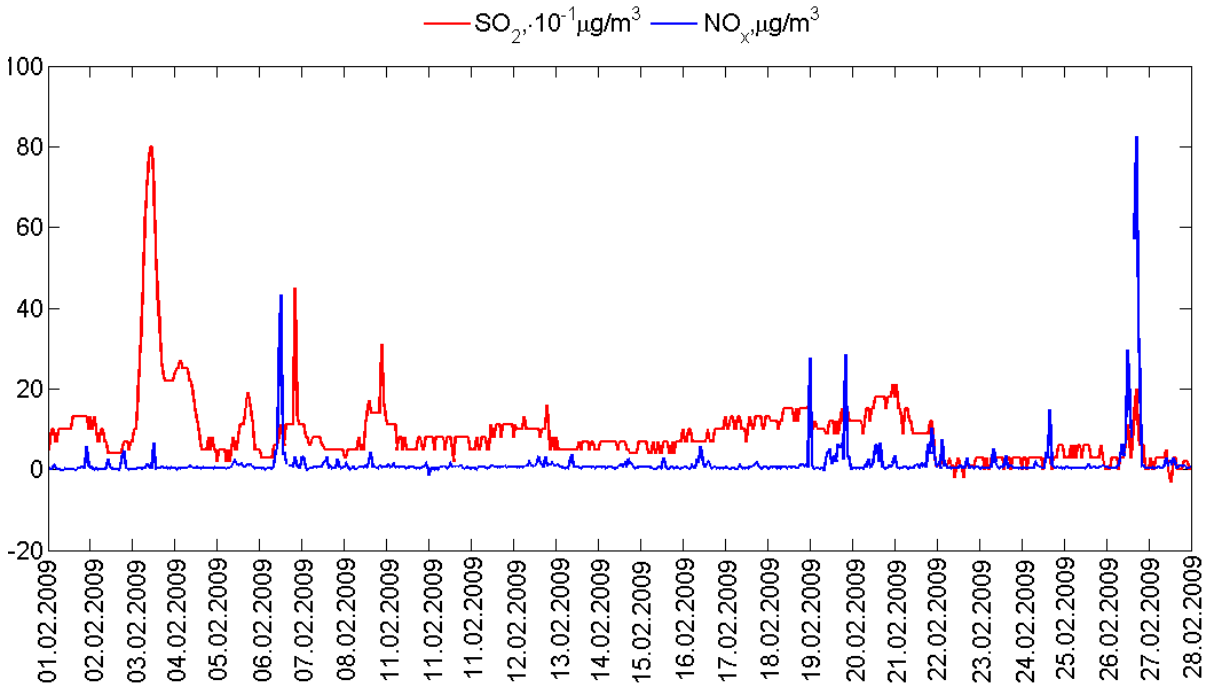

Figure 8 Hourly NO, NO_2, NO_x and SO_2 data from 01.02.2009 to 28.02.2009

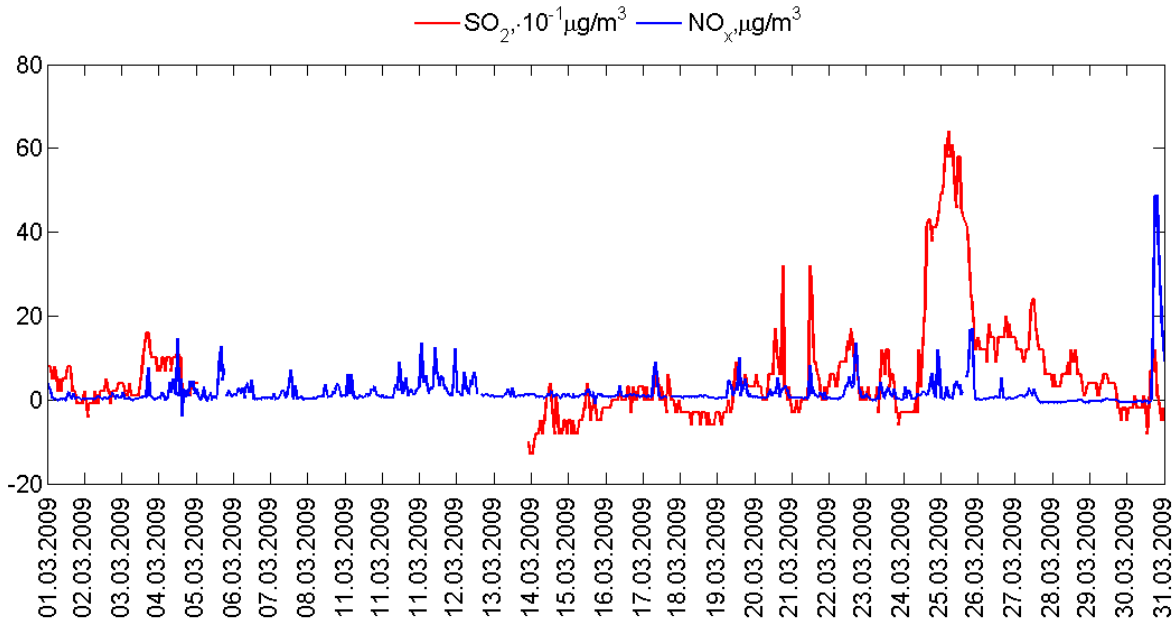

Figure 9 Hourly NO, NO_2, NO_x and SO_2 data from 01.03.2009 to 31.03.2009

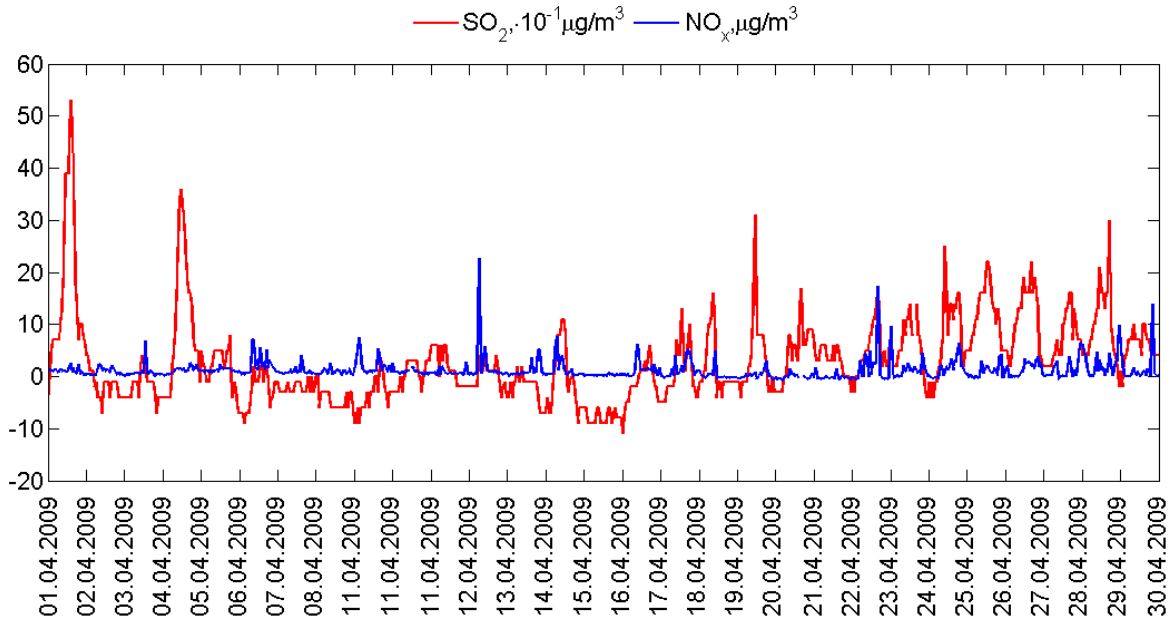

Figure 10 Hourly NO, NO_2, NO_x and SO_2 data from 01.04.2009 to 30.04.2009

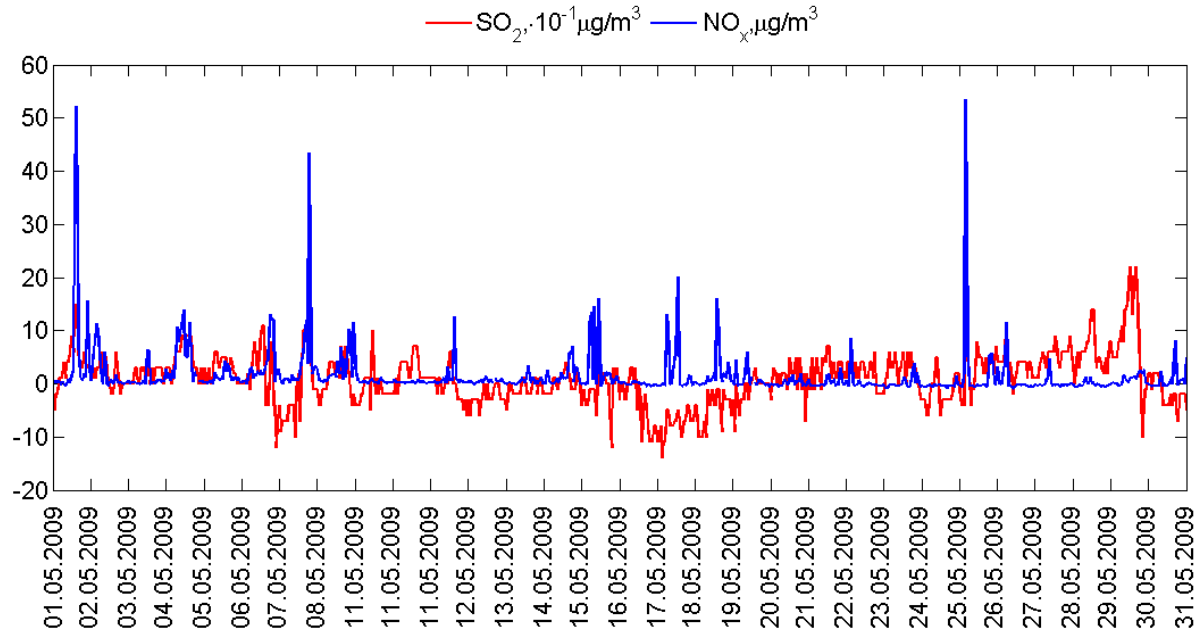

Figure 11 Hourly NO, NO_2, NO_x and SO_2 data from 01.05.2009 to 31.05.2009

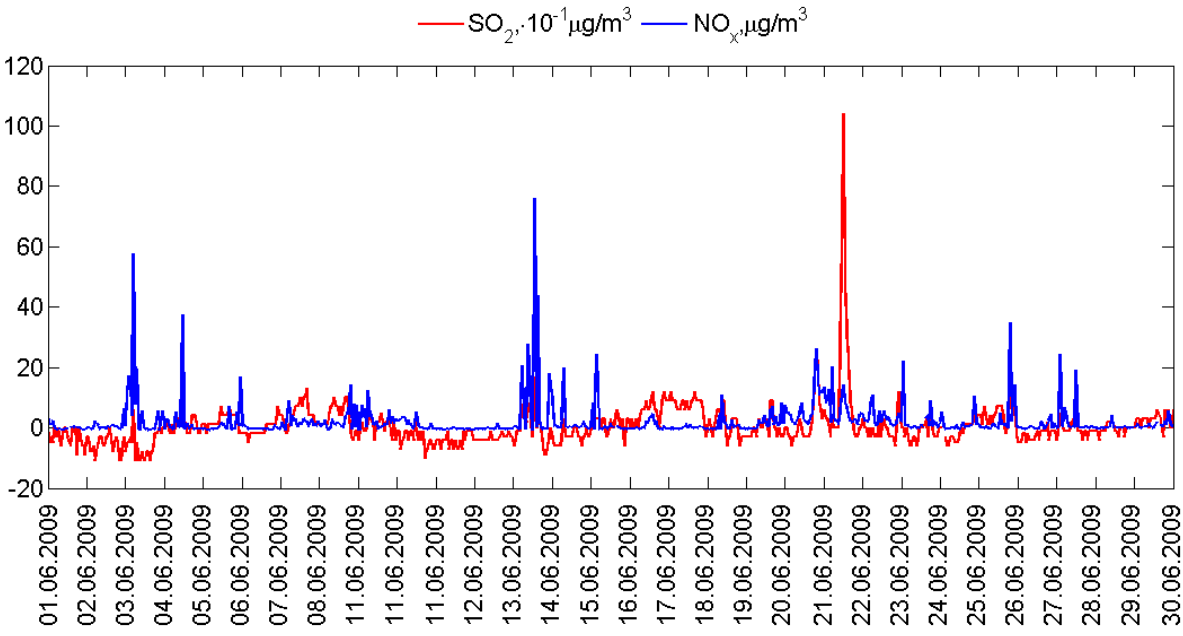

Figure 12 Hourly NO, NO_2, NO_x and SO_2 data from 01.06.2009 to 30.06.2009

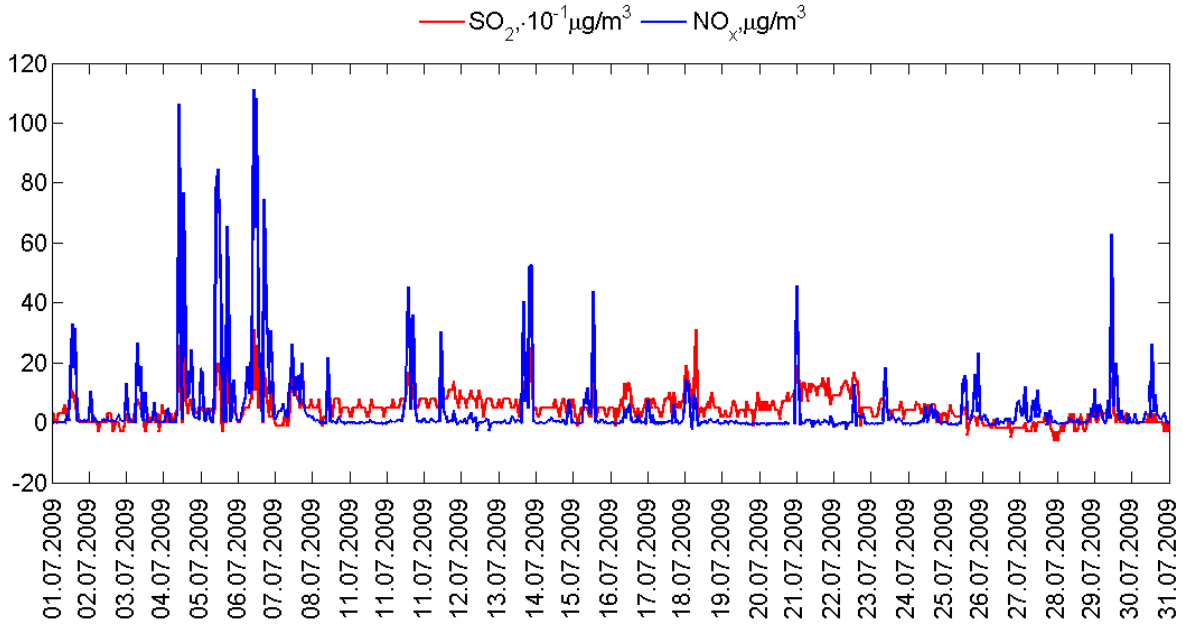

Figure 13 Hourly NO, NO_2, NO_x and SO_2 data from 01.07.2009 to 31.07.2009

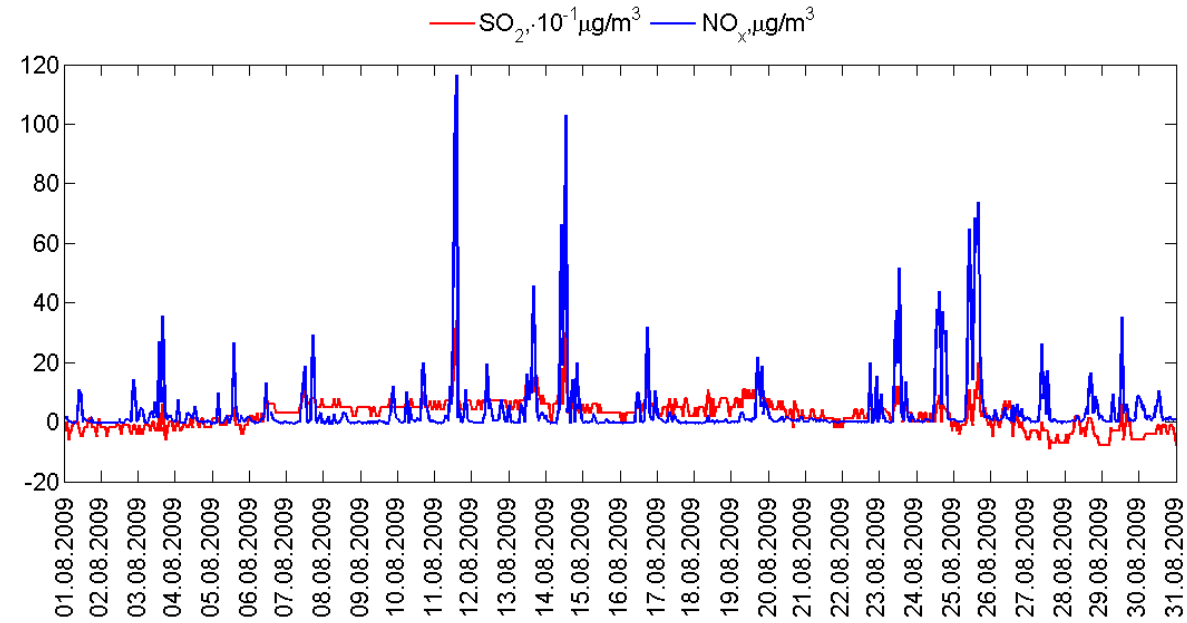

Figure 14 Hourly NO, NO_2, NO_x and SO_2 data from 01.08.2009 to 31.08.2009

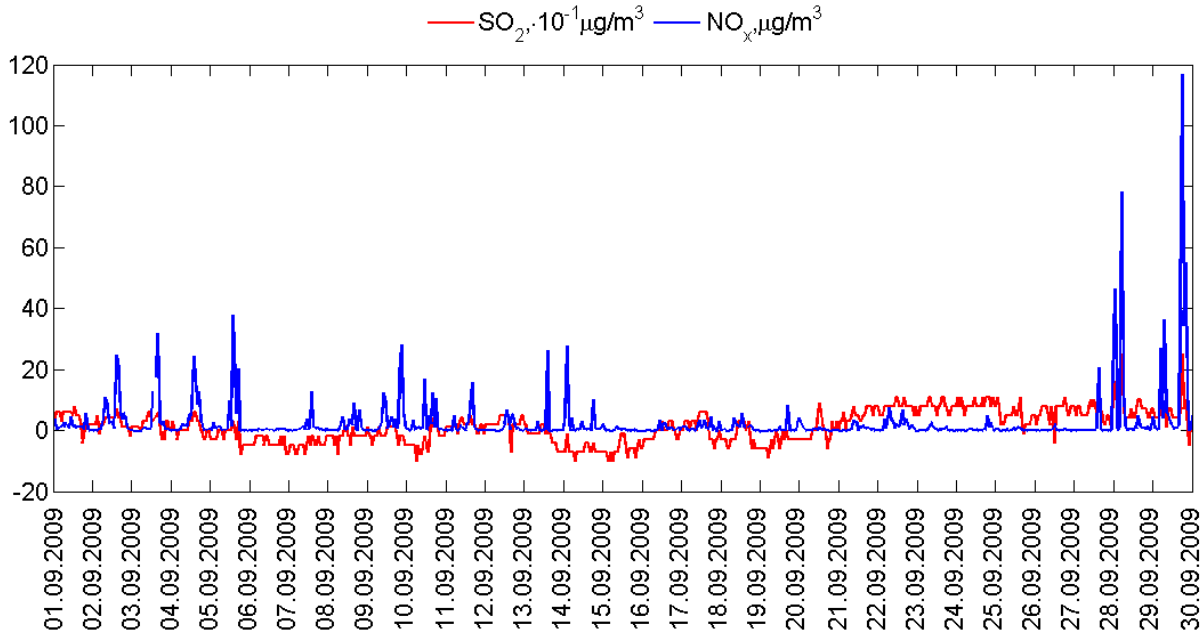

Figure 15 Hourly NO, NO_2, NO_x and SO_2 data from 01.09.2009 to 30.09.2009

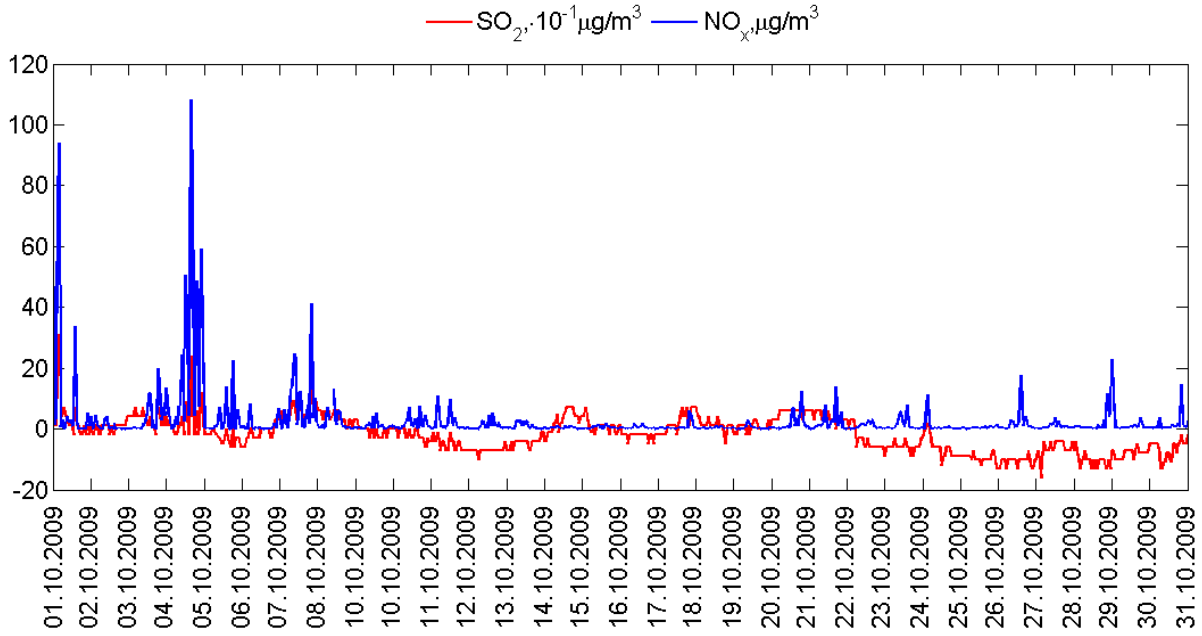

Figure 16 Hourly NO, NO_2, NO_x and SO_2 data from 01.10.2009 to 31.10.2009

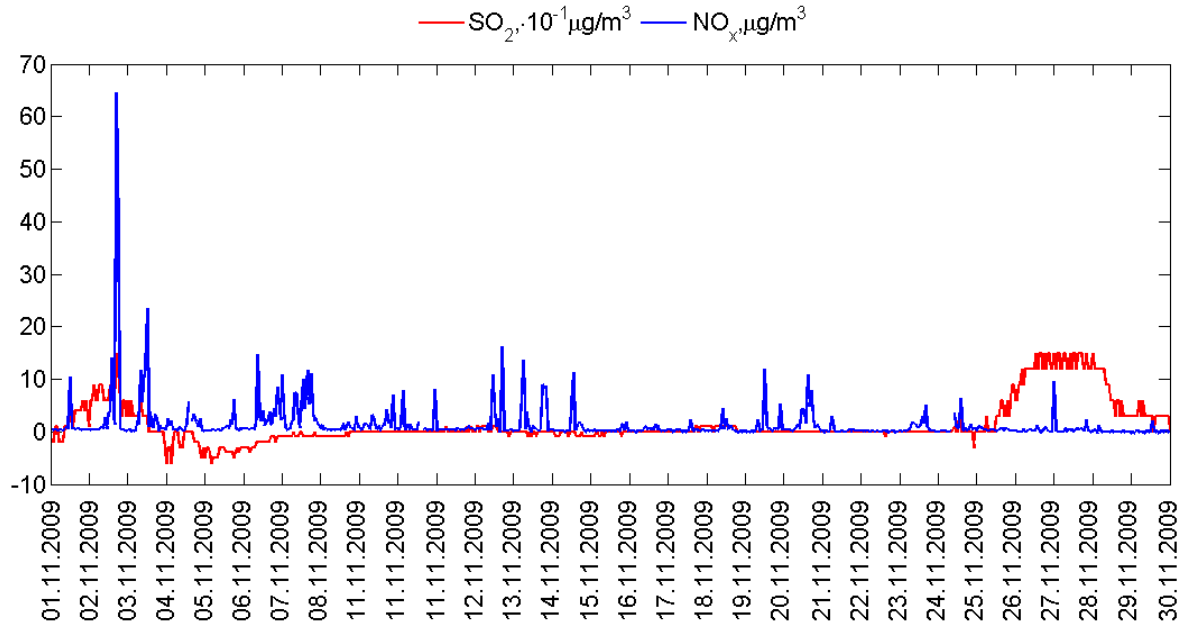

Figure 17 Hourly NO, NO_2, NO_x and SO_2 data from 01.11.2009 to 30.11.2009

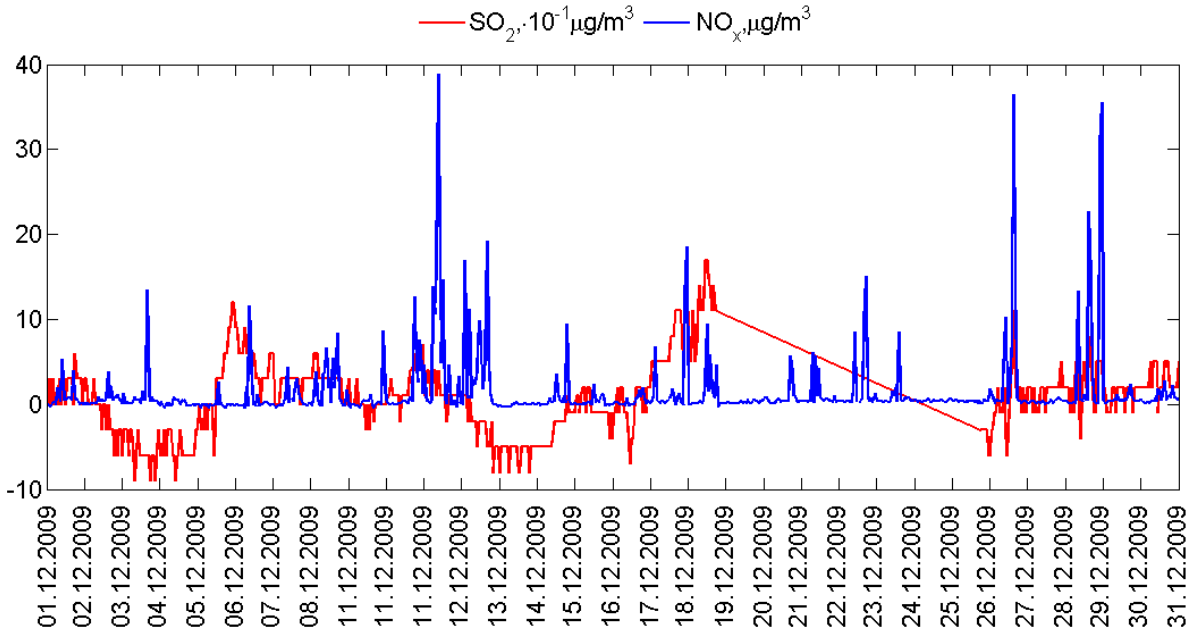

Figure 18 Hourly NO, NO_2, NO_x and SO_2 data from 01.12.2009 to 31.12.2009

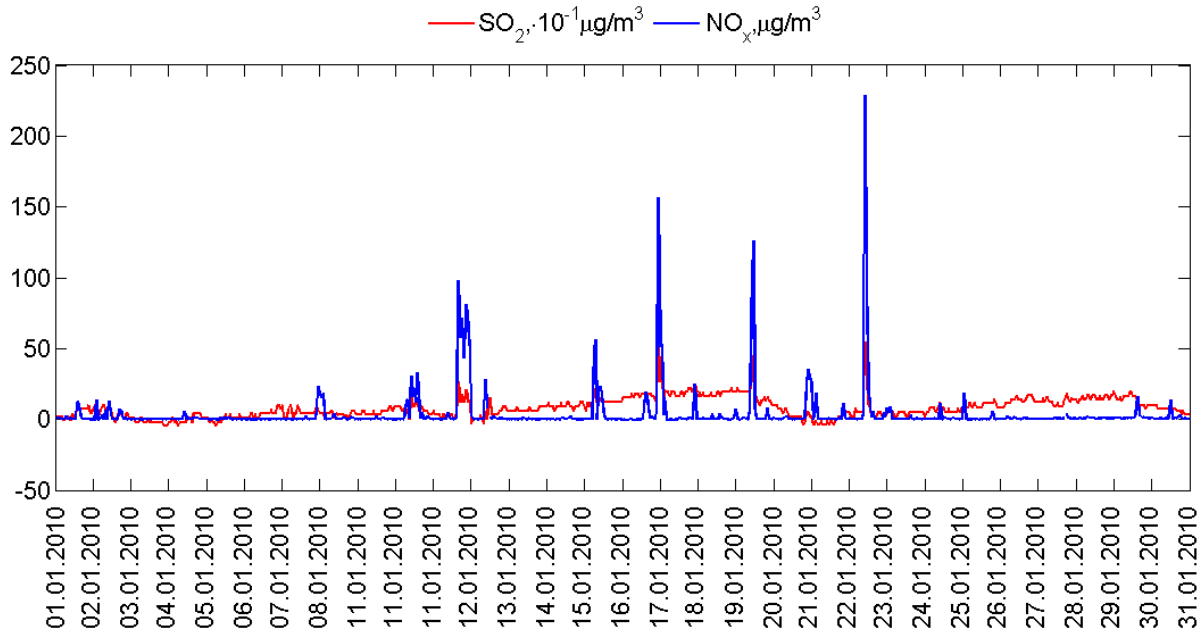

Figure 19 Hourly NO, NO_2, NO_x and SO_2 data from 01.01.2010 to 31.01.2010

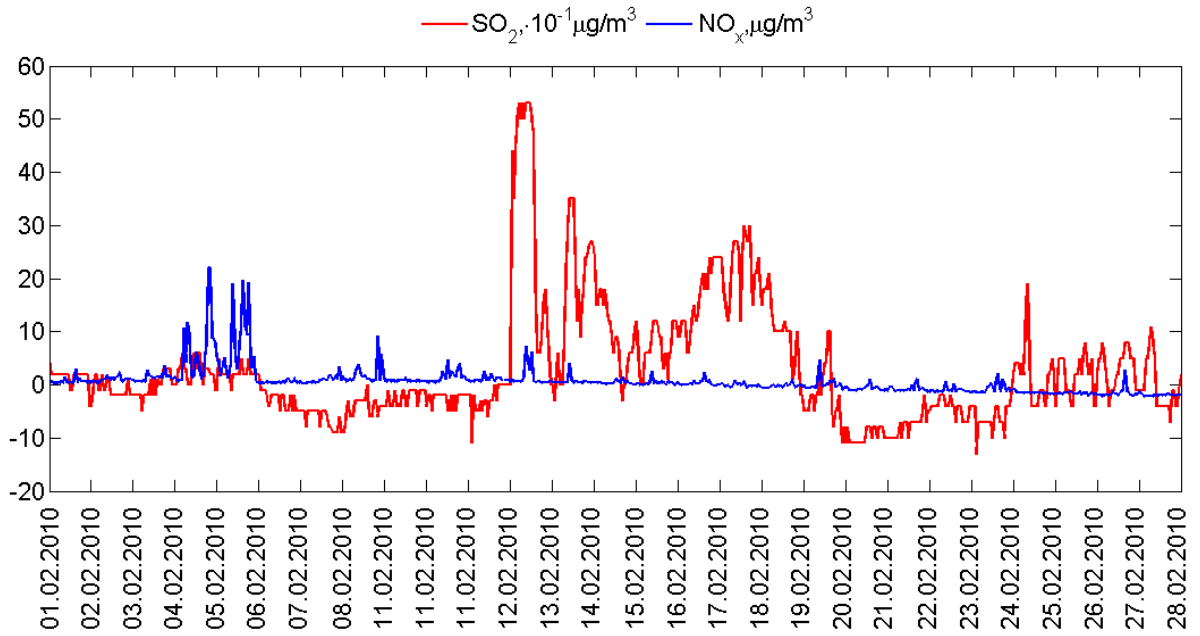

Figure 20 Hourly NO, NO_2, NO_x and SO_2 data from 01.02.2010 to 28.02.2010

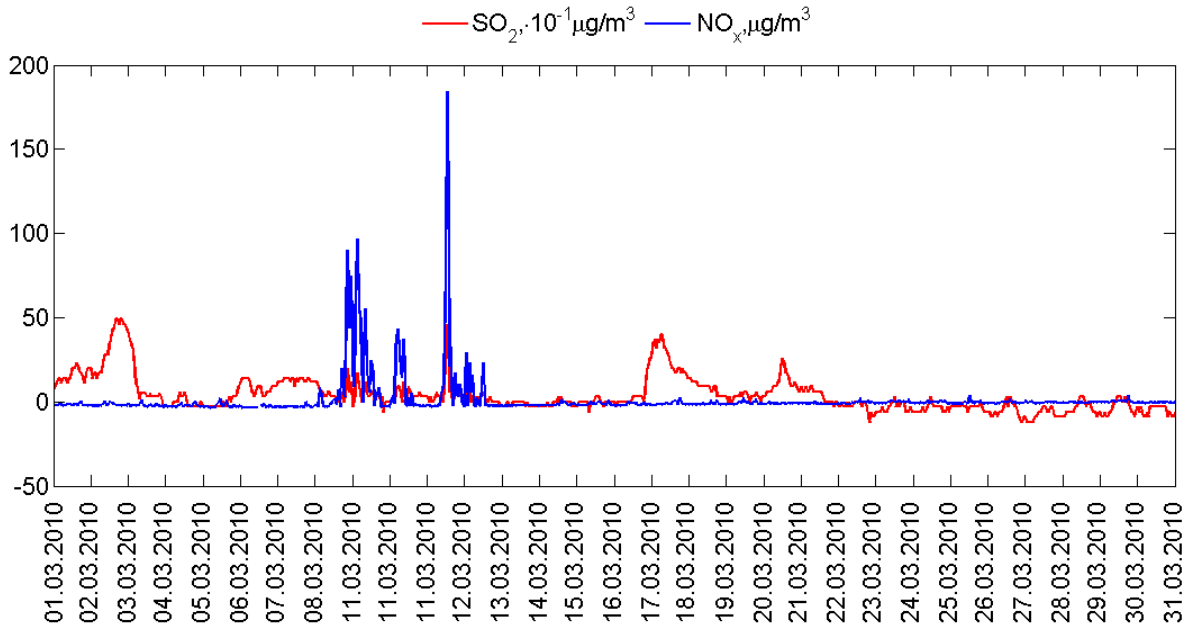

Figure 21 Hourly NO, NO_2, NO_x and SO_2 data from 01.03.2010 to 31.03.2010

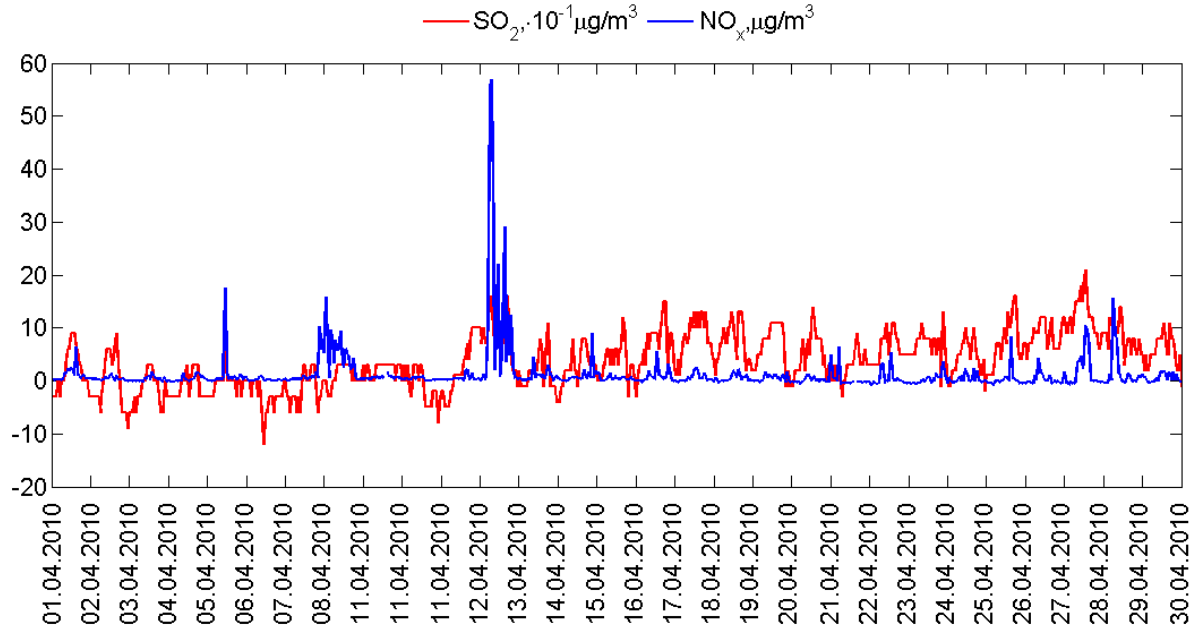

Figure 22 Hourly NO, NO_2, NO_x and SO_2 data from 01.04.2010 to 30.04.2010

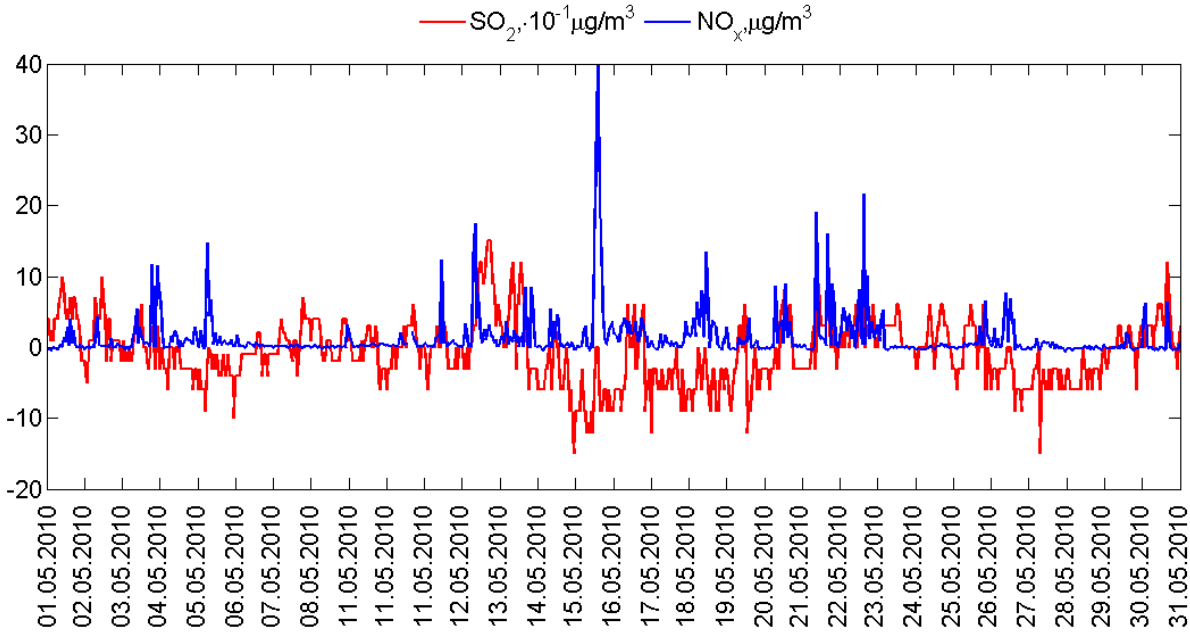

Figure 23 Hourly NO, NO_2, NO_x and SO_2 data from 01.05.2010 to 31.05.2010

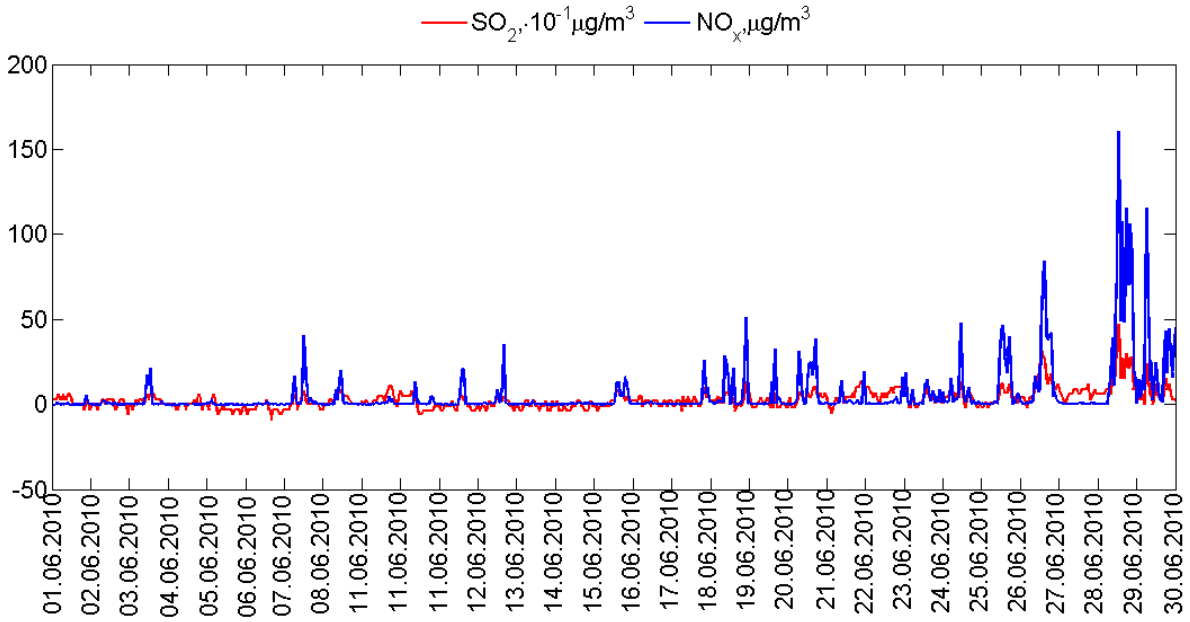

Figure 24 Hourly NO, NO_2, NO_x and SO_2 data from 01.06.2010 to 30.06.2010

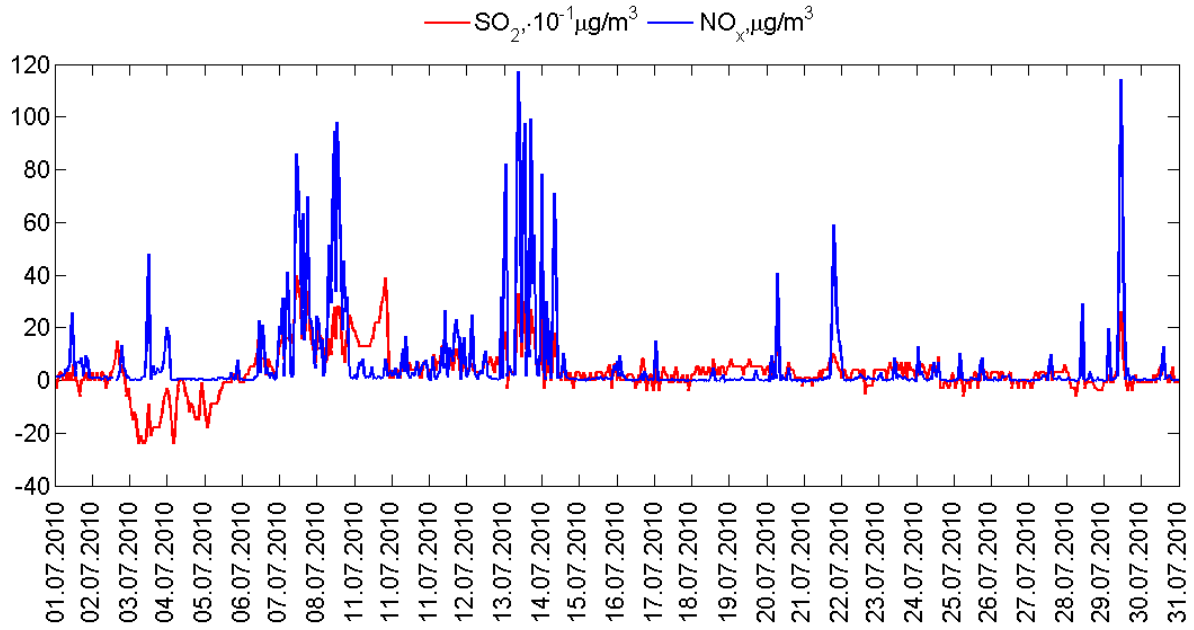

Figure 25 Hourly NO, NO_2, NO_x and SO_2 data from 01.07.2010 to 31.07.2010

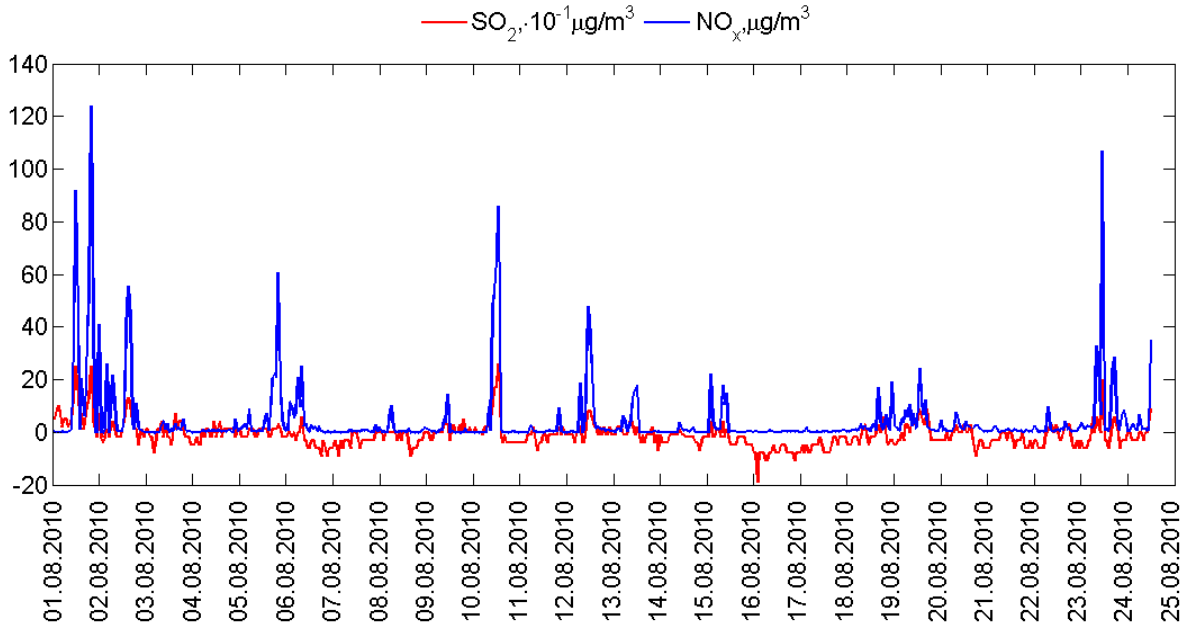

Figure 26 Hourly NO, NO_2, NO_x and SO_2 data from 01.08.2010 to 24.08.2010

Appendix 2 Daily data from the filter samples from the Zeppelin station and Ny-Ålesund

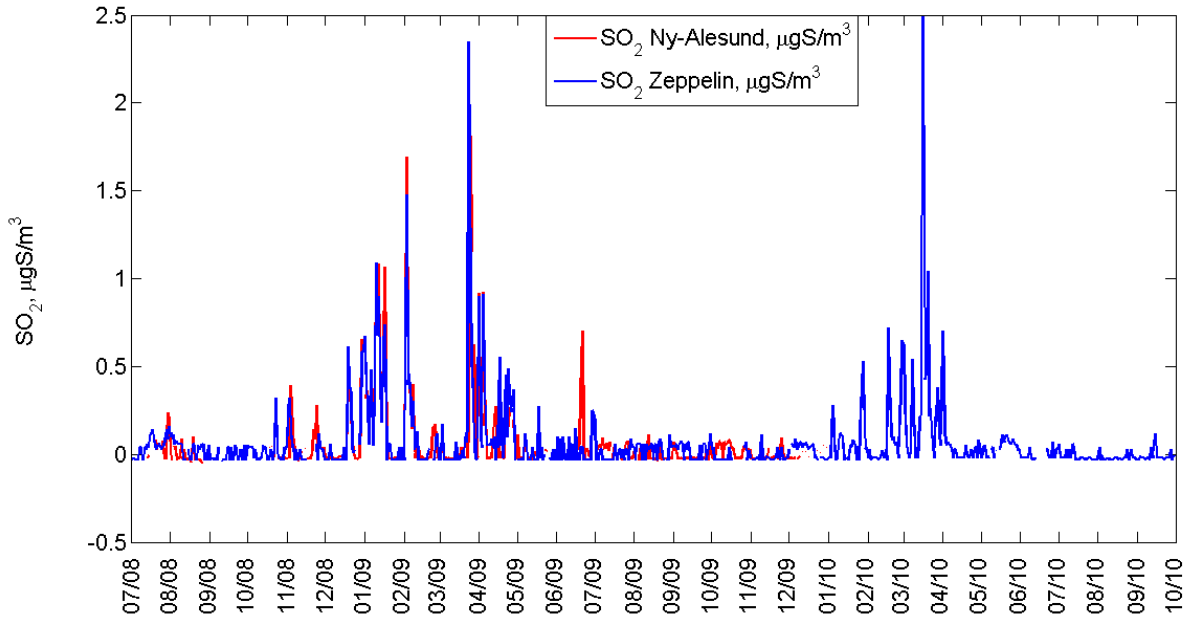

Figure1 SO_2(g) daily concentration in µg S/m^3

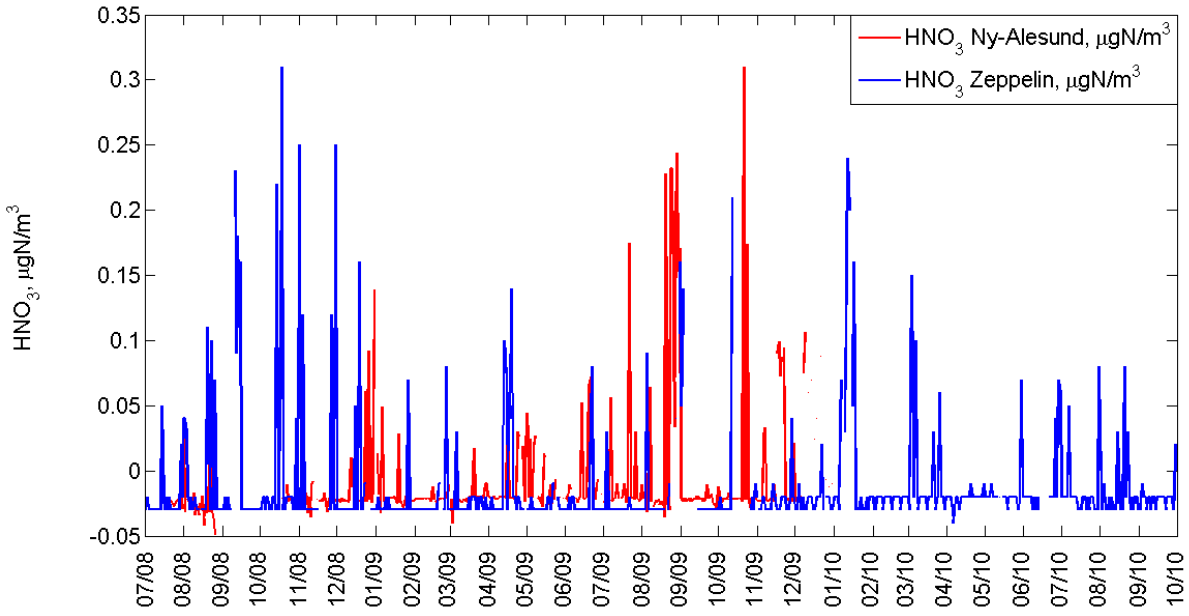

Figure2 HNO_3(g) daily concentration in µg N/ m^3

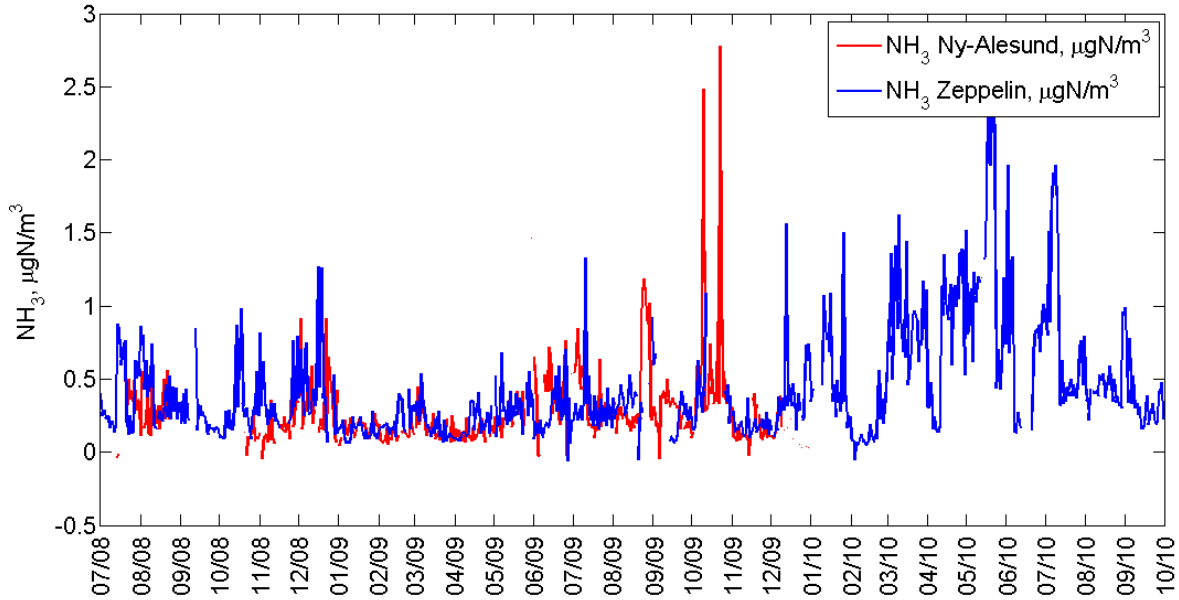

Figure3 NH_3(g) daily concentration in µg N/ m^3

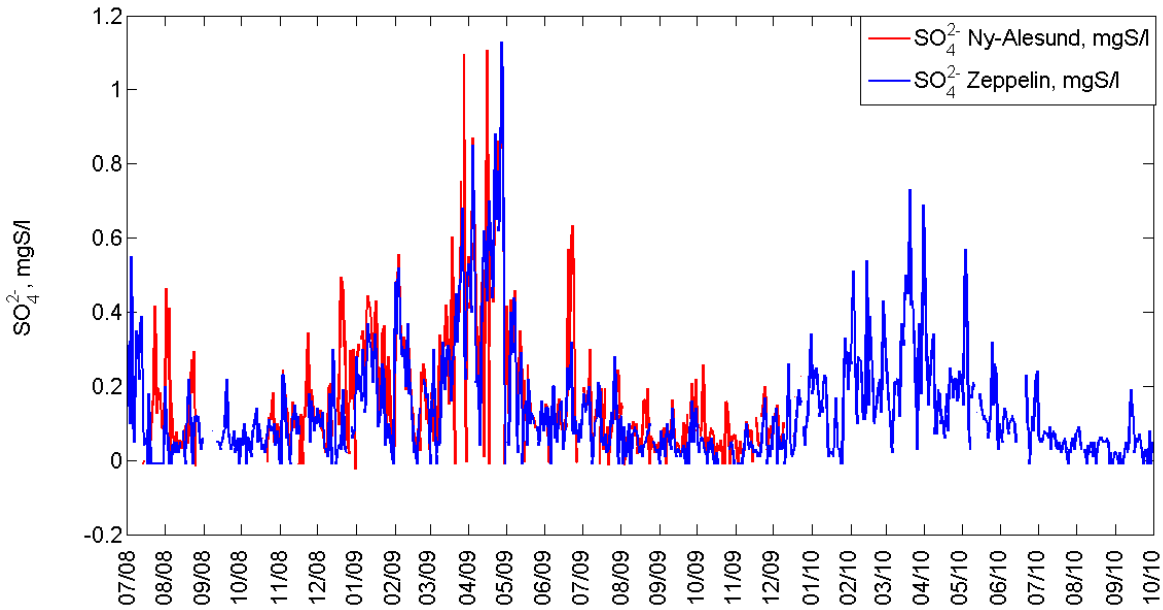

Figure 4 SO_4^{2-}(p) daily concentration in mgS/l

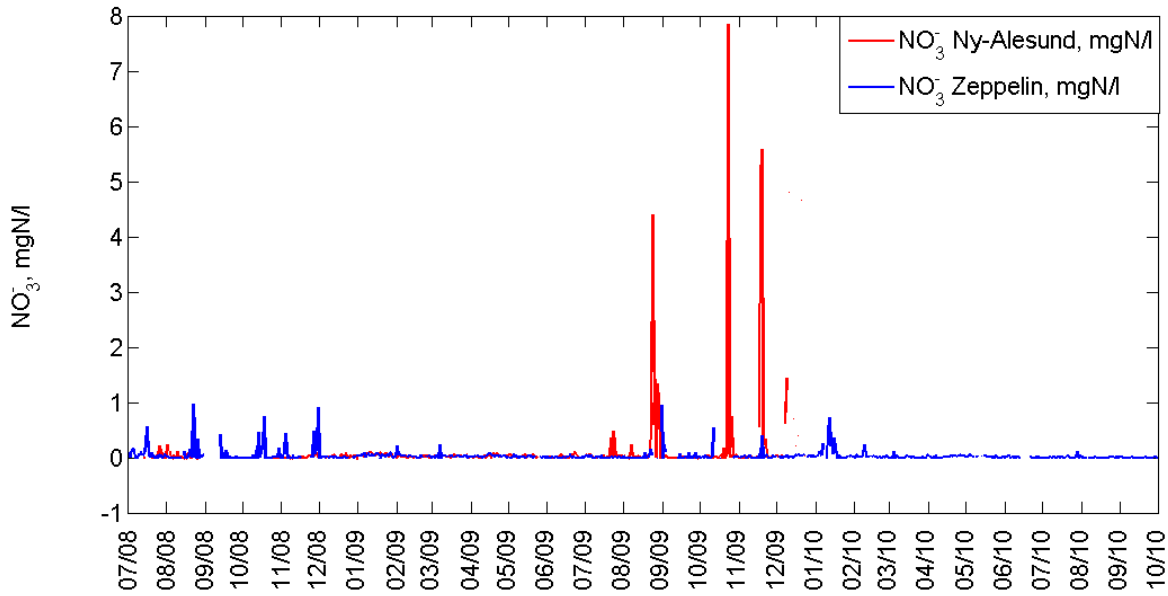

Figure 5 NO_3^-(p) daily concentration in mgN/l

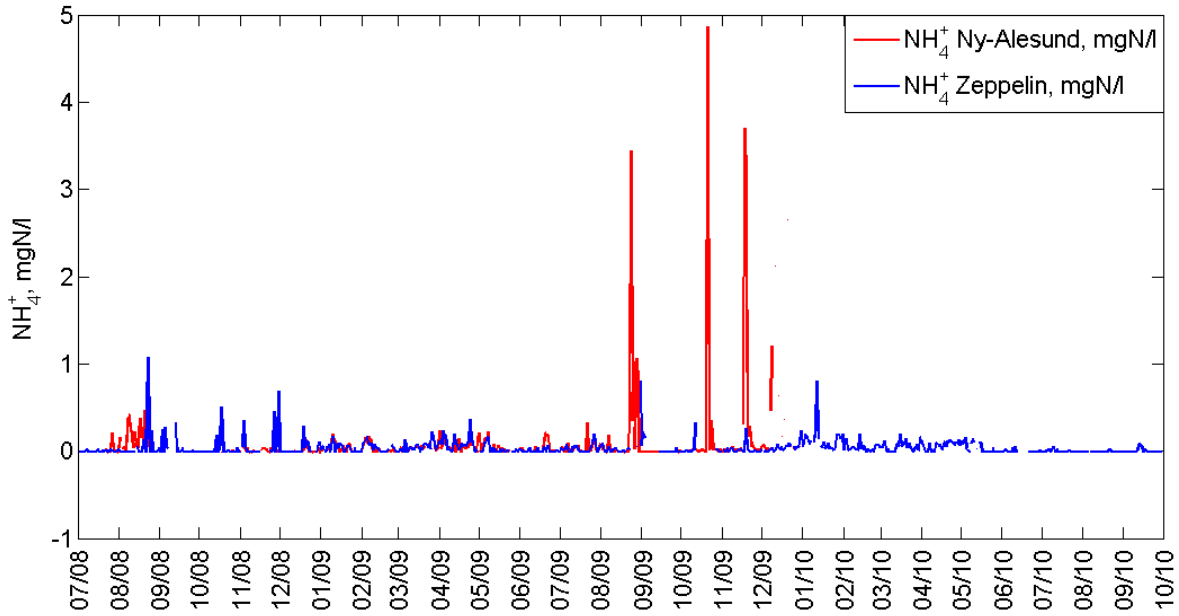

Figure 6 NH_4^+ (p) daily concentration in mgN/l

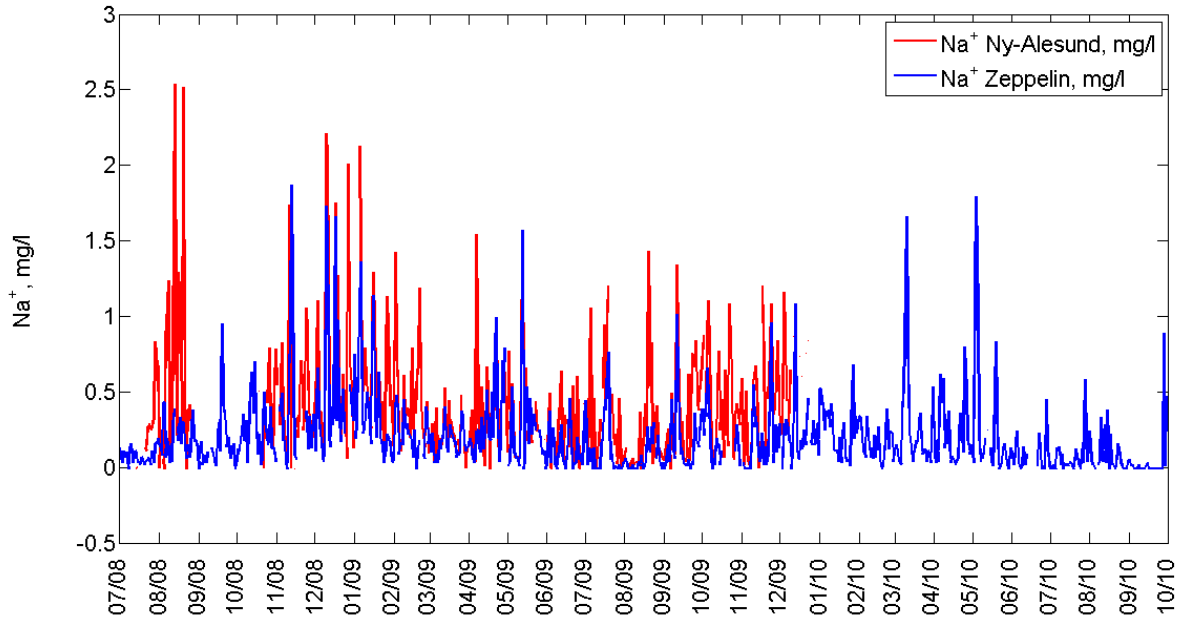

Figure 7 Na^{+} (p) daily concentration in mg/l

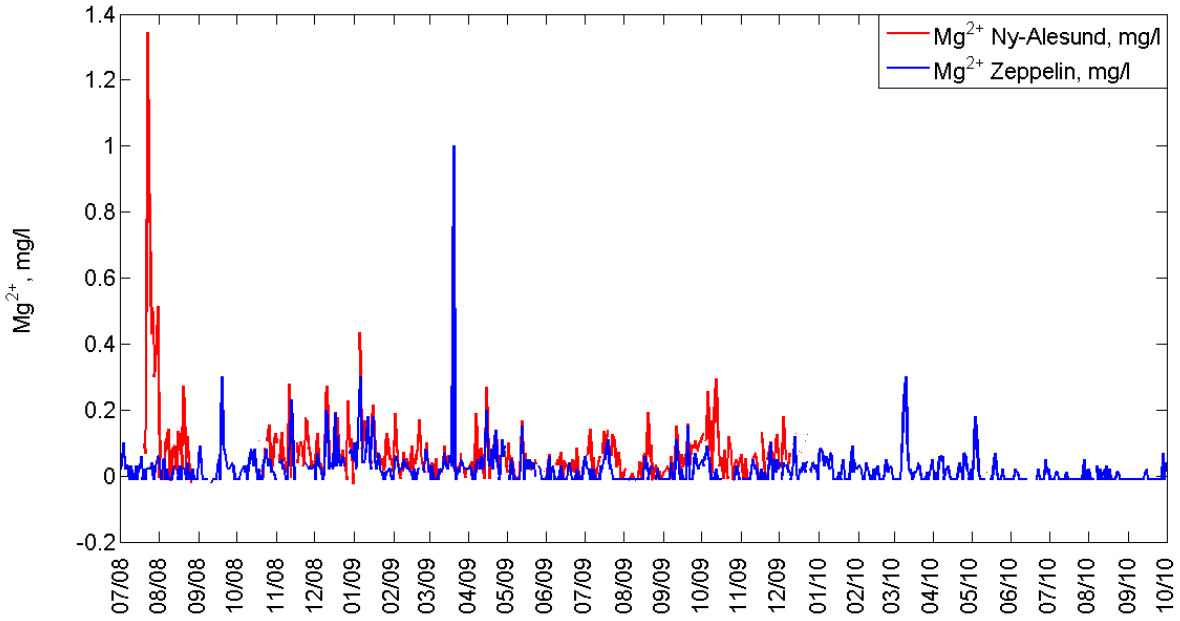

Figure 8 Mg^{2+} (p) daily concentration in mg/l

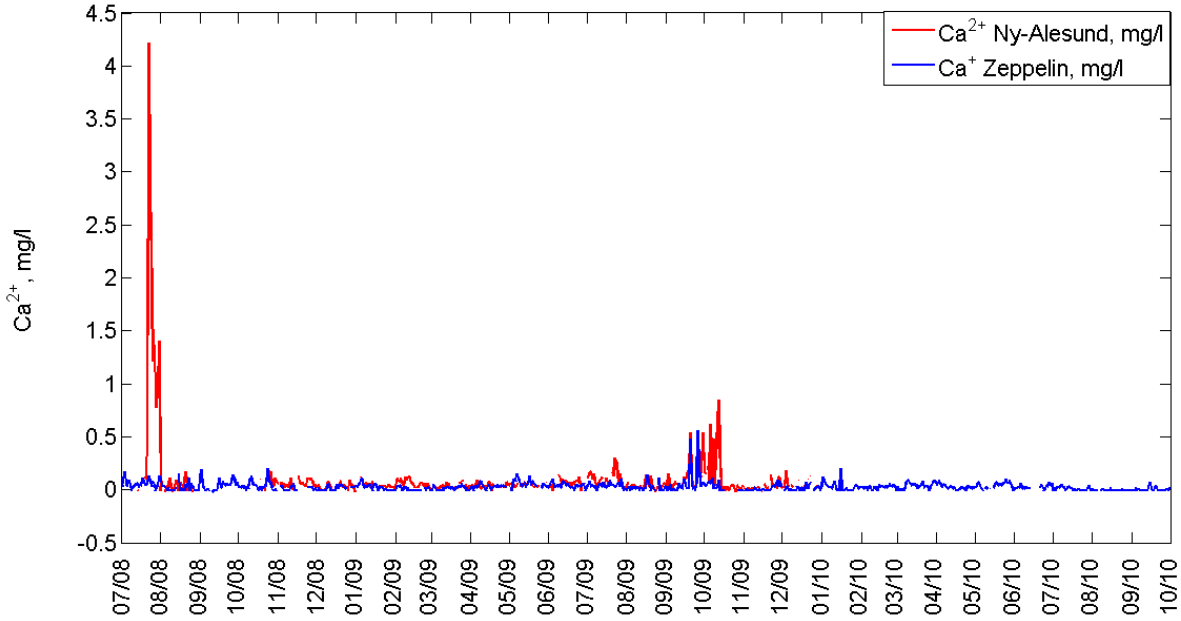

Figure 9 Ca^{2+} (p) daily concentration in mg/l

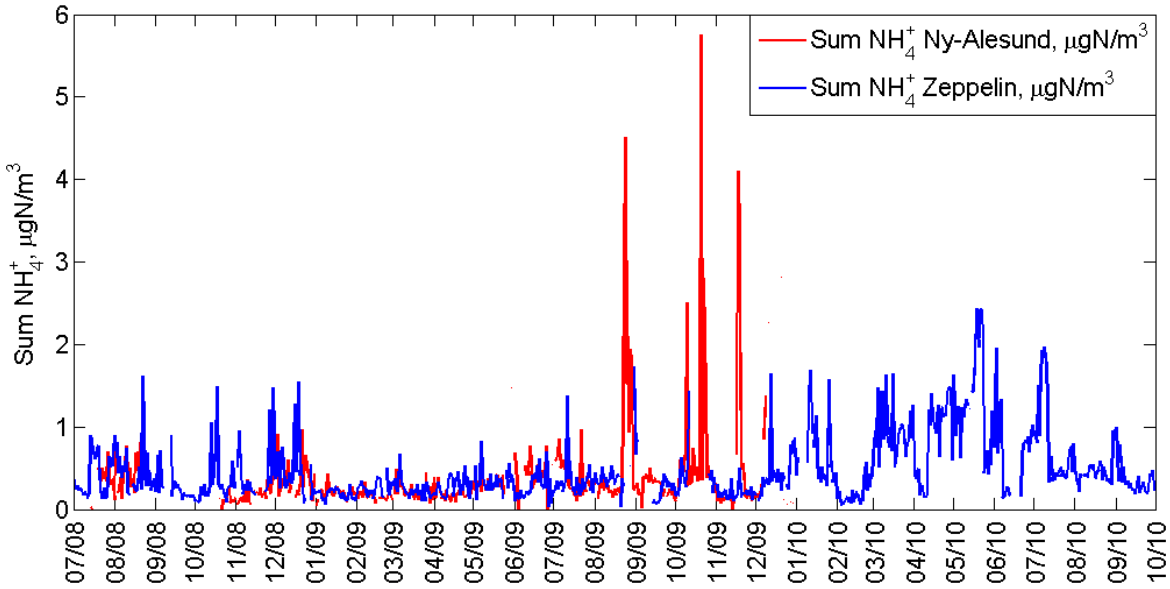

Figure 10 $NH_3(g)$+ NH_4^+ (p) daily concentration in µg N/ m^3

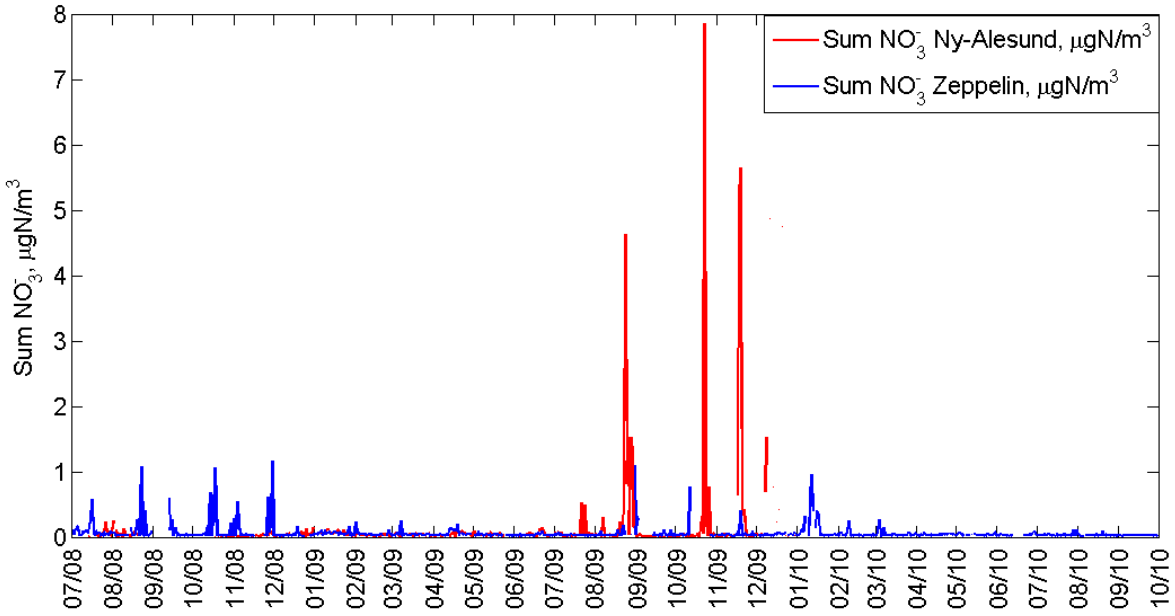

Figure 11 $HNO_3(g)+NO_3^-(p)$ daily concentration in µg N/ m^3

References

Aamaas, B. et al. 2011. "Elemental Carbon Deposition to Svalbard Snow from Norwegian Settlements and Long-Range Transport." *Tellus B* 63(3):340–51. Retrieved April 26, 2014 (http://www.tellusb.net/index.php/tellusb/article/view/16215).

Aas, Kjetil Schanke et al. n.d. "A Comparison between Simulated and Observed Surface Energy Balance at the Svalbard Archipelago." *Journal of Applied Meteorology and Climatology*.

Aas, W. et al. 2012. "Lessons Learnt from the First EMEP Intensive Measurement Periods." *Atmospheric Chemistry and Physics* 12:8073–94. Retrieved April 28, 2014 (http://www.atmos-chem-phys.net/12/8073/2012/).

AMAP, 1998. AMAP Assessment Report: Arctic Pollution Issues. Arctic Monitoring and Assessment Programme (AMAP), Oslo, Norway. xii+859 pp. Chapter 9. Acidifying Pollutants, Arctic Haze, and Acidification in the Arctic.

Alvarado, M. J. et al. 2010. "Nitrogen Oxides and PAN in Plumes from Boreal Fires during ARCTAS-B and Their Impact on Ozone: An Integrated Analysis of Aircraft and Satellite Observations." *Atmospheric Chemistry and Physics* 10:9739–60. Retrieved March 19, 2014 (http://www.atmos-chem-phys.net/10/9739/2010/).

Arsene, C. et al. Formation of Methane Sulfinic Acid in the Gas-Phase OH-Radical Initiated Oxidation of Dimethyl Sulfoxide. *Environmental science & technology* 36, vol.23, pp5155–63. Retrieved (http://www.ncbi.nlm.nih.gov/pubmed/12523433), 2002

Arya, S. P. *Air Pollution Meteorology and Dispersion*. New York: Oxford University press, 1999

Barrie, L., and U. Platt. 1997. "Arctic Tropospheric Chemistry: An Overview." *Tellus B* 49(5):450–54. Retrieved April 22, 2014 (http://www.tellusb.net/index.php/tellusb/article/view/15984).

Basurko, Oihane C., Gorka Gabiña, and Zigor Uriondo. 2012. "Energy Audits of Fishing Vessels : Lessons Learned and the Way Forward." in *Second International Symposium on Fishing Vessel Energy Efficiency E-Fishing, Vigo, Spain, May 2012*. Vigo.

Beine, H. J. et al. 1996. "Measurements of NO_x and Aerosol Particles at the Ny-Ålesund Zeppelin Mountain Station on Svalbard: Influence of Regional and Local Pollution Sources." *Atmospheric Environment* 30(7):1067–79.

Beine, H. J., S. Argentini, A. Maurizi, G. Mastrantonio, and A. Viola. 2001. "The Local Wind Field at Ny-Ålesund and the Zeppelin Mountain at Svalbard." *Meteorology and*

Atmospheric Physics 78:107–13.

Beine, Harald J. et al. 1997. "High-Latitude Springtime Photochemistry . Part I : NOx , PAN and Ozone Relationships." *Journal of Atmospheric Chemistry* 27:127–53.

Berresheim, H. et al. 2002. "Gas-Aerosol Relationships of H 2 SO 4 , MSA, and OH: Observations in the Coastal Marine Boundary Layer at Mace Head, Ireland." *Journal of Geophysical Research* 107(D19):PAR 5–1–PAR 5–12. Retrieved March 23, 2014 (http://doi.wiley.com/10.1029/2000JD000229).

Braathen, G. O., Ø. Hov, and F. Stordal. 1990. *Arctic Atmospheric Research Station on the Zeppelin Mountain (474m A.s.l.) near Ny-Ålesund on Svalbard (78°54'29" N, 11°52'53"E)*. Lillestrøm, Norway.

Chameides, W. L. et al. 1992. "Ozone Precursor Relationships in the Ambient Atmosphere." *Journal of Geophysical Research* 97(D5):6037–55.

Ciciotti, Tiziana, Paolo Braico, Emiliano Liberatori, Luigi Mazari Villanova, and Roberto Sparapani, eds. 2013. *Research Activity in Ny-Ålesund 2011-2012*.

Colarco, P. R. et al. 2004. "Transport of Smoke from Canadian Forest Fires to the Surface near Washington, D.C.: Injection Height, Entrainment, and Optical Properties." *Journal of Geophysical Research* 109(D6):D06203. Retrieved May 27, 2014 (http://doi.wiley.com/10.1029/2003JD004248).

Corbett, James J., and James J. Winebrake. 2008. "Emissions Tradeoffs among Alternative Marine Fuels: Total Fuel Cycle Analysis of Residual Oil, Marine Gas Oil, and Marine Diesel Oil." *Journal of the Air & Waste Management Association* 58(4):538–42. Retrieved March 24, 2014 (http://secure.awma.org/onlinelibrary/doihandler.aspx?doicode=10.3155-1047-3289.58.4.538).

Det Norske Veritas AS. 2009. *Marpol 73/78 Annex VI Regulations for the Prevention of Air Pollution from Ships. Technical and Operational Implications*.

Dütsch, Marina Lara, and Lars Robert Hole. 2012. *Evaluation of the WRF Model Based on Observations Made by Controlled Meteorological Balloons in the Atmospheric Boundary Layer of Svalbard*.

Eckhardt, S. et al. 2013. "The Influence of Cruise Ship Emissions on Air Pollution in Svalbard – a Harbinger of a More Polluted Arctic?" *Atmospheric Chemistry and Physics* 13(16):8401–9. Retrieved January 26, 2014 (http://www.atmos-chem-phys.net/13/8401/2013/).

eKlima. Free access to weather- and climate data from Norwegian Meteorological Institute from historical data to real time observations [online]. –URL: http://sharki.oslo.dnmi.no/portal/page?_pageid=73,39035,73_39049&_dad=portal&_schema=PORTAL

Eleftheriadis, K., S. Vratolis, and S. Nyeki. 2009. "Aerosol Black Carbon in the European Arctic: Measurements at Zeppelin Station, Ny-Ålesund, Svalbard from 1998-2007." *Geophysical Research Letters* 36(2):L02809, pp.1–5. Retrieved March 26, 2014 (http://doi.wiley.com/10.1029/2008GL035741).

Eneroth, Kristina, Kim Holmén, Torunn Berg, Norbert Schmidbauer, and Sverre Solberg. 2007. "Springtime Depletion of Tropospheric Ozone, Gaseous Elemental Mercury and Non-Methane Hydrocarbons in the European Arctic, and Its Relation to Atmospheric Transport." *Atmospheric Environment* 41(38):8511–26. Retrieved March 19, 2014 (http://linkinghub.elsevier.com/retrieve/pii/S1352231007006231).

Esau, Igor, and Irina Repina. 2012. "Wind Climate in Kongsfjorden, Svalbard, and Attribution of Leading Wind Driving Mechanisms through Turbulence-Resolving Simulations." *Advances in Meteorology* 2012:1–16. Retrieved May 7, 2014 (http://www.hindawi.com/journals/amete/2012/568454/).

Evenset, Anita, and Guttorm N. Christensen. 2011. *Environmental Impacts of Expedition Cruise Traffic around Svalbard*. Tromsø.

Fan, S. M., and D. J. Jacob. 1992. "Surface Ozone Depletion in Arctic Spring Sustained by Bromine Reactions on Aerosols." *Nature* 359:522–24.

Finlayson-Pitts, Barbara J., and James N. Jr. Pitts. 2000. *Chemistry of the Upper and Lower Atmosphere: Theory, Experiments, and Applications*. ACADEMIC PRESS.

FLEXTRA Air mass trajectories [online]. –URL: http://tarantula.nilu.no/trajectories/

Forest fires in Russia [online]. –URL: http://www.hzg.de/science_and_industrie/klimaberatung/csc_web/010253/index_0010253.html.en

Hanna, Steven R., Gary A. Briggs, and Rayford P. Jr. Hosker. 1982. *Handbook on Atmospheric Diffusion*. Retrieved (http://www.wmo.int/pages/prog/www/DPFSERA/documents/workbook.pdf).

Heintzenberg, Jost, and Caroline Leck. 1994. "Seasonal Variation of the Atmospheric Aerosol near the Top of the Marine Boundary Layer over Spitsbergen Related to the Arctic Sulphur Cycle*." *Tellus B* 46:52–67. Retrieved

(http://www.tellusb.net/index.php/tellusb/article/view/15751).

Hermansen O. et al., Air Quality Ny-Ålesund. Monitoring of Local Air Quality 2008-2010. Measurement results. Scientific report. NILU, March 2011

Ingerø, Odd Olsen (Governor of Svalbard). 2010. *Start Notice - Administration Plan for the Nature Reserves in East Svalbard*. Retrieved (http://oldweb.sysselmannen.no/hoved.aspx?m=44380&amid=3180767).

Jaeglé, L. et al. 1998. "Sources and Chemistry of NOx in the Upper Troposphere over the United States." *Geophysical Research Letters* 25(10):1705–8. Retrieved March 19, 2014 (https://www.atmos.washington.edu/~jaegle/group/Publications_files/Geophys Res Lett 1998 Jaegle.pdf).

Kalli, Juha, Tapio Karvonen, and Teemu Makkonen. 2009. *Sulphur Content in Ships Bunker Fuel in 2015 A Study on the Impacts of the New IMO Regulations and Transportation Costs*. Helsinki.

Kupfer, Heike, Andreas Herber, and Gert König-Langlo. 2006. *Radiation Measurements and Synoptic Observations at Ny-Ålesund, Svalbard*. Alfred-Wegener-Institut für Polar- und Meeresforschung. Retrieved April 22, 2014 (http://epic.awi.de/26713/1/10543.pdf).

Lee, Chulkyu et al. 2011. "SO 2 Emissions and Lifetimes: Estimates from Inverse Modeling Using in Situ and Global, Space-Based (SCIAMACHY and OMI) Observations." *Journal of Geophysical Research* 116(D6):D06304. Retrieved January 23, 2014 (http://doi.wiley.com/10.1029/2010JD014758).

Lewin, E., and B. Zachau-Christiansen. 1977. "Efficiency of 0.5 N KOH Impregnated Filters for SO2-Collection." *Atmospheric Environment* 11(1):861–62.

Li, Shao-Meng et al. 1990. "Arctic Boundary Layer Ozone Variations Associated with Nitrate, Bromine, and Meteorology: A Case Study." *Journal of Geophysical Research* 95(D13):22,433–22,440. Retrieved (http://doi.wiley.com/10.1029/JD095iD13p22433).

Lyons, T. J., and W. D. Scott. 1990. *Principles of Air Pollution Meteorology*. London: Belhaven Press.

Mäkiranta, Eeva. 2009. *Observations of Atmospheric Boundary Layer over Sea Ice in a Svalbard Fjord.* Helsinki: University of Helsinki. Department of Physics.

Mäkiranta, Eeva, Timo Vihma, Anna Sjöblom, and Esa-Matti Tastula. 2011. "Observations and Modelling of the Atmospheric Boundary Layer Over Sea-Ice in a Svalbard Fjord." *Boundary-Layer Meteorology* 140(1):105–23. Retrieved April 23, 2014

(http://link.springer.com/10.1007/s10546-011-9609-1).

Maturilli, M., a. Herber, and G. König-Langlo. 2013. "Climatology and Time Series of Surface Meteorology in Ny-Ålesund, Svalbard." *Earth System Science Data* 5(1):155–63. Retrieved March 27, 2014 (http://www.earth-syst-sci-data.net/5/155/2013/).

Molenaar, E. J. 2012. "Fisheries Regulation in the Maritime Zones of Svalbard." *The International Journal of Marine and Coastal Law* 27:3–58. Retrieved March 24, 2014 (http://booksandjournals.brillonline.com/content/journals/10.1163/157180812x610541).

Müller, D. et al. 2007. "Multiwavelength Raman Lidar Observations of Particle Growth during Long-Range Transport of Forest-Fire Smoke in the Free Troposphere." *Geophysical Research Letters* 34(5):L05803. Retrieved May 27, 2014 (http://doi.wiley.com/10.1029/2006GL027936).

Nasjonalt folkehelseinstitutt. Luftkvalitetskriterier. [online]. Available: http://www.fhi.no/eway/default.aspx?pid=233&trg=MainArea_5661&MainArea_5661=5631:0:15,3152:1:0:0:::0:0

NILU. 1996. *EMEP Manual for Sampling and Chemical Analysis*.

Norges Rederiforbund. 2003. *Miljøvennlig Skipsfart – Miljøprogram 2003 – 2007*. Oslo.

Oke, T. R. 2002. *Boundary Layer Climates*. 2nd ed. Taylor & Francis e-Library.

Petzold, A. et al. 2008. "Experimental Studies on Particle Emissions from Cruising Ship, Their Characteristic Properties, Transformation and Atmospheric Lifetime in the Marine Boundary Layer." *Atmospheric Chemistry and Physics* 8(9):2387–2403. Retrieved (http://www.atmos-chem-phys.net/8/2387/2008/).

Quinn, P. K. et al. 2007. "Arctic Haze: Current Trends and Knowledge Gaps." *Tellus B* 59(1):99–114. Retrieved March 26, 2014 (http://www.tellusb.net/index.php/tellusb/article/view/16972).

Ramírez-Anguita, Juan M., Àngels González-Lafont, and José M. Lluch. 2008. "Formation Pathways of DMSO from DMS-OH in the Presence of O2 and NOx: A Theoretical Study." *Journal of Computational Chemistry* 30(2):173–82.

Reimann, Stefan, Roland Kallenborn, and Norbert Schmidbauer. 2009. "Severe Aromatic Hydrocarbon Pollution in the Arctic Town of Longyearbyen (Svalbard) Caused by Snowmobile Emissions." *Environmental science & technology* 43(13):4791–95. Retrieved (http://www.ncbi.nlm.nih.gov/pubmed/19673266).

Sander, Gunnar, Aina Holst, and John Shears. 2006. *Environmental Impact*

Assessment of the Research Activities in Ny-Ålesund 2006.

Schau, Erwin M., Harald Ellingsen, Anders Endal, and Svein Aa. Aanondsen. 2009. "Energy Consumption in the Norwegian Fisheries." *Journal of Cleaner Production* 17(3):325–34. Retrieved March 21, 2014 (http://linkinghub.elsevier.com/retrieve/pii/S0959652608001947).

Seinfeld, John H., and Spyros N. Pandis. 2006. *Atmospheric Chemistry and Physics: From Air Pollution to Climate Change*. 2nd ed. John Wiley & Sons, Inc.

Shears, John, Fredrik Theisen, Are Bjørdal, and Stefan Norris. 1998. *Environmental Impact Assessment. Ny-Ålesund International Scientific Research and Monitoring Station, Svalbard*. Tromsø.

Shiobara M. et al. Long-term monitoring of clouds and aerosols by ground-based remote sensing instruments operated by NIPR in Ny-Ålesund, Abstracts for the 11th Ny-Ålesund Science Managers Committee Seminar, National Research Council of Italy, Rome, 9 -11 October 2013, p.30.

Smith, S. J. et al. 2011. "Anthropogenic Sulfur Dioxide Emissions: 1850–2005." *Atmospheric Chemistry and Physics* 11:1101–16. Retrieved March 22, 2014 (http://www.atmos-chem-phys.net/11/1101/2011/).

Solberg, Sverre, Norbert Schmidbauer, Arne Semb, Frode Stordal, and Øystein Hov. 1996. "Boundary-Layer Ozone Depletion as Seen in the Norwegian Arctic in Spring." *Journal of Atmospheric Chemistry* 23:301–32.

Solberg S. et al., Reactive Nitrogen Compounds at Spitsbergen in the Norwegian Arctic, Journal of Atmospheric Chemistry, 28, pp 209–225, 1997.

Stohl, A. 2006. "Characteristics of Atmospheric Transport into the Arctic Troposphere." *Journal of Geophysical Research* 111(D11):D11306. Retrieved April 2, 2014 (http://doi.wiley.com/10.1029/2005JD006888).

Teledyne Advanced Pollution Instrumentation. 2010. *Model 200E Nitrogen Oxide Analyzer. Technical Manual*. SAN DIEGO.

Teledyne Advanced Pollution Instrumentation. 2011. *Model 100E UV Fluorescence SO2 Analyzer. Operation Manual*. SAN DIEGO.

Treffeisen, R. et al. 2007. "Arctic Smoke – Aerosol Characteristics during a Record Smoke Event in the European Arctic and Its Radiative Impact." *Atmospheric Chemistry and Physics* 7:3035–53.

TSI. 2002a. *Model 3010 Condensation Particle Counter. Instruction Manual*.

TSI. 2002b. *Model 3025A Ultrafine Condensation Particle Counter. Instruction Manual*.

Tunved, P., J. Ström, and R. Krejci. 2013. "Arctic Aerosol Life Cycle: Linking Aerosol Size Distributions Observed between 2000 and 2010 with Air Mass Transport and Precipitation at Zeppelin Station, Ny-Ålesund, Svalbard." *Atmospheric Chemistry and Physics* 13:3643–60. Retrieved March 24, 2014 (http://www.atmos-chem-phys.net/13/3643/2013/).

Tyedmers, Peter. 2004. "Fisheries and Energy Use." Pp. 683–93 in *Encyclopedia of Energy*, vol. 2, edited by C Cleveland. Amsterdam: Elsevier Inc.

Vestreng, V., R. Kallenborn, and E. Økstad. 2009. *Climate Influencing Emissions , Scenarios and Mitigation Options at Svalbard*.

Virkkula, Aki et al. 2006. "Chemical Size Distributions of Boundary Layer Aerosol over the Atlantic Ocean and at an Antarctic Site." *Journal of Geophysical Research* 111(D5):D05306. Retrieved April 4, 2014 (http://doi.wiley.com/10.1029/2004JD004958).

Wallace, John M., and Peter V. Hobbs. 2006. *Atmospheric Science: An Introductory Survey*. 2nd ed. Elsevier Inc.

Weinbruch, Stephan et al. 2012. "Chemical Composition and Sources of Aerosol Particles at Zeppelin Mountain (Ny Ålesund, Svalbard): An Electron Microscopy Study." *Atmospheric Environment* 49:142–50. Retrieved March 26, 2014 (http://linkinghub.elsevier.com/retrieve/pii/S135223101101260X).

WMO, Manual for the GAW precipitation chemistry programme. Guidelines, Data Quality Objectives and Standard Operating Procedures (WMO TD No. 1251). WMO report № 160, 2004

Vickers, D. and L. Mahrt, Quality control and flux sampling problems for tower and aircraft data, Journal of Atmospheric and Oceanic Technology, 14(3):512{526, 1997.

Yin, F., D. Grosjean, and Seinfeld J. H. 1990. "Photooxidation of Dimethyl Sulfide and Dimethyl Disulfide . I : Mechanism Development." *Journal of Atmospheric Chemistry* 11:309–64.

Zhan, Jianqiong, and Yuan Gao. 2014. "Impact of Summertime Anthropogenic Emissions on Atmospheric Black Carbon at Ny-Ålesund in the Arctic." *Polar Research* 33(21821). Retrieved March 18, 2014 (http://www.polarresearch.net/index.php/polar/article/view/21821/xml).

Ziegler, Friederike, and Per-Anders Hansson. 2003. "Emissions from Fuel

Combustion in Swedish Cod Fishery." *Journal of Cleaner Production* 11:303–14. Retrieved (http://linkinghub.elsevier.com/retrieve/pii/S0959652602000501).